Summer 8-16-2018

Higher-Order Accurate Finite Difference Method for Thermal Analysis in Double-Layered Solid Structures -- Gradient Preserved Method

Yun Yan
Louisiana Tech University

HIGHER-ORDER ACCURATE FINITE DIFFERENCE METHOD FOR THERMAL ANALYSIS IN DOUBLE-LAYERED SOLID STRUCTURES — GRADIENT PRESERVED METHOD

by

Yun Yan, B.S. M.S.

A Dissertation Presented in Partial Fulfillment
of the Requirements for the Degree
Doctor of Philosophy

COLLEGE OF ENGINEERING AND SCIENCE
LOUISIANA TECH UNIVERSITY

May 2018

LOUISIANA TECH UNIVERSITY

THE GRADUATE SCHOOL

May 7, 2018

Date

We hereby recommend that the dissertation prepared under our supervision by Yun Yan

entitled HIGHER-ORDER ACCURATE FINITE DIFFERENCE METHOD FOR THERMAL ANALYSIS IN DOUBLE-LAYERED SOLID STRUCTURES — GRADIENT PRESERVED METHOD

be accepted in partial fulfillment of the requirements for the Degree of Doctor of Philosophy in Computational Analysis and Modeling

Supervisor of Dissertation Research

Head of Department

Computational Analysis and Modeling

Department

Recommendation concurred in:

Advisory Committee

Approved:

Director of Graduate Studies

Approved:

Dean of the Graduate School

Dean of the College

GS Form 13a
(6/07)

ABSTRACT

Layered structures have appeared in many systems such as biological tissues, micro-electronic devices, thin films, fins, reactor walls, thermoelectric power conversion, thermal coating, metal oxide semiconductors, and thermal processing of DNA origami nanostructures. Analyzing heat transfer in layered structures is of crucial importance for the design and operation of devices and the optimization of thermal processing of materials. There are many numerical methods dealing with the layered structures or interface problems. The existing numerical methods such as the immersed interface method and the matched interface boundary method, if using three-grid points across the interface, usually provide only a second-order truncation error, which reduces the accuracy of the overall numerical solution even if the higher-order compact finite difference method is employed at other points. Obtaining a higher-order accurate numerical scheme using three-grid points across the interface so that the overall numerical scheme is stable and convergent with higher-order accuracy is mathematically challenging.

The objective of this dissertation is to develop a higher-order accurate finite difference method using three-grid points across the interface. To this end, we first consider three mathematical models, the steady-state heat conduction model, the unsteady-state heat conduction model and the nanoscale heat conduction model. The well-posedness of these three models are proved. After that, compact higher-order

finite difference schemes for solving these three models are developed, respectively. In particular, for the interior points, the well-known padé scheme (three-point fourth-order compact finite difference scheme) is applied. On the boundary and interface, by preserving the first-order derivative, u_x, fourth-order finite difference schemes for the interface conditions, third-order or fourth-order finite difference schemes for the Neumann boundary conditions and the Robin boundary conditions, are developed, respectively. As such, the overall schemes are at least third-order accurate. The stability and convergence of the scheme for the steady-state case with Dirichlet boundary are proven. Finally, four different examples are given to test the obtained numerical schemes. Results showed that the convergence rate is close to 4.0, which coincides with the theoretical analysis. Further research will focus on the analysis of the stability and convergence of the schemes for the unsteady-state heat conduction case and the nanoscale heat conduction case, and the extension of our schemes to multidimensional cases.

APPROVAL FOR SCHOLARLY DISSEMINATION

The author grants to the Prescott Memorial Library of Louisiana Tech University the right to reproduce, by appropriate methods, upon request, any or all portions of this Dissertation. It is understood that "proper request" consists of the agreement, on the part of the requesting party, that said reproduction is for his personal use and that subsequent reproduction will not occur without written approval of the author of this Dissertation. Further, any portions of the Dissertation used in books, papers, and other works must be appropriately referenced to this Dissertation.

Finally, the author of this Dissertation reserves the right to publish freely, in the literature, at any time, any or all portions of this Dissertation.

Author Yun Yan

Date 05/17/2018

TABLE OF CONTENTS

LIST OF TABLES

LIST OF FIGURES

ACKNOWLEDGMENTS

Dr. Weizhong Dai, the most important person I should thank at this moment. Without his support, input, direction and patience, I would not be able to finish this dissertation. He is such an elegant, brilliant and diligent man, just like his own equation, *Success* = 89% *Hard work* + 10% *Intelligence* + 1% *Luck.* We had countless hours of conversation on almost every topic. He can always explain and solve a problem in a very simple and clear way. He taught me a lot and gave me lots of advice on research, teaching, career, life in general and much more. Without him, I would never have found my passion for research and my own equation, *Happiness* = x_1% *Hard work* + x_2% *Intelligence* + x_3% *Luck* + x_4% *Love.* I am so lucky, more than 1%, to have the chance to learn under such a wise mathematician.

I would also like to thank the professors I met at Louisiana Tech University. I want to give my thanks to Dr. Erica P. Murray, the first professor aside from my advisor, for her suggestions and sincerity at the very beginning of my PhD life. Moreover, I would like to thank the rest of my committee members, Dr. Sumeet Dua, Dr. Katie A. Evans, and Dr. Don Liu for their help and feedback to improve this dissertation. I want to thank Dr. Songming Hou for providing me with plenty of time to talk with me either regarding research or life and for his valuable suggestions on this work. I am grateful to Dr. Paula W. Brown for her assistance in improving my English, both verbally and writing. I would like to thank Mr. Danny Eddy, Dr.

Dave Meng, Dr. Scarlett S. Bracey, and Dr. Jonathan B. Walters for their help when I was their teaching assistant.

I am very grateful to the College of Engineering and Science for providing me an assistantship during my study in PhD CAM program. Special thanks gives to Dr. William Edwin Koss for allowing the Program of Mathematics and Statistics to select me as the recipient of the Dr. Walter E. Koss Scholarship for the academic year 2014-2015. Thanks to all the faculty and staffs at Louisiana Tech for their support and help. Each person has influenced my research or life in some way.

My gratitude goes above all to my family. To my parents, siblings and my wife, thank you for your love and support as I pursued my hopes and dreams; thank you for your unmatched support you have given me through the years. Without your love and sacrifice, I could never have completed this work.

I want to acknowledge the help that has come from all my friends, for their understanding and assistance in these past four years. First, I'd like to thank the friends I made in Ruston, Louisiana. They helped me in various ways at different periods and I had a much more colorful life here because of them. I would also like to thank the friends I made before I started my PhD journey, in particular, Zhiyan Yang (12 years), Qifang Li (9 years), Zhipin Lin (9 years) and Jia Zhang (7 years). I thank them for their support and for their willingness to lend a listening ear when needed even from afar. Last but not least, I would like to thank my academic siblings, Fei Han, Casey O. Orndorff, Yushan Lin, Joshua P. Wilson and Aniruddha Bora. I enjoyed my conversations with them on research and life. I am very happy to be a member of this academic family. It is a special pleasure to thank Bora, Zhiping,

Jia and Rui Liu for their help on either improving my dissertation or preparing my defense. I will keep in touch.

Thanks to all who smiled at me while I was on campus even though we did not know each other.

All the people I mentioned above made my PhD journey much more enjoyable. I cannot thank them enough.

CHAPTER 1

INTRODUCTION

1.1 General Overview

Layered structures have appeared in many engineering systems such as biological tissues, micro-electronic devices, thin films, reactor walls, thermoelectric power conversion, thermal coating, metal oxide semiconductors and thermal processing of DNA origami nano structures [1-8]. In particular, the multi-layered metal thin-films, for example, gold-coated metal mirrors, are often used in high-power infrared-laser systems to avoid damage at the front surface of a single layer film caused by the high-power laser energy [7]. Furthermore, to achieve high thermoelectric efficiency, a low thermal conductivity is required. Low thermal conductivity is often realized by nano-structuring with the introduction of a high density of materials [4]. All semiconductor devices possess metal contacts; hence, the study of heat conduction through metal-semiconductor interfaces is a technological problem [8]. Thus, analysis of heat conduction in layered structures is of crucial importance for the design and operation of devices and the optimization of thermal processing of materials.

There are many models and numerical methods in the literature dealing with thermal analysis in layered structures. The governing equations include steady-state heat conduction, unsteady-state heat conduction, where the equations vary

from elliptic partial differential equations, parabolic partial differential equations, Boltzmann transport equations to dual-phase-lagging equations, etc. The numerical methods include finite difference method, finite element method, finite volume method, Monte Carlo method, mesh-free method, etc. Moreover, the numerical methods that deal with the interface include Peskin's immersed boundary method [9-14], the immersed interface method [15-25], the ghost fluid method [26-28], the matched interface and boundary method [29-34], finite element method [35-44] and some body-fitting approaches [45, 46]. For time-dependent problems, summation-by-parts operators with simultaneous approximation terms is another good choice besides the above methods [47-50].

Although there are many numerical methods such as the aforementioned immersed interface method and the matched interface boundary method, the existing numerical method using three-grid points across the interface usually provides only a second-order truncation error, which reduces the accuracy of the overall numerical solution even if the higher-order compact finite difference method is employed at other points. It is desirable to have a higher-order numerical scheme using three points across the interface because fourth-order three-points in space compact numerical scheme has been obtained for the interior points [51]. As such, the overall scheme will provide a much more accurate solution. At the same time, the solution system is a tridiagonal linear system, which can be easily solved using the well-known Thomas algorithm. Using as small a number of grid points as possible to obtain a reasonable accurate solution is particularly interesting in micro/nano scale heat conduction because of the very small dimension. However, obtaining a higher-order accurate

numerical scheme using three-grid points across the interface so that the overall numerical scheme is unconditionally stable and convergent with higher-order accuracy is mathematically challenging.

1.2 Research Objectives

The objective of this dissertation is to develop a higher-order accurate finite difference method using three-grid points across the interface. By coupling with a three-point fourth-order compact finite difference scheme at the interior points, we aim to obtain a stable and convergent numerical scheme and achieve a higher-order accurate solution. To this end, this dissertation research will focus on the development of a higher-order accurate finite difference method for the thermal analysis in steady-state, unsteady-state and micro/nano scale based on the one-dimensional double-layered elliptic, parabolic and dual-phase-lagging equations with different kinds of interface conditions and boundary conditions in order to avoid the complex geometry.

The organization of the rest of the dissertation is given as follows. In Chapter 2, the literature that leads to the current work is reviewed. In Chapter 3, the models for thermal analysis in one dimensional steady-state, unsteady-state and micro/nano scale (only nanoscale will be used for the rest of the dissertation) of heat conduction in double-layered structures are considered, in which the elliptic equation, the traditional heat conduction equation, and the dual-phase-lagging equation are given. The well-posedness of these three models are analyzed. In Chapter 4, we give the idea of the gradient preserved method, and then apply it to developing the numerical schemes for the steady-state heat conduction model with the Dirichlet boundary. The solvability,

stability, and convergence of the numerical scheme are analyzed theoretically. In Chapter 5, by using the gradient preserved method and three-points compact finite difference method, we propose higher-order accurate finite difference schemes for obtaining the approximate solutions for the steady-state heat conduction model (with Neumann and Robin boundaries), the unsteady-state heat conduction model and the nanoscale heat conduction model. In Chapter 6, we test these new numerical methods by four examples for accuracy and applicability. In Chapter 7, summary of the current work is given and future work is discussed.

CHAPTER 2

LITERATURE REVIEW AND PREVIOUS WORK

This chapter will review the heat conduction equations, existing numerical methods dealing with interface, and compact finite difference method, which are related to this dissertation.

2.1 Heat Conduction Equations

Based on Fourier's law, the heat flux and the temperature gradient in solid structure satisfy

$$q\left(\vec{r},t\right)=-k\nabla u\left(\vec{r},t\right), \tag{2.1}$$

where $\vec{q}$ is the heat flux, $u\left(\vec{r},t\right)$ is the temperature, k is the conductivity, $\vec{r}$ is the space vector, t is the time, and ∇ is the gradient operator. Coupling with the energy equation

$$\rho C u_t\left(\vec{r},t\right)=-\nabla\cdot q\left(\vec{r},t\right)+f\left(\vec{r},t\right), \tag{2.2}$$

where ρ is the density, C is the specific heat, and $f\left(x,t\right)$ is the heat source term, one may obtain

$$\rho C u_t\left(\vec{r},t\right)=k\nabla^2 u\left(\vec{r},t\right)+f\left(\vec{r},t\right), \tag{2.3}$$

which is often called the unsteady-state heat conduction equation. If the temperature is time-independent, i.e. $u_t(\vec{r},t)=0$, it is called the steady-state, and the equation can be reduced to

$$-k\nabla^2 u(\vec{r}) = f(\vec{r}), \tag{2.4}$$

which is called an elliptic equation. In particular, for the one-dimensional case, the unsteady-state equation can be written as

$$\rho C u_t(x,t) = k u_{xx}(x,t) + f(x,t), \tag{2.5}$$

and the steady-state equation (elliptic equation) is

$$-k u_{xx}(x) = f(x). \tag{2.6}$$

In general, if k is dependent on x, the unsteady-state and steady-state equations can be written as

$$\rho C u_t(x,t) = \frac{\partial}{\partial x}\left(k(x)\, u_x(x,t)\right) + f(x,t), \tag{2.7}$$

and

$$-\frac{d}{dx}\left(k(x)\, u_x(x)\right) = f(x), \tag{2.8}$$

respectively. The boundary condition could be the Dirichlet boundary condition

$$u|_{\partial\Omega} = g(x,t), \tag{2.9}$$

where $\partial\Omega$ is the boundary, $g(x,t)$ is a given function, or the Neumann boundary condition

$$\frac{\partial u}{\partial \vec{n}}|_{\partial\Omega} = g(x,t), \tag{2.10}$$

where $\vec{n}$ is the outward normal vector on the boundary, or the Robin boundary condition

$$\alpha \frac{\partial u}{\partial \vec{n}}|_{\partial\Omega} + \beta u|_{\partial\Omega} = g\left(x,t\right), \tag{2.11}$$

where α, β are constants.

In 1997, Tzou introduced the phase-lag concept to allow for the heat flux and the temperature gradient to occur at different instants of time in nanoscale heat transfer [53]. This can be represented as

$$q\left(\vec{r},t+\tau_q\right) = -k\nabla u\left(\vec{r},t+\tau_T\right), \tag{2.12}$$

where τ_q, τ_T are the delay times for the heat flux and the temperature gradient, respectively. In the heat diffusion model at the nanoscale, $\tau_q = \tau_T = 0$, which implies an infinite speed of heat propagation (zero delay time between heat input at one location and its detection at other locations). On the other hand, in the thermal wave theory of heat conduction, $\tau_T = 0$, a first-order Taylor series expansion of the above equation with respect to t, gives the classical thermal wave model

$$q\left(\vec{r},t\right) + \tau_q q_t\left(\vec{r},t\right) = -k\nabla u\left(\vec{r},t\right), \tag{2.13}$$

as originally proposed by Cattaneo and Vernotle [54, 55]. This wave equation relaxes the assumption of infinite speed of heat propagation. The heat flux delay time (or phonon mean free time) is related to the wave speed w, by expression $\tau_q = \frac{\eta}{w^2}$, where η is the thermal diffusivity. It is clear that when the wave speed is infinite, the wave equation reduces to the classical heat diffusion equation. In order to obtain a solution

for q and u, we combine the energy equation (2.2) and obtain

$$\frac{k}{\rho C}u_t\left(\vec{r},t\right)=\nabla^2 u\left(\vec{r},t\right)-\frac{\rho C\tau_q}{k}u_{tt}\left(\vec{r},t\right)+\frac{1}{k}\left(f\left(\vec{r},t\right)+\tau_q f_t\left(\vec{r},t\right)\right). \tag{2.14}$$

For the dual-lag model, the case $\tau_q < \tau_T$ implies that the flux (or heat flow) causes a temperature gradient to occur across the medium. On the other hand, when $\tau_q > \tau_T$, the temperature gradient (which occurs first) induces the flux or heat flow. A first-order Taylor series approximation of Eq. (2.12) leads to the expression

$$q\left(\vec{r},t\right)+\tau_q q_t\left(\vec{r},t\right)\simeq -k\left[\nabla u\left(\vec{r},t\right)+\tau_T\frac{\partial\left(\nabla u\left(\vec{r},t\right)\right)}{\partial t}\right]. \tag{2.15}$$

As discussed by Tzou, the lags or delayed responses can be caused by the following factors: (1) A lag is caused by the time it takes for heat to be transferred from the heated electrons to the phonons, which is usually of the order of a picosecond. (2) For dielectric films, insulators, and semiconductors, the dominant mechanism of heat transport is phonon collisions and scattering. In this case, the lag is caused by the phonon mean free time. (3) Heat transport at low temperatures can be delayed because of a reduced collision rate among molecules. (4) Porous media can cause a delay in response caused by the time it takes for heat flow to circulate around the air pockets in the medium. As such, it is seen that the lags may belong to the intrinsic or to the structural properties of the materials. Combining with the energy equation, we eliminate q and obtain the dual-phase-lagging equation as

$$\frac{\rho C}{k}u_t(\vec{r},t)+\frac{\rho C\tau_q}{k}u_{tt}(\vec{r},t)=\nabla^2 u(\vec{r},t)+\tau_T\frac{\partial(\nabla u(\vec{r},t))}{\partial t}+\frac{1}{k}(f(\vec{r},t)+\tau_q f_t(\vec{r},t)). \tag{2.16}$$

The dual-phase-lagging equation as a new modified constitutive equation replacing the Fourier law to simulate the heat transfer in some special cases such as

nanoscales, ultrafast laser-pulsed processes, living tissues, and carbon nanotubes has been widely used. A recent review article [1], published by Ghazanfarian and his collaborators in 2015, indicates that more than three-hundred articles on the thermal lagging behavior in heat and mass transfer have been published and all or part of which are involved with the phase-lagging models.

2.2 Interface Problems

There are lots of research papers in the literature that address interface problems. In this dissertation, we only discuss a few commonly used finite difference methods for interface problems.

Peskin proposed an immersed boundary method (IBM) to simulate the blood flows in heart, where the interface problem comes from the singular source at the time-varying boundary [11-13]. One of the important ideas in the IBM is the use of a discrete delta function to distribute a singular source to nearby grid points. For example, the Peskin original discrete cosine delta function is

$$\delta_\varepsilon(x) = \begin{cases} \frac{1}{4\varepsilon}\left(1+\cos\left(\frac{\pi x}{2\varepsilon}\right)\right), & |x| < 2\varepsilon, \\ 0, & |x| \geq 2\varepsilon. \end{cases} \tag{2.17}$$

Consider the following interface problem

$$u_{xx} = \delta(x - x_I), \quad x = x_I \in (0,1); \quad u(0) = u(1) = 0, \tag{2.18}$$

where x_I is the location of the interface. It can be seen that the finite difference method

$$\left(u_{j-1} - 2u_j + u_{j+1}\right)/h^2 = \delta_h(x - x_I) \tag{2.19}$$

with δ_h given by Eq. (2.17) is only first-order accurate. However, due to the simplicity, efficiency and robustness of the IBM, it has been applied in many engineering computations [56-58]. In addition, higher-order version of the IBM has been gradually proposed by Peskin and his coworkers [9, 10]. In particular, Tornberg and Engquist developed a globally fourth-order scheme for problems with singular sources at the interface by using some sophisticated discrete delta functions with a narrow support [59].

In 1994, LeVeque and Li proposed the immersed interface method (IIM) for solving elliptic equations with interface problems [18]. The idea of IIM is to use Taylor series expansion on the grid points near the interface, and then by matching the interface conditions, to determine the weights of these points. The method in determining the finite difference coefficients is to minimize the local truncation error. By defining polynomials up to the second order at each side of the interface, the IIM is a second-order accurate method, although its local truncation error at points around the interface is only first-order. The original IIM has been improved in many ways, such as the discrete maximum principle [19], a multi-grid method [15] and a fast algorithm if the problem comes with piecewise constant coefficient [21]. The coupling of the IIM with the level set approach to handle moving interfaces has also been proposed [16, 17]. The IIM has been successfully applied to many important problems [10, 60-62]. More details on reviewing the IIM can be found in the book written by Li and Ito [63].

In 1999, Osher and his coworkers proposed the ghost fluid method (GFM) [26]. In GFM, the interface jump conditions are captured implicitly by extending values

across the interface into a ghost fluid based on the level set method. Although the GFM is typically first-order accurate, it is widely used due to its simplicity when dealing with complex interface.

In 2006, the matched interface and boundary (MIB) method was originally developed for simulating electromagnetic wave scatting and propagation [31, 64]. For elliptic interface problems, the MIB can be treated as a generalization of the IBM, the IIM and the GFM. In the MIB technique, the solution on each side of the interface is smoothly extended to the other side of the interface by using fictitious values. To get those fictitious values, first, the extrapolation of fictitious values are numerically realized by enforcing given boundary conditions. Secondly, the number of fictitious values is determined by the order of the central finite difference scheme. However, as pointed out in [33], the MIB can be fitted in an interpolation formulation without relating to any fictitious node value. The purpose of using fictitious values is to make the MIB presentation clear.

In 2010, Pan and his collaborators developed an interpolation matched interface and boundary (IMIB) method with second-order accuracy based on the original MIB method [65]. Since the IMIB is the generalization of MIB, GFM and IIM, and one of the most important idea of this dissertation comes from the IMIB method, we give more details on this method by using a one-dimensional elliptic interface problem as

$$\frac{d^2\left(\beta\left(x\right)u\left(x\right)\right)}{dx^2} = f\left(x\right),\ 0 < x < 1, \tag{2.20}$$

with a Dirichlet boundary condition:

$$u(0) = 0,\ u(1) = 0, \tag{2.21}$$

and conditions across the interface I:

$$u_{I^+} - u_{I^-} = 0, \tag{2.22}$$

$$\beta_{I^+} (u_x)_{I^+} - \beta_{I^-} (u_x)_{I^-} = 0, \tag{2.23}$$

where the function $\beta(x)$ might be discontinuous at the interface, the superscript $-$ or $+$ denotes the limiting value of a function at different sides of the interface.

First, we design an equal-distant mesh and denote grid size to be $h = 1/M$, where M is a positive integer, as shown in Figure 2.1. Grid points in the mesh are denoted as $x_j = jh$, $0 \le j \le M$, where the interface is located at grid point $x_I = mh + \theta h$. F_m, F_{m+1} are two fictitious values at locations x_m and x_{m+1}, respectively.

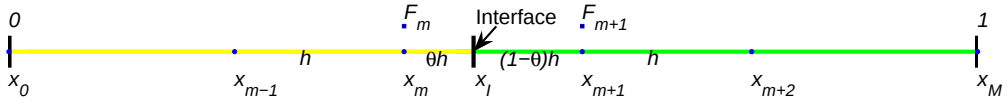

Figure 2.1: One-dimensional mesh for IMIB.

We now give the derivations on the IMIB method. Using Taylor series expansion, we can obtain the approximations of the values u and its first-order derivative u_x on the left-hand and right-hand side of the interface as

$$u_{I^-} = \left(-\frac{\theta}{2} + \frac{\theta^2}{2}\right) u_{m-1} + \left(1 - \theta^2\right) u_m + \left(\frac{\theta}{2} + \frac{\theta^2}{2}\right) F_{m+1}, \tag{2.24}$$

$$u_{I^+} = \left(1 - \frac{3\theta}{2} + \frac{\theta^2}{2}\right) F_m + \left(2\theta - \theta^2\right) u_{m+1} + \left(-\frac{\theta}{2} + \frac{\theta^2}{2}\right) u_{m+2}, \tag{2.25}$$

and

$$(u_x)_{I^-} = \left(-\frac{1}{2}+\theta\right)u_{m-1} - 2\theta u_m + \left(\frac{1}{2}+\theta\right)F_{m+1}, \tag{2.26}$$

$$(u_x)_{I^+} = \left(-\frac{3}{2}+\theta\right)F_m + (2-2\theta)\,u_{m+1} + \left(-\frac{1}{2}+\theta\right)u_{m+2}, \tag{2.27}$$

respectively. Then, we can discretize u_{xx} at grid points x_m and x_{m+1}, as

$$\frac{\left(\frac{F_{m+1}-u_m}{h} - \frac{F_m-u_{m-1}}{h}\right)}{h} = f_m, \tag{2.28}$$

$$\frac{\left(\frac{u_{m+2}-u_{m+1}}{h} - \frac{u_{m+1}-F_m}{h}\right)}{h} = f_{m+1}. \tag{2.29}$$

Combining Eqs. (2.22)-(2.29) together, we obtain a system of 8 equations with 10 unknowns $\{u_{I^-}, u_{I^+}, (u_x)_{I^-}, (u_x)_{I^+}, F_m, F_{m+1}, u_{m-1}, u_m, u_{m+1}, u_{m+2}\}$. After deleting u_{I^-}, u_{I^+}, $(u_x)_{I^-}$, $(u_x)_{I^+}$, F_m and F_{m+1}, we obtain the following scheme

$$\begin{aligned}
&\left(2-\theta^2\right)u_{m-1} - \left(5-2\theta-\theta^2\right)u_m + (2-\theta)^2\,u_{m+1} - (1-\theta)^2\,u_{m+2} \\
=&\,(3-2\theta)\,a + \left(2-3\theta+\theta^2\right)bh + \left(1+2\theta-2\theta^2\right)h^2 f_m, \qquad (2.30)\\
&-\theta^2 u_{m-1} - \left(1+\theta^2\right)u_m - \left(2+4\theta-\theta^2\right)u_{m+1} + (1+2\theta-\theta)^2\,u_{m+2} \\
=&-(1+2\theta)\,a + \left(\theta+\theta^2\right)bh + \left(1+2\theta-2\theta^2\right)h^2 f_{m+1}. \qquad (2.31)
\end{aligned}$$

Eq. (2.30) and Eq. (2.31) can be rewritten as

$$\frac{u_{m+1}-2u_m+u_{m-1}}{h^2} = \frac{1+2\theta-2\theta^2}{2}f_m + \frac{1-2\theta+\theta^2}{2}f_{m+1} + \frac{a}{h^2} + \frac{b\,(1-\theta)}{h}, \tag{2.32}$$

$$\frac{u_{m+2}-2u_{m+1}+u_m}{h^2} = \frac{\theta^2}{2}f_m + \frac{2-\theta^2}{2}f_{m+1} - \frac{a}{h^2} + \frac{b\theta}{h}. \tag{2.33}$$

Given that $f_{m+1} = f_m + (f_{I^+} - f_{I^-}) + O(h)$, the above schemes can be changed to

$$\frac{u_{m+1}-2u_m+u_{m-1}}{h^2} = f_m + \frac{a}{h^2} + \frac{b\,(1-\theta)}{h} + \frac{1-2\theta+\theta^2}{2}\,(f_{I^+} - f_{I^-}), \tag{2.34}$$

$$\frac{u_{m+2}-2u_{m+1}+u_m}{h^2} = f_{m+1} - \frac{a}{h^2} + \frac{b\theta}{h} - \frac{\theta^2}{2}\,(f_{I^+} - f_{I^-}). \tag{2.35}$$

As pointed in [65], Eqs. (2.30)-(2.31) are the same as the second-order MIB [32], Eqs. (2.32)-(2.33) are equivalent to the IIM [18] and interpolation formulation of MIB [33]. Also, if $f_{I^+} - f_{I^-} = 0$, Eqs. (2.34)-(2.35) are just the same as the GFM [27].

All the above methods have been extended to treat time-dependent equations with interface problems. Another good choice in dealing with the time-dependent interface problems is the summation-by-parts operators with simultaneous approximation terms [50, 66]. The method can facilitate the derivation of higher-order spatial discretization that are provably time stable based on the energy method. For example, the interface procedures for the heat equation have been considered by Giles [67], by Roe *et al.* [68] and by Henshaw and Chand [69].

In 2014, Sun and Dai provided a fourth-order accuracy in space scheme for solving heat conduction in a double-layered film with the Neumann boundary condition [70]. Dai *et. al* also developed a fourth-order compact finite-difference scheme for solving the 1-D Pennes' bioheat transfer equation in a triple-layered skin structure [71]. For heat conduction in nanoscale, Dai and his collaborators proposed several schemes based on different mathematical models [72-76], but all of them are only second-order accuracy in spatial dimension.

Apart from the methods mentioned above, many other approaches have been proposed in the literature, such as the finite element method [35-44], discontinuous Galerkin approach [77], integral equation approach [78], etc. We will not give more details on these methods as our focus is on the finite difference method.

2.3 Compact Finite Difference Method

From numerical analysis, we know that the derivative $g_x(x)$ at x_i can be approximated using

$$\begin{aligned} g_x(x_i) &\simeq \frac{g(x_i) - g(x_{i-1})}{h}, \text{ with truncation error } O(h), \\ g_x(x_i) &\simeq \frac{g(x_{i+1}) - g(x_{i-1})}{2h}, \text{ with truncation error } O\left(h^2\right), \end{aligned}$$

and in general,

$$g_x(x_i) \simeq \sum_{j=-n}^{n} \alpha_j g(x_{i+j}), \text{ with truncation error } O(h^n).$$

Here, $x_{i+1} = x_i + h$, $x_{i-1} = x_i - h$, and $x_{i+j} = x_i + jh$. This implies that to obtain a truncation error of $O(h^n)$, one may need to use $2n+1$ values of $g(x)$ to approximate $g_x(x_i)$. This becomes inconvenient when solving partial differential equations near the boundary. To overcome this trouble, in 1992, Lele proposed a new method called the compact finite difference method [51]. The idea is to use as few grid points as possible to obtain as higher order of truncation error as possible. For example, if one wants to obtain the approximation of $g_x(x_i)$, the relationship between $\{g_x(x_i)\}$ and $\{g(x_i)\}$ can be written in an implicit way as

$$\begin{aligned} &\beta(g_x)_{i-2} + \alpha(g_x)_{i-1} + (g_x)_i + \alpha(g_x)_{i+1} + \beta(g_x)_{i+2} \\ =&c\frac{g_{i+3} - g_{i-3}}{6h} + b\frac{g_{i+2} - g_{i-2}}{4h} + a\frac{g_{i+1} - g_{i-1}}{2h}, \end{aligned} \tag{2.36}$$

where α, β, a, b, c are constants to be determined, and $(g_x)_i$, g_i representing $g_x(x_i)$, $g(x_i)$ and so on. Using the Taylor series expansion at x_i on both sides, and matching them, one may obtain

$$a + b + c = 1 + 2\alpha + 2\beta, \text{ with truncation error } O\left(h^2\right),$$

$$
\begin{aligned}
a+2^2b+3^2c &= 2\cdot\frac{3!}{2!}\left(\alpha+2^2\beta\right),\ \text{with truncation error } O\left(h^4\right),\\
a+2^4b+3^4c &= 2\cdot\frac{5!}{4!}\left(\alpha+2^4\beta\right),\ \text{with truncation error } O\left(h^6\right),\\
a+2^6b+3^6c &= 2\cdot\frac{7!}{6!}\left(\alpha+2^6\beta\right),\ \text{with truncation error } O\left(h^8\right),\\
a+2^8b+3^8c &= 2\cdot\frac{9!}{8!}\left(\alpha+2^8\beta\right),\ \text{with truncation error } O\left(h^{10}\right).
\end{aligned}
$$

Solving the above system, we obtain the following several cases as

(1) When $\beta=0$, $c=0$, $a=\frac{2}{3}(\alpha+2)$, $b=\frac{1}{3}(4\alpha-1)$, Eq. (2.36) gives a fourth-order approximation for $g_x(x_i)$. In particular, when $\alpha=\frac{1}{4}$, $b=0$, Eq. (2.39) becomes a three-point scheme. This is the most useful compact scheme since only three grid points are involved.

(2) When $\beta=0$, $c=0$, $\alpha=\frac{1}{3}$, $a=\frac{14}{9}$, $b=\frac{1}{9}$, Eq. (2.36) gives a sixth-order approximation for $g_x(x_i)$.

(3) When $\beta=\frac{1}{36}$, $\alpha=\frac{4}{9}$, $c=0$, $b=\frac{25}{54}$, $a=\frac{40}{27}$, Eq. (2.36) gives a eighth-order approximation for $g_x(x_i)$.

(4) When $\beta=\frac{1}{20}$, $c=\frac{1}{100}$, $b=\frac{101}{150}$, $a=\frac{17}{12}$, Eq. (2.36) gives a tenth-order approximation for $g_x(x_i)$.

At the boundary, one may use a similar way and write the compact scheme as, for example,

$$
(g_x)_1+\alpha(g_x)_2=\frac{1}{h}\left(ag_1+bg_2+cg_3+dg_4\right). \tag{2.37}
$$

Thus, when $a=\frac{-11+2\alpha}{6}$, $b=\frac{6-\alpha}{2}$, $c=\frac{2\alpha-3}{2}$, $d=\frac{2-\alpha}{6}$, Eq. (2.37) gives a third-order truncation error of $O(h^3)$. In particular, when $\alpha=3$, $a=-\frac{17}{6}$, $b=\frac{3}{2}$, $c=\frac{3}{2}$, $d=-\frac{1}{6}$, Eq. (2.37) gives a fourth-order truncation error of $O(h^4)$.

Similarly, we may write the relationship between $\{g_{xx}(x_i)\}$ and $\{g(x_i)\}$ in an implicit way to obtain the approximation of $g_{xx}(x_i)$ as

$$\begin{aligned}&\beta(g_{xx})_{i-2}+\alpha(g_{xx})_{i-1}+(g_{xx})_i+\alpha(g_{xx})_{i+1}+\beta(g_{xx})_{i+2}\\ =&c\frac{g_{i+3}-2g_i+g_{i-3}}{9h^2}+b\frac{g_{i+2}-2g_i+g_{i-2}}{4h^2}+a\frac{g_{i+1}-2g_i+g_{i-1}}{h^2}.\end{aligned}\tag{2.38}$$

Again, using the Taylor series expansion at x_i on both sides, and matching them, one may obtain

$$\begin{aligned}a+b+c &= 1+2\alpha+2\beta, \text{ with truncation error } O\left(h^2\right),\\ a+2^2b+3^2c &= \frac{4!}{2!}\left(\alpha+2^2\beta\right), \text{ with truncation error } O\left(h^4\right),\\ a+2^4b+3^4c &= \frac{6!}{4!}\left(\alpha+2^4\beta\right), \text{ with truncation error } O\left(h^6\right),\\ a+2^6b+3^6c &= \frac{8!}{6!}\left(\alpha+2^6\beta\right), \text{ with truncation error } O\left(h^8\right),\\ a+2^8b+3^8c &= \frac{10!}{8!}\left(\alpha+2^8\beta\right), \text{ with truncation error } O\left(h^{10}\right).\end{aligned}$$

Solving the above system, we obtain the following several cases.

(1) When $\beta=0$, $c=0$, $a=\frac{4}{3}(1-\alpha)$, $b=\frac{1}{3}(-1+10\alpha)$, Eq. (2.38) gives a fourth-order truncation error of $O(h^4)$. In particular, choosing $\alpha=\frac{1}{10}$, $b=0$, $a=\frac{12}{10}$, Eq. (2.38) reduces to the well-known Padé scheme. This is the most useful compact scheme since only three grid points are involved. This dissertation research will apply this scheme to the interior points.

(2) When $\beta=0$, $c=0$, $\alpha=\frac{2}{11}$, $a=\frac{12}{11}$, $b=\frac{3}{11}$, Eq. (2.38) gives a sixth-order truncation error of $O(h^6)$.

(3) When $\beta\neq 0$, $c\neq 0$, $a=\frac{6-9\alpha-12\beta}{4}$, $b=\frac{2454\alpha-294}{535}$, $c=\frac{696-1191\alpha}{428}$, Eq. (2.38) gives another sixth-order truncation error of $O(h^6)$.

(4) When $\alpha = \frac{344}{1179}$, $\beta = \frac{38\alpha - 9}{214}$, $c = 0$, $b = \frac{1038}{899}$, $a = \frac{1038}{899}$, Eq. (2.38) gives the eighth-order truncation error of $O\left(h^8\right)$.

(5) When $\beta = \frac{43}{1798}$, $\alpha = \frac{334}{899}$, $c = \frac{79}{1798}$, $b = \frac{1038}{1798}$, $a = \frac{1065}{1798}$, Eq. (2.38) gives the tenth-order truncation error of $O\left(h^{10}\right)$.

For the boundary, one may use

$$\left(g_{xx}\right)_1 + \alpha \left(g_{xx}\right)_2 = \frac{1}{h^2}\left(ag_1 + bg_2 + cg_3 + dg_4\right), \tag{2.39}$$

and determine those constants using a similar way. For example, when $a = \alpha + 2$, $b = (-2\alpha + 5)$, $c = \alpha + 4$, $d = -1$, Eq. (2.39) gives a second-order truncation error of $O(h^2)$; when $\alpha = 11$, $a = 13$, $b = -27$, $c = 15$, $d = -14$, Eq. (2.39) gives a third-order truncation error of $O(h^3)$.

The compact finite difference method has been widely used in many areas based on different differential equations. For example, fourth-order accurate (in space) schemes have been proposed for the traditional heat conduction equation with Neumann boundary [79-82]. Although the authors used different techniques to deal with the boundary, they all used the fourth-order Padé scheme for the interior points. For convection-diffusion equations, fourth-order accurate schemes have also been developed [83-87]. Moreover, compact finite difference schemes of sixth-order accuracy for solving the parabolic type of partial differential equations have been proposed and applied to areas of heat conduction, geodynamic simulation and so on [88-90]. For equations related to quantum mechanics, complex values and nonlinear terms are frequently appeared in the governing equations, such as the well-known Schrödinger equation, the complex Ginzburg-Landau equation, etc. Compact finite

difference schemes have been developed for solving this type of equations [91, 92]. Furthermore, fourth-order accurate compact finite difference schemes have been applied to equations with third order mixed derivatives in space and time, such as the dual-phase-lagging model for micro/nano heat transfer [93, 94].

In summary, we have reviewed several heat conduction equations which will be used in our dissertation research, some existing interfacial methods and compact finite difference method. As mentioned in Chapter 1, the existing finite difference methods using three-grid points across the interface typically provide only a second-order truncation error, which reduces the accuracy of the overall numerical solution, even though the higher-order compact finite difference method is employed at other points. Thus, obtaining a higher-order accurate numerical scheme using three-grid points across the interface so that the overall numerical scheme is stable and convergent with higher-order accuracy is the objective of this dissertation.

CHAPTER 3

MATHEMATICAL MODELS

In this chapter, we consider heat transfer in a double-layered solid structure as shown in Figure 3.1. Three mathematical models which are for steady-state, unsteady-state and nanoscale heat conduction are discussed, respectively. For simplicity, only one-dimensional cases are studied.

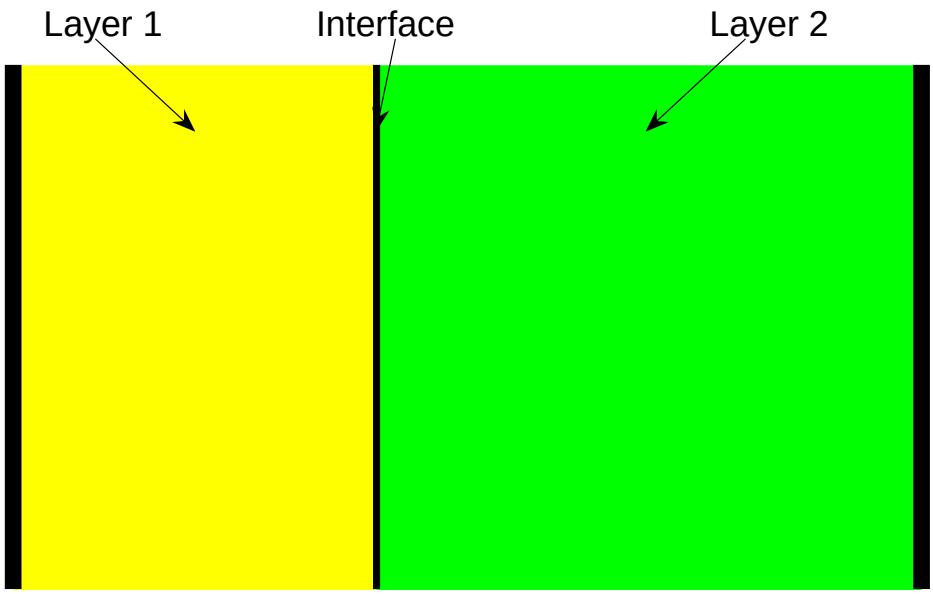

Figure 3.1: Double-layered solid structure.

3.1 Steady State Heat Conduction Model

Under the steady-state, the temperature in the double-layered structure is independent on time. As such, the heat conduction in the double-layered structure can be expressed as two simple elliptic equations with interfacial condition and boundary condition as follows:

$$k_1 u_{xx}(x) = f_1(x), \quad 0 < x < l, \tag{3.1}$$

$$k_2 u_{xx}(x) = f_2(x), \quad l < x < L, \tag{3.2}$$

interfacial condition at $x = l$:

$$u_{I^+} - u_{I^-} = a, \tag{3.3}$$

$$k_2 (u_x)_{I^+} - k_1 (u_x)_{I^-} = b, \tag{3.4}$$

and boundary condition of either Dirichlet boundary condition:

$$u(0) = \phi_1, \ u(L) = \phi_2, \tag{3.5a}$$

or Neumann boundary condition:

$$u_x(0) = \phi_1, \ u_x(L) = \phi_2, \tag{3.5b}$$

or Robin boundary condition:

$$-\alpha_1 u_x(0) + \gamma_1 u(0) = \phi_1, \quad \alpha_2 u_x(L) + \gamma_2 u(L) = \phi_2. \tag{3.5c}$$

Here, $u(x)$ is the temperature of the structure, $f_1(x)$, $f_2(x)$ are smooth functions (They are the opposite numbers of the original source terms to avoid minus signs below), a, b, ϕ_1, ϕ_2 are real-value constants, k_1, k_2, α_1, α_2, γ_1, γ_2 are positive constants

related to thermal properties of the structure, and u_{I^+}, u_{I^-}, $(u_x)_{I^+}$, $(u_x)_{I^-}$ denote $u(l+0)$, $u(l-0)$, $u_x(l+0)$, $u_x(l-0)$, respectively.

We call a problem is well-posed if the problem has a unique solution that depends continuously on the data used to define the problem. It can be seen that the above model with the Robin boundary is well-posed. In fact, multiplying the heat conduction equations (3.1) and (3.2) by $u(x)$ and then integrating over $[0, l]$ and $[l, L]$, respectively, we obtain

$$\int_0^l k_1 u_{xx} u dx + \int_l^L k_2 u_{xx} u dx = \int_0^l f_1 u dx + \int_l^L f_2 u dx. \tag{3.6}$$

Using the integration by parts, we further obtain

$$k_1 \int_0^l (u_x)^2 dx + k_2 \int_l^L (u_x)^2 dx - k_1 u_x u|_0^l - k_2 u_x u|_l^L = \int_0^l f_1 u dx + \int_l^L f_2 u dx. \tag{3.7}$$

From the homogeneous interfacial condition, $a = b = 0$, and homogeneous Robin boundary condition, $\phi_1 = \phi_2 = 0$, the left-hand-side (LHS) of Eq. (3.7) can be changed to

$$\begin{aligned} LHS =& k_1 \int_0^l (u_x)^2 dx + k_2 \int_l^L (u_x)^2 dx - k_1 (u_x)_{I^-} u_{I^-} + k_1 u_x(0) u(0) \\ & - k_2 u_x(L) u(L) + k_2 (u_x)_{I^+} u_{I^+} \\ =& k_1 \int_0^l (u_x)^2 dx + k_2 \int_l^L (u_x)^2 dx + k_1 \frac{\gamma_1}{\alpha_1} u^2(0) + k_2 \frac{\gamma_2}{\alpha_2} u^2(L). \end{aligned} \tag{3.8}$$

On the other hand, the right-hand-side (RHS) of Eq. (3.7) can be evaluated by Young's inequality, $ab \le \frac{1}{4\varepsilon} a^2 + \varepsilon b^2$, $\varepsilon > 0$, as

$$\begin{aligned} RHS =& \int_0^l f_1 u dx + \int_l^L f_2 u dx \\ \le& \frac{1}{4\varepsilon_1} \int_0^l (f_1)^2 dx + \varepsilon_1 \int_0^l u^2 dx + \frac{1}{4\varepsilon_2} \int_l^L (f_2)^2 dx + \varepsilon_2 \int_l^L u^2 dx, \end{aligned} \tag{3.9}$$

where ε_1, ε_2 are positive constants. Note that by Cauchy-Schwarz's inequality, $\left(\int_a^b f(x)\,g(x)\,dx\right)^2 \le \int_a^b f^2(x)\,dx \int_a^b g^2(x)\,dx$, one may obtain

$$\begin{aligned}
[u(x)-u(0)]^2 &= \left(\int_0^x u_x dx\right)^2 \\
&\le \int_0^l 1^2 dx \int_0^l (u_x)^2\,dx \\
&\le l\int_0^l (u_x)^2\,dx, \quad 0<x<l, \qquad (3.10)\\
[u(L)-u(x)]^2 &= \left(\int_x^L u_x dx\right)^2 \\
&\le \int_l^L 1^2 dx \int_l^L (u_x)^2\,dx \\
&\le (L-l)\int_l^L (u_x)^2\,dx, \quad l<x<L. \qquad (3.11)
\end{aligned}$$

Then, by $(a+b)^2 \le 2a^2+2b^2$, we have

$$\begin{aligned}
u^2(x) &= [u(x)-u(0)+u(0)]^2 \\
&\le 2[u(x)-u(0)]^2 + 2u^2(0) \\
&\le 2l\int_0^l (u_x)^2\,dx + 2u^2(0), \quad 0<x<l, \qquad (3.12)\\
u^2(x) &= [u(L)-u(x)-u(L)]^2 \\
&\le 2[u(L)-u(x)]^2 + 2u^2(L) \\
&\le 2(L-l)\int_l^L (u_x)^2\,dx + 2u^2(L), \quad l<x<L. \qquad (3.13)
\end{aligned}$$

Integrating both sides of Eq. (3.12) and Eq. (3.13) over $(0,l)$ and (l,L), respectively, we further obtain

$$\begin{aligned}
\int_0^l u^2(x)\,dx &\le 2l^2\int_0^l (u_x)^2\,dx + 2lu^2(0), \quad 0<x<l, \qquad (3.14)\\
\int_l^L u^2(x)\,dx &\le 2(L-l)^2\int_l^L (u_x)^2\,dx + 2(L-l)u^2(L), \quad l<x<L. \qquad (3.15)
\end{aligned}$$

Thus, Eq. (3.7) becomes

$$\begin{aligned}
&k_1\int_0^l (u_x)^2\,dx + k_2\int_l^L (u_x)^2\,dx + k_1\frac{\gamma_1}{\alpha_1}u^2(0) + k_2\frac{\gamma_2}{\alpha_2}u^2(L)\\
\leq&\frac{1}{4\varepsilon_1}\int_0^l (f_1)^2\,dx + \varepsilon_1\int_0^l u^2dx + \frac{1}{4\varepsilon_2}\int_l^L (f_2)^2\,dx + \varepsilon_2\int_l^L u^2dx\\
\leq&\frac{1}{4\varepsilon_1}\int_0^l (f_1)^2\,dx + \varepsilon_1\left[2l^2\int_0^l (u_x)^2\,dx + 2lu^2(0)\right]\\
&+\frac{1}{4\varepsilon_2}\int_l^L (f_2)^2\,dx + \varepsilon_2\left[2(L-l)^2\int_l^L (u_x)^2\,dx + 2(L-l)u^2(L)\right],
\end{aligned}\tag{3.16}$$

i.e.

$$\begin{aligned}
&\left(k_1 - 2\varepsilon_1 l^2\right)\int_0^l (u_x)^2\,dx + \left(k_2 - 2\varepsilon_2(L-l)^2\right)\int_l^L (u_x)^2\,dx\\
&+\left(k_1\frac{\gamma_1}{\alpha_1} - 2\varepsilon_1 l\right)u^2(0) + \left(k_2\frac{\gamma_2}{\alpha_2} - 2\varepsilon_2(L-l)\right)u^2(L)\\
\leq&\frac{1}{4\varepsilon_1}\int_0^l (f_1)^2\,dx + \frac{1}{4\varepsilon_2}\int_l^L (f_2)^2\,dx.
\end{aligned}\tag{3.17}$$

Choosing $\varepsilon_1 = \min\left\{\frac{1}{4}\frac{k_1}{l^2}, \frac{1}{4}\frac{k_1\gamma_1}{\alpha_1 l}\right\}$, $\varepsilon_2 = \min\left\{\frac{1}{4}\frac{k_2}{(L-l)^2}, \frac{1}{4}\frac{k_2\gamma_2}{\alpha_2(L-l)^2}\right\}$, we obtain

$$\begin{aligned}
&\frac{k_1}{2}\int_0^l (u_x)^2\,dx + \frac{k_2}{2}\int_l^L (u_x)^2\,dx + \frac{k_1\gamma_1}{2\alpha_1}u^2(0) + \frac{k_2\gamma_2}{2\alpha_2}u^2(L)\\
\leq&\frac{1}{4\varepsilon_1}\int_0^l (f_1)^2\,dx + \frac{1}{4\varepsilon_2}\int_l^L (f_2)^2\,dx.
\end{aligned}\tag{3.18}$$

Thus, if there are two solutions $u_1(x)$ and $u_2(x)$ satisfying Eqs. (3.1-3.4) and Eq. (3.5c), we let $u(x) = u_1(x) - u_2(x)$. Then $u(x)$ satisfies Eq. (3.18) with $f_1 = f_2 \equiv 0$, implying that $u_x \equiv 0$, implying the difference between $u_1(x)$ and $u_2(x)$ is a constant, and $u(0) = u(L) \equiv 0$, indicating the constant is 0, and hence, $u_1(x) = u_2(x)$, which means this solution is unique. The solution is continuously dependent on the boundary condition and source term based on Eq. (3.18). Thus, we finish the proof of the well-posedness of the steady-state heat conduction model with Robin

boundary condition. It should be pointed out that Eq. (3.18) is often called the energy estimation.

Similarly, under the Dirichlet boundary condition, an energy estimation can be obtained as

$$\begin{aligned} &\frac{k_1}{2}\int_0^l (u_x)^2\,dx + \frac{k_2}{2}\int_l^L (u_x)^2\,dx \\ \leq &\frac{l^2}{k_1}\int_0^l (f_1)^2\,dx + \frac{(L-l)^2}{k_2}\int_l^L (f_2)^2\,dx. \end{aligned} \tag{3.19}$$

From Eq. (3.19), we can prove that the model is well-posed under the Dirichlet boundary condition.

For the Neumann boundary case, we first assume $u_1(x)$ and $u_2(x)$ to be two different solutions satisfying the same initial and boundary conditions, same interfacial conditions and same source terms. Letting $u(x) = u_1(x) - u_2(x)$, then $u(x)$ satisfies Eqs. (3.1)-(3.4) and Eq. (3.5b) in homogeneous case. Multiplying homogenous Eqs. (3.1) and (3.2) by $u(x)$ and then integrating over $[0, l]$ and $[l, L]$, respectively, we obtain

$$\int_0^l k_1 u_{xx} u dx + \int_l^L k_2 u_{xx} u dx = 0. \tag{3.20}$$

Using the integration by parts at the homogenous boundary and interfacial condition, Eq. (3.20) becomes

$$\begin{aligned} &k_1\int_0^l (u_x)^2\,dx + k_2\int_l^L (u_x)^2\,dx - k_1 u_x u|_0^l - k_2 u_x u|_l^L \\ =&k_1\int_0^l (u_x)^2\,dx + k_2\int_l^L (u_x)^2\,dx \\ =&0. \end{aligned} \tag{3.21}$$

Thus, $u_x = 0$ on $[0, L]$, and hence $u(x)$ is a constant. This indicates that the solution is unique within a constant difference. To show the solution depending on the source term and boundary condition, we multiply Eqs. (3.1)-(3.2) by u_{xx}, and integrate over $[0, l]$ and $[l, L]$, respectively. This gives

$$\begin{aligned}
&k_1 \int_0^l (u_{xx})^2 \, dx + k_2 \int_l^L (u_{xx})^2 \, dx \\
=&\int_0^l f_1 u_{xx} dx + \int_l^L f_2 u_{xx} dx \\
\leq&\frac{1}{2k_1} \int_0^l (f_1)^2 \, dx + \frac{1}{2k_2} \int_l^L (f_2)^2 \, dx + \frac{k_1}{2} \int_0^l (u_{xx})^2 \, dx + \frac{k_2}{2} \int_l^L (u_{xx})^2 \, dx, \qquad (3.22)
\end{aligned}$$

implying that

$$k_1 \int_0^l (u_{xx})^2 \, dx + k_2 \int_l^L (u_{xx})^2 \, dx \leq \frac{1}{k_1} \int_0^l (f_1)^2 \, dx + \frac{1}{k_2} \int_l^L (f_2)^2 \, dx. \qquad (3.23)$$

Using a similar argument as in Eqs. (3.14)-(3.15), we further obtain

$$\begin{aligned}
&k_1 \int_0^l (u_x)^2 \, dx + k_2 \int_l^L (u_x)^2 \, dx \\
\leq&2k_1 l^2 \int_0^l (u_{xx})^2 \, dx + 2k_2 (L-l)^2 \int_l^L (u_{xx})^2 \, dx + 2k_1 l u_x^2(0) + 2k_2 (L-l) u_x^2(L) \\
\leq&c \left[k_1 \int_0^l (u_{xx})^2 \, dx + k_2 \int_l^L (u_{xx})^2 \, dx + k_1 u_x^2(0) + k_2 u_x^2(L) \right] \\
\leq&c \left[\frac{1}{k_1} \int_0^l (f_1)^2 \, dx + \frac{1}{k_2} \int_l^L (f_2)^2 \, dx + k_1 u_x^2(0) + k_2 u_x^2(L) \right], \qquad (3.24)
\end{aligned}$$

where $c = \max\left\{2l^2,\ 2(L-l)^2,\ 2l,\ 2(L-l)\right\}$. Thus, the following theorem can be obtained.

Theorem 3.1. *Assume that $f(x)$ is continuously differentiable. Then the steady-state heat conduction model, Eqs. (3.1)-(3.5), is well-posed.*

3.2 Unsteady State Heat Conduction Model

For the unsteady-state case, the temperature $u(x,t)$ is dependent on time. As such, the heat conduction in the double-layered structure can be expressed as two simple parabolic equations with initial condition, interfacial condition and boundary condition as follows:

$$\rho_1 C_1 u_t(x,t) = k_1 u_{xx}(x,t) + f_1(x,t), \quad 0 < x < l, \ 0 < t \leq T, \tag{3.25}$$

$$\rho_2 C_2 u_t(x,t) = k_2 u_{xx}(x,t) + f_2(x,t), \quad l < x < L, \ 0 < t \leq T, \tag{3.26}$$

initial condition:

$$u(x,0) = \psi_1(x), \quad 0 \leq x \leq l, \quad u(x,0) = \psi_2(x), \ l \leq x \leq L, \tag{3.27}$$

interfacial condition at $x = l$:

$$u_{I^+}(t) - u_{I^-}(t) = a(t), \ 0 \leq t \leq T, \tag{3.28}$$

$$k_2 (u_x)_{I^+}(t) - k_1 (u_x)_{I^-}(t) = b(t), \quad 0 \leq t \leq T, \tag{3.29}$$

and boundary condition of either Dirichlet boundary condition:

$$u(0,t) = \phi_1(t), \quad u(L,t) = \phi_2(t), \quad 0 \leq t \leq T, \tag{3.30a}$$

Neumann boundary condition:

$$u_x(0,t) = \phi_1(t), \quad u_x(L,t) = \phi_2(t), \ 0 \leq t \leq T, \tag{3.30b}$$

or Robin boundary condition:

$$-\alpha_1 u_x(0,t) + \gamma_1 u(0,t) = \phi_1(t), \quad \alpha_2 u_x(L,t) + \gamma_2 u(L,t) = \phi_2(t), \quad 0 \leq t \leq T. \tag{3.30c}$$

Here, k_1, k_2 are conductivities, ρ_1, ρ_2 are densities, C_1, C_2 are specific heats, $f_1(x,t)$, $f_2(x,t)$ are source terms, $\psi_1(x)$, $\psi_2(x)$, $a(t)$, $b(t)$, $\phi_1(t)$, $\phi_2(t)$ are given functions,

$\alpha_1, \alpha_2, \gamma_1, \gamma_2$ are positive constants, and $u_{I^+}(t)$, $u_{I^-}(t)$, $(u_x)_{I^+}(t)$, $(u_x)_{I^-}(t)$ denote $u(l+0,t)$, $u(l-0,t)$, $u_x(l+0,t)$, $u_x(l-0,t)$, respectively.

Similar to the steady-state case, we can obtain the following theorem.

Theorem 3.2 *Assume that* $f_1(x,t)$, $f_2(x,t)$, $\psi_1(x)$, $\psi_2(x)$, $a(t)$, $b(t)$, $\phi_1(t)$, $\phi_2(t)$ *are continuously differentiable. Then the above heat conduction model is well-posed.*

Proof. Assume $u_1(x,t)$, $u_2(x,t)$ satisfy Eqs. (3.25)-(3.26) with the same interfacial and boundary conditions, but different source terms, $\hat{f}_1(x,t)$, $\hat{f}_2(x,t)$ for $u_1(x,t)$, $\tilde{f}_1(x,t)$, $\tilde{f}_2(x,t)$ for $u_2(x,t)$, and different initial conditions, $\hat{\psi}_1(x)$, $\hat{\psi}_2(x)$ for $u_1(x,t)$, $\tilde{\psi}_1(x)$, $\tilde{\psi}_2(x)$ for $u_2(x,t)$. Letting $u(x,t) = u_1(x,t) - u_2(x,t)$, $f_1(x,t) = \hat{f}_1(x,t) - \tilde{f}_1(x,t)$, $f_2(x,t) = \hat{f}_2(x,t) - \tilde{f}_2(x,t)$, $\psi_1(x) = \hat{\psi}_1(x) - \tilde{\psi}_1(x)$, $\psi_2(x) = \hat{\psi}_2(x) - \tilde{\psi}_2(x)$, we obtain $u(x,t)$ satisfying Eqs. (3.25)-(3.27) with homogeneous interfacial and boundary conditions.

We now multiply Eqs. (3.25)-(3.26) by $u(x,t)$, integrate them over $(0,l)$ and (l,L), respectively, and then use the integration by parts at homogenous interfacial and boundary conditions. This gives

$$\begin{aligned}
&\rho_1 C_1 \int_0^l u_t u dx + \rho_2 C_2 \int_l^L u_t u dx + k_1 \int_0^l (u_x)^2 dx + k_2 \int_l^L (u_x)^2 dx \\
\leq & k_1 (u_x)_{I^-}(t) u_{I^-}(t) - k_1 u_x(0,t) u(0,t) + k_2 u_x(L,t) u(L,t) \\
& - k_2 (u_x)_{I^+}(t) u_{I^+}(t) + \rho_1 C_1 \int_0^l f_1 u dx + \rho_2 C_2 \int_l^L f_2 u dx \\
\leq & -\frac{k_1 \alpha_1}{\gamma_1} u^2(0,t) - \frac{k_2 \alpha_2}{\gamma_2} u^2(L,t) + \frac{\rho_1 C_1}{2} \int_0^l u^2 dx \\
& + \frac{\rho_2 C_2}{2} \int_l^L u^2 dx + \frac{\rho_1 C_1}{2} \int_0^l (f_1)^2 dx + \frac{\rho_2 C_2}{2} \int_l^L (f_2)^2 dx, \qquad (3.31)
\end{aligned}$$

(Here, we use the Robin boundary as an example), implying that

$$\begin{aligned}
&\frac{d}{dt}\left[\rho_1 C_1 \int_0^l u^2 dx + \rho_2 C_2 \int_l^L u^2 dx\right] + 2k_1 \int_0^l (u_x)^2 dx \\
&+ 2k_2 \int_l^L (u_x)^2 dx + \frac{2k_1\alpha_1}{\gamma_1} u^2(0,t) + \frac{2k_2\alpha_2}{\gamma_2} u^2(L,t) \\
\leq &\rho_1 C_1 \int_0^l u^2 dx + \rho_2 C_2 \int_l^L u^2 dx + \rho_1 C_1 \int_0^l (f_1)^2 dx + \rho_2 C_2 \int_l^L (f_2)^2 dx. \qquad (3.32)
\end{aligned}$$

Introducing $E(t) = \rho_1 C_1 \int_0^l u^2 dx + \rho_2 C_2 \int_l^L u^2 dx$, Eq. (3.32) can be rewritten as

$$\frac{dE(t)}{dt} \leq E(t) + \rho_1 C_1 \int_0^l (f_1)^2 dx + \rho_2 C_2 \int_l^L (f_2)^2 dx. \qquad (3.33)$$

By Gronwall's inequality, we obtain an energy estimation as

$$E(t) \leq e^t \left[E(0) + \int_0^t \left(\rho_1 C_1 \int_0^l (f_1)^2 dx + \rho_2 C_2 \int_l^L (f_2)^2 dx\right) d\tau\right]. \qquad (3.34)$$

Thus, $u_1(x,t)$ and $u_2(x,t)$ satisfy the same initial condition and the same source term, which means the left hand side of Eq. (3.34) will be 0, we can obtain $E(t) = 0$, indicating $u \equiv 0$, and hence, the solution is unique. It can be seen from Eq. (3.34) that the solution is continuously dependent on the initial condition and the source term.

Likewise, we can derive energy estimations similar to Eq. (3.34) for Dirichlet and Neumann boundaries. Hence, the model is well-posed for all the three types of boundaries.

3.3 Nanoscale Heat Conduction Model

For the heat conduction in the nanoscale double-layered structure, traditional methods are the two-temperature model coupled within the acoustic mismatch model or the diffuse mismatch model [95, 96], and the non-equilibrium molecular dynamical

model [4]. Here, we employ a recently developed model within the dual-phase-lagging framework for layered structures as follows [76]:

$$\begin{aligned}&\rho_1 C_1 \left(u_t\left(x,t\right)+\tau_q^{(1)}u_{tt}\left(x,t\right)\right)\\ =&k_1\left(u_{xx}\left(x,t\right)+\tau_T^{(1)}u_{xxt}\left(x,t\right)\right)+f_1\left(x,t\right),\quad 0<x<l,\quad 0<t\leq T,\end{aligned}\tag{3.35}$$

$$\begin{aligned}&\rho_2 C_2 \left(u_t\left(x,t\right)+\tau_q^{(2)}u_{tt}\left(x,t\right)\right)\\ =&k_2\left(u_{xx}\left(x,t\right)+\tau_T^{(2)}u_{xxt}\left(x,t\right)\right)+f_2\left(x,t\right),\quad l<x<L,\quad 0<t\leq T,\end{aligned}\tag{3.36}$$

subject to the initial and temperature-jump (Robin) boundary conditions as

$$u\left(x,0\right)=\psi_1\left(x\right),\quad u_t\left(x,0\right)=\varphi_1\left(x\right),\quad 0\leq x\leq l,\tag{3.37}$$

$$u\left(x,0\right)=\psi_2\left(x\right),\ u_t\left(x,0\right)=\varphi_2\left(x\right),\ l\leq x\leq L,\tag{3.38}$$

$$-\alpha_1 u_x\left(0,t\right)+u\left(0,t\right)=\phi_1\left(t\right),\ 0\leq t\leq T,\tag{3.39}$$

$$\alpha_2 u_x\left(L,t\right)+u\left(L,t\right)=\phi_2\left(t\right),\ 0\leq t\leq T,\tag{3.40}$$

and the interfacial condition at $x=l$ as

$$u_{I^+}\left(t\right)-u_{I^+}\left(t\right)=0,\quad 0\leq t\leq T,\tag{3.41}$$

$$\begin{aligned}&k_2\left(\left(u_x\right)_{I^+}\left(t\right)+\tau_T^{(2)}\left(u_{xt}\right)_{I^+}\left(t\right)\right)-k_1\left(\left(u_x\right)_{I^-}\left(t\right)+\tau_T^{(1)}\left(u_{xt}\right)_{I^-}\left(t\right)\right)\\ =&0,\quad 0\leq t\leq T.\end{aligned}\tag{3.42}$$

Here, k_1, k_2 are conductivities, ρ_1, ρ_1, are densities, C_1 C_2 are specific heats, $\tau_q^{(1)}$ and $\tau_q^{(2)}$, $\tau_T^{(1)}$ and $\tau_T^{(2)}$ stand for heat flux q and temperature gradient ∇u phase lags, respectively, $u\left(x,t\right)$ is the temperature, $f_1\left(x,t\right)$, $f_2\left(x,t\right)$ are source terms, $\psi_1\left(x\right)$, $\psi_2\left(x\right)$, $\varphi_1\left(x\right)$, $\varphi_2\left(x\right)$, $a\left(t\right)$, $b\left(t\right)$, $\phi_1\left(t\right)$, $\phi_2\left(t\right)$ are given functions, α_1, α_2 are positive

constants, and $u_{I^+}(t)$, $u_{I^-}(t)$, $(u_x)_{I^+}(t)$, $(u_x)_{I^-}(t)$, $(u_{xt})_{I^+}(t)$, $(u_{xt})_{I^-}(t)$ denote $u(l+0,t)$, $u(l-0,t)$, $u_x(l+0,t)$, $u_x(l-0,t)$, $u_{xt}(l+0,t)$, $u_{xt}(l-0,t)$, respectively.

Under the homogeneous interfacial and boundary conditions, Sun *et al.* [76] used a similar argument as aforementioned and obtained an energy estimation as

$$E(t) \leq E(0) + \frac{1}{2}\int_0^t \left[\frac{1}{\rho_1 C_1}\int_0^l (f_1)^2\, dx + \frac{1}{\rho_2 C_2}\int_l^L (f_2)^2\, dx\right] d\tau, \tag{3.43}$$

where $E(t) = \rho_1 C_1 \tau_q^{(1)} \int_0^l u_t^2 dx + \rho_2 C_2 \tau_q^{(2)} \int_l^L u_t^2 dx + k_1 \int_0^l u_x^2 dx + k_2 \int_l^L u_x^2 dx + \frac{k_1}{\alpha_1} u^2(0,t) + \frac{k_2}{\alpha_2} u^2(L,t)$. Thus, if $u_1(x,t)$ and $u_2(x,t)$ satisfy the above nanoscale heat conduction model, then $u(x,t) = u_1(x,t) - u_2(x,t)$ satisfies Eq. (3.43) with $E(0) = 0$ and $f_1 = f_2 \equiv 0$. Hence, $E(t) \equiv 0$, and $u(x,t) \equiv 0$. This implies that the solution is unique and is further continuously dependent on the initial condition and the source term. Thus, we obtain the following theorem.

Theorem 3.3. *Assume that* $f_1(x,t)$, $f_2(x,t)$, $\psi_1(x)$, $\psi_2(x)$, $\varphi_1(x)$, $\varphi_2(x)$, $a(t)$, $b(t)$, $\phi_1(t)$, $\phi_2(t)$ *are continuously differentiable. Then the nanoscale heat conduction model is well-posed.*

In summary, we have proposed the steady-state heat conduction model, unsteady-state heat conduction model, and nanoscale heat conduction model for thermal analysis in double-layered solid structures in this chapter. In general, obtaining the analytical solutions for these three models are tedious if not impossible, particularly for the nanoscale heat conduction model. In this dissertation, we will seek their numerical solutions, and aim at the development of higher-order accurate compact finite difference schemes for solving the above three heat conduction models, respectively.

CHAPTER 4

NUMERICAL METHODS: PART I — GRADIENT PRESERVED METHOD

In this chapter, a generalization of the compact finite difference method and a new idea called the gradient preserved method will be proposed. In particular, we will use the steady-state heat conduction model with Dirichlet boundary to illustrate these two methods.

4.1 Generalization of Compact Finite Difference Method

As we can see in the previous literature review, the accuracy of the compact finite difference method is relatively lower at boundary as compared with that at interior points. This is because we can only use one side of the points to approximate the derivative at boundary points. However, lower accuracy at boundary will reduce the globe accuracy even if the higher-order compact finite difference method is used for interior points. Our generalization of compact finite difference method is proposed here to solve this troublesome.

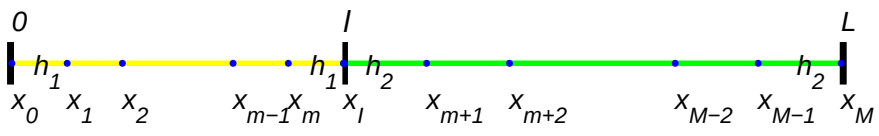

Figure 4.1: One-dimensional mesh for a double-layered solid structure.

We first design a one-dimensional mesh and denote grid sizes to be $h_1 = l/m$, $h_2 = (L-l)/(M-m)$, respectively, where m, M $(m < M)$ are positive integers, as shown in Figure 4.1. Grid points in the mesh are denoted as $x_j = jh_1$, $0 \le j \le m$; $x_j = l + (j-m)\,h_2$, $m+1 \le j \le M$, where the interface is located at grid point $x_I = (m+1)\,h_1 = l$. Based on the mesh, we have the following theorem.

Theorem 4.1 *Assume that* $g(x) \in C^6[0,1]$. *Then*

$$\begin{aligned}
16g(x_1) - g(x_2) =& 15g(x_0) + 14h_1 g_x(x_0) + 6h_1^2 g_{xx}(x_0) \\
&+ \frac{4}{3}h_1^3 g_{x^3}(x_0) - \frac{2h_1^5}{15}g_{x^5}(x_0) + O\left(h_1^6\right), \qquad (4.1a)\\
16g(x_{M-1}) - g(x_{M-2}) =& 15g(x_M) - 14h_2 g_x(x_M) + 6h_2^2 g_{xx}(x_M) \\
&- \frac{4}{3}h_2^3 g_{x^3}(x_M) + \frac{2h_2^5}{15}g_{x^5}(x_M) + O\left(h_2^6\right), \qquad (4.1b)\\
g(x_1) - g(x_0) =& h_1 g_x(x_0) + \frac{5}{12}h_1^2 g_{xx}(x_0) + \frac{1}{12}h_1^2 g_{xx}(x_1) \\
&+ \frac{h_1^3}{12}g_{x^3}(x_0) - \frac{h_1^5}{180}g_{x^5}(x_0) + O\left(h_1^6\right) \text{(see [82, 84])}, \qquad (4.2a)\\
g(x_{M-1}) - g(x_M) =& -h_2 g_x(x_M) + \frac{5}{12}h_2^2 g_{xx}(x_M) + \frac{1}{12}h_2^2 g_{xx}(x_{M-1}) \\
&- \frac{h_2^3}{12}g_{x^3}(x_M) + \frac{h_2^5}{180}g_{x^5}(x_M) + O\left(h_2^6\right) \text{(see [82, 84])}, \qquad (4.2b)\\
32g(x_1) - g(x_2) =& 31g(x_0) + 30h_1 g_x(x_0) + \frac{35}{3}h_1^2 g_{xx}(x_0) \\
&+ \frac{8}{3}h_1^2 g_{xx}(x_1) - \frac{1}{3}h_1^2 g_{xx}(x_2) \\
&+ 2h_1^3 g_{x^3}(x_0) + \frac{h_1^6}{15}g_{x^6}(x_0) + O\left(h_1^7\right), \qquad (4.3a)\\
32g(x_{M-1}) - g(x_{M-2}) =& 31g(x_M) - 30h_2 g_x(x_M) + \frac{35}{3}h_2^2 g_{xx}(x_M) \\
&+ \frac{8}{3}h_2^2 g_{xx}(x_{M-1}) - \frac{1}{3}h_2^2 g_{xx}(x_{M-2}) \\
&- 2h_2^3 g_{x^3}(x_M) + \frac{h_2^6}{15}g_{x^6}(x_M) + O\left(h_2^7\right). \qquad (4.3b)
\end{aligned}$$

Proof. Denote $D^j g(x)$ as the jth order derivative of $g(x)$. The Taylor series expansion at location x_0 gives

$$\begin{aligned} g(x_1) =& g(x_0) + h_1 g_x(x_0) + \frac{h_1^2}{2} g_{xx}(x_0) + \frac{h_1^3}{6} g_{x^3}(x_0) + \frac{h_1^4}{24} g_{x^4}(x_0) \\ &+ \frac{h_1^5}{120} g_{x^5}(x_0) + \frac{h_1^6}{720} g_{x^6}(x_0) + ... \\ =& \left(D^0 + h_1 D^1 + \frac{h_1^2}{2} D^2 + \frac{h_1^3}{6} D^3 + \frac{h_1^4}{24} D^4 + \frac{h_1^5}{120} D^5 + \frac{h_1^6}{720} D^6 + ... \right) g(x_0), \quad (4.4) \\ g(x_2) =& g(x_0) + 2h_1 g_x(x_0) + \frac{4h_1^2}{2} g_{xx}(x_0) + \frac{8h_1^3}{6} g_{x^3}(x_0) + \frac{16h_1^4}{24} g_{x^4}(x_0) \\ &+ \frac{32h_1^5}{120} g_{x^5}(x_0) + \frac{64h_1^6}{720} g_{x^6}(x_0) + ... \\ =& \left(D^0 + 2h_1 D^1 + \frac{4h_1^2}{2} D^2 + \frac{8h_1^3}{6} D^3 + \frac{16h_1^4}{24} D^4 + \frac{32h_1^5}{120} D^5 + \frac{64h_1^6}{720} D^6 + ... \right) g(x_0). \quad (4.5) \end{aligned}$$

Multiplying Eq. (4.4) by -16, then adding it to Eq. (4.5), we obtain

$$-16g(x_1) + g(x_2) = -\left(15D^0 + 14h_1 D^1 + \frac{12}{2} h_1^2 D^2 + \frac{8h_1^3}{6} D^3 - \frac{16h_1^5}{120} D^5 - \frac{48h_1^6}{720} D^6 + ... \right) g(x_0). \quad (4.6)$$

Thus, Eq. (4.1a) holds. By the Taylor series expansion at location x_M, we have

$$\begin{aligned} g(x_{M-1}) =& \left(D^0 - h_2 D^1 + \frac{h_2^2}{2} D^2 - \frac{h_2^3}{6} D^3 + \frac{h_2^4}{24} D^4 - \frac{h_2^5}{120} D^5 + \frac{h_2^6}{720} D^6 + ... \right) g(x_M), \quad (4.7) \\ g(x_{M-2}) =& \left(D^0 - 2h_2 D^1 + \frac{4h_2^2}{2} D^2 - \frac{8h_2^3}{6} D^3 + \frac{16h_2^4}{24} D^4 - \frac{32h_2^5}{120} D^5 + \frac{64h_2^6}{720} D^6 + ... \right) g(x_M). \quad (4.8) \end{aligned}$$

Multiplying Eq. (4.7) by -16, then adding it to Eq. (4.8), we obtain

$$\begin{aligned} & -16g(x_{M-1}) + g(x_{M-2}) \\ =& -\left(15D^0 - 14h_2 D^1 + \frac{12h_2^2}{2} D^2 - \frac{8h_2^3}{6} D^3 + \frac{16h_2^5}{120} D^5 - \frac{48h_2^6}{720} D^6 + ... \right) g(x_M). \quad (4.9) \end{aligned}$$

Thus, Eq. (4.1b) holds. The Taylor series expansion at location x_0 also gives

$$\begin{aligned} h_1^2 g_{xx}(x_1) =& h_1^2 \left(D^0 + h_1 D^1 + \frac{h_1^2}{2} D^2 + \frac{h_1^3}{6} D^3 + \frac{h_1^4}{24} D^4 + \frac{h_1^5}{120} D^5 + ... \right) D^2 g(x_0) \\ =& \left(h_1^2 D^2 + h_1^3 D^3 + \frac{h_1^4}{2} D^4 + \frac{h_1^5}{6} D^5 + \frac{h_1^6}{24} D^6 + \frac{h_1^7}{120} D^7 + ... \right) g(x_0). \quad (4.10) \end{aligned}$$

Multiplying Eq. (4.4) by -12, then adding it to Eq. (4.10), we obtain

$$\begin{aligned} &-12g\left(x_1\right)+h^2g_{xx}\left(x_1\right) \\ =&-\left(12D^0+12h_1D^1+5h_1^2D^2+h_1^3D^3-\frac{h_1^5}{15}D^5-\frac{h_1^6}{40}D^6+...\right)g\left(x_0\right). \end{aligned} \tag{4.11}$$

Rearranging the terms in Eq. (4.11) yields

$$\begin{aligned} &-12g\left(x_1\right)+12g\left(x_0\right) \\ =&-\left(12h_1D^1+5h_1^2D^2+h_1^3D^3-\frac{h_1^5}{15}D^5-\frac{h_1^6}{40}D^6+...\right)g\left(x_0\right)-h_1^2g_{xx}\left(x_1\right). \end{aligned} \tag{4.12}$$

Dividing Eq. (4.12) by -12, Eq. (4.2a) comes. The Taylor series expansion at location x_M also gives

$$\begin{aligned} h_2^2g_{xx}\left(x_{M-1}\right)=&h_2^2\left(D^0-h_2D^1+\frac{h_2^2}{2}D^2-\frac{h_2^3}{6}D^3+\frac{h_2^4}{24}D^4-\frac{h_2^5}{120}D^5+...\right)D^2g\left(x_M\right) \\ =&\left(h_2^2D^2-h_2^3D^3+\frac{h_2^4}{2}D^4-\frac{h_2^5}{6}D^5+\frac{h_2^6}{24}D^6-\frac{h_2^7}{120}D^7+...\right)g\left(x_M\right). \end{aligned} \tag{4.13}$$

Multiplying Eq. (4.7) by -12, then adding it to Eq. (4.13), we obtain

$$\begin{aligned} &-12g\left(x_{M-1}\right)+h^2g_{xx}\left(x_{M-1}\right) \\ =&-\left(12D^0-12h_2D^1+5h_2^2D^2-h_2^3D^3+\frac{h_2^5}{15}D^5-\frac{h_2^6}{40}D^6+...\right)g\left(x_M\right). \end{aligned} \tag{4.14}$$

Dividing Eq. (4.14) by -12 and rearranging the terms, Eq. (4.2b) comes.

Changing x_1 to x_2, x_{M-1} to x_{M-2}, h_1 to $2h_1$, h_2 to $2h_2$, Eqs. (4.2a)-(4.2b) become

$$\begin{aligned} g\left(x_2\right)-g\left(x_0\right)=&\left(2h_1D+\frac{20}{12}h_1^2D^2+\frac{8}{12}h_1^3D^3+\frac{32h_1^5}{180}D^5-\frac{64h_1^6}{480}D^6\right)g\left(x_0\right) \\ &+\frac{4}{12}h_1^2g_{xx}\left(x_2\right)+O\left(h_1^7\right), \end{aligned} \tag{4.15a}$$

and

$$g(x_{M-2}) - g(x_M) = \left(-2h_2D + \frac{20}{12}h_2^2D^2 - \frac{8}{12}h_2^3D^3 - \frac{32h_2^5}{180}D^5 - \frac{64h_2^6}{480}D^6\right)g(x_M) + \frac{4}{12}h_2^2 g_{xx}(x_{M-2}) + O\left(h_2^7\right). \tag{4.15b}$$

Multiplying Eq. (4.2a) and Eq. (4.2b) by -32 and then adding them to Eq. (4.15a) and Eq. (4.15b), respectively, we obtain

$$\begin{aligned} -32g(x_1) + g(x_2) + 31g(x_0) = &-30h_1 g_x(x_0) - \frac{35}{3}h_1^2 g_{xx}(x_0) \\ &- \frac{8}{3}h_1^2 g_{xx}(x_1) + \frac{1}{3}h_1^2 g_{xx}(x_2) \\ &- 2h_1^3 g_{x^3}(x_0) - \frac{h_1^6}{15}g_{x^6}(x_0) + O\left(h_1^7\right), \end{aligned} \tag{4.16a}$$

$$\begin{aligned} -32(x_{M-1}) + g(x_{M-2}) + 31g(x_M) = &30h_2 g_x(x_M) - \frac{35}{3}h_2^2 g_{xx}(x_M) \\ &- \frac{8}{3}h_2^2 g_{xx}(x_{M-1}) + \frac{1}{3}h_2^2 g_{xx}(x_{M-2}) \\ &+ 2h_2^3 g_{x^3}(x_M) - \frac{h_2^6}{15}g_{x^6}(x_M) + O\left(h_2^7\right). \end{aligned} \tag{4.16b}$$

Thus, Eqs. (4.3a)-(4.3b) hold.

From Eqs. (4.1a), (4.2a) and (4.3a), we can see the absolute values of the leading terms in $g_{x^5}(x_0)$ of truncation errors for approximating $g_x(x_0)$ are $\frac{h_1^4}{105}$, $\frac{h_1^4}{180}$, $\frac{h_1^5}{450}$, respectively. Same results can be obtained for $g_x(x_M)$. Further, one may see that Eqs. (4.1a), (4.2a) and (4.3a) are some special cases of the expression:

$$(g_{xx})_0 + \alpha(g_{xx})_1 + \beta(g_{xx})_2 = ag_0 + bg_1 + cg_2 + \xi(g_x)_0 + \zeta(g_{x^3})_0, \tag{4.17}$$

where α, β, a, b, c, ξ, ζ are constants to be determined. Similarly, Eqs. (4.1b), (4.2b), (4.3b) are some special cases of another expression:

$$(g_{xx})_M + \alpha(g_{xx})_{M-1} + \beta(g_{xx})_{M-2} = ag_M + bg_{M-1} + cg_{M-2} + \xi(g_x)_M + \zeta(g_{x^3})_M. \tag{4.18}$$

Eqs. (4.17)-(4.18) can be considered as couple of generalizations of the compact finite difference method, Eq. (2.38), at boundary.

Since the interfacial condition can be treated as an inside-boundary condition, we have some similar formulas as listed in Eqs. (4.1)-(4.3), which are included in the following theorem.

Theorem 4.2 *Assume that* $g(x) \in C^6[0,1]$. *Then*

$$\begin{aligned} 16g(x_m) - g(x_{m-1}) =& 15g(x_{I^-}) - 14h_1 g_x(x_{I^-}) + 6h_1^2 g_{xx}(x_{I^-}) \\ & - \frac{4}{3}h_1^3 g_{x^3}(x_{I^-}) + \frac{2h_1^5}{15} g_{x^5}(x_{I^-}) + O\left(h_1^6\right), \end{aligned} \tag{4.19a}$$

$$\begin{aligned} 16g(x_{m+1}) - g(x_{m+2}) =& 15g(x_{I^+}) + 14h_2 g_x(x_{I^+}) + 6h_2^2 g_{xx}(x_{I^+}) \\ & + \frac{4}{3}h_2^3 g_{x^3}(x_{I^+}) - \frac{2h_2^5}{15} g_{x^5}(x_{I^+}) + O\left(h_2^6\right), \end{aligned} \tag{4.19b}$$

$$\begin{aligned} g(x_m) - g(x_{I^-}) =& -h_1 g_x(x_{I^-}) + \frac{5}{12}h_1^2 g_{xx}(x_{I^-}) + \frac{1}{12}h_1^2 g_{xx}(x_m) \\ & - \frac{1}{12}h_1^3 g_{x^3}(x_{I^-}) - \frac{h_1^5}{180} g_{x^5}(x_M) + O\left(h_1^6\right), \end{aligned} \tag{4.20a}$$

$$\begin{aligned} g(x_{m+1}) - g(x_{I^+}) =& h_2 g_x(x_{I^+}) + \frac{5}{12}h_2^2 g_{xx}(x_{I^+}) + \frac{1}{12}h_2^2 g_{xx}(x_{m+1}) \\ & + \frac{1}{12}h_2^3 g_{x^3}(x_{I^+}) - \frac{h_2^5}{180} g_{x^5}(x_{I^+}) + O\left(h_2^6\right), \end{aligned} \tag{4.20b}$$

$$\begin{aligned} 32g(x_m) - g(x_{m-1}) =& 31g(x_{I^-}) - 30h_1 g_x(x_{I^-}) + \frac{35}{3}h_1^2 g_{xx}(x_{I^-}) \\ & + \frac{8}{3}h_1^2 g_{xx}(x_m) - \frac{1}{3}h_1^2 g_{xx}(x_{m-1}) \\ & - 2h_1^3 g_{x^3}(x_{I^-}) + \frac{h_1^6}{15} g_{x^6}(x_{I^-}) + O\left(h_1^7\right), \end{aligned} \tag{4.21a}$$

$$\begin{aligned} 32g(x_{m+1}) - g(x_{m+2}) =& 31g(x_{I^+}) + 30h_2 g_x(x_{I^+}) + \frac{35}{3}h_2^2 g_{xx}(x_{I^+}) \\ & + \frac{8}{3}h_2^2 g_{xx}(x_{m+1}) - \frac{1}{3}h_2^2 g_{xx}(x_{m+2}) \\ & + 2h_2^3 g_{x^3}(x_{I^+}) + \frac{h_2^6}{15} g_{x^6}(x_{I^+}) + O\left(h_2^7\right). \end{aligned} \tag{4.21b}$$

Again, Eqs. (4.19a), (4.20a) and (4.21a) can be seen to be some special cases of the following expression

$$(g_{xx})_{I^-} + \alpha (g_{xx})_m + \beta (g_{xx})_{m-1} = a g_{I^-} + b g_m + c g_{m-1} + \xi (g_x)_{I^-} + \zeta (g_{x^3})_{I^-} , \quad (4.22)$$

and Eqs. (4.19b), (4.20b), (4.21b) are some special cases of the expression

$$(g_{xx})_{I^+} + \alpha (g_{xx})_{m+1} + \beta (g_{xx})_{m+2} = a g_{I^+} + b g_{m+1} + c g_{m+2} + \xi (g_x)_{I^+} + \zeta (g_{x^3})_{I^+} . \quad (4.23)$$

Thus, Eqs. (4.22)-(4.23) can be considered as couple of generalizations of the compact finite difference method, Eq. (2.38), at interface.

It should be pointed out that the first-order and third-order derivatives are included in our generalized version of compact finite difference method, which will be used in the next section.

4.2 Gradient Preserved Method

We consider the steady-state heat conduction model proposed in Section 3.1:

$$k_1 u_{xx} (x) = f_1 (x) , \quad 0 < x < l, \quad (4.24)$$

$$k_2 u_{xx} (x) = f_2 (x) , \quad l < x < L, \quad (4.25)$$

with the interfacial condition at $x = l$:

$$u_{I^+} - u_{I^-} = a, \quad (4.26)$$

$$k_2 (u_x)_{I^+} - k_1 (u_x)_{I^-} = b, \quad (4.27)$$

and the Dirichlet boundary condition:

$$u (0) = \phi_1, \quad u (L) = \phi_2. \quad (4.28)$$

We now develop a fourth-order compact finite difference scheme using three-points in space. We use the one-dimensional mesh as shown in Figure 4.1 and denote u_j as the approximation of $u(x_j)$, and so on for others.

For the interior points, $x_1 \le x_j \le x_{m-1}$ and $x_{m+2} \le x_j \le x_{M-1}$, the fourth-order Padé scheme gives

$$\frac{k_1(u_{j-1}-2u_j+u_{j+1})}{h_1^2} = \frac{1}{12}\left[(f_1)_{j-1}+10(f_1)_j+(f_1)_{j+1}\right], \quad 1 \le j \le m-1, \tag{4.30}$$

$$\frac{k_2(u_{j-1}-2u_j+u_{j+1})}{h_2^2} = \frac{1}{12}\left[(f_2)_{j-1}+10(f_2)_j+(f_2)_{j+1}\right], \quad m+2 \le j \le M-1. \tag{4.31}$$

At the boundary points, x_0 and x_M, we simply set

$$u_0 = \phi_1, \; u_M = \phi_2. \tag{4.32}$$

To derive a scheme at interface, $x = x_I$, we first obtain two tridiagonal equations around the interface x_I, in which one contains u_{m-1}, u_m and u_{m+1}, the other contains u_m, u_{m+1} and u_{m+2}.

From Eqs. (4.24)-(4.25), we have $u_{xx}(x_{I^-}) = \frac{f_1(x_{I^-})}{k_1}$, $u_{x^3}(x_{I^-}) = \frac{(f_1)_x(x_{I^-})}{k_1}$ and $u_{xx}(x_{I^+}) = \frac{f_2(x_{I^+})}{k_2}$, $u_{x^3}(x_{I^+}) = \frac{(f_2)_x(x_{I^+})}{k_2}$. Substituting them into Eq. (4.21a) and Eq. (4.21b) yields

$$\begin{aligned} &u(x_{m-1}) - 32u(x_m) + 31u(x_{I^-}) - 30h_1u_x(x_{I^-}) \\ =& -\frac{h_1^2}{3k_1}\left(35f_1(x_{I^-}) + 8f_1(x_m) - f_1(x_{m-1})\right) + \frac{2h_1^3}{k_1}(f_1)_x(x_{I^-}) + O\left(h_1^6\right), \end{aligned} \tag{4.33}$$

$$\begin{aligned} &u(x_{m+2}) - 32u(x_{m+1}) + 31u(x_{I^+}) + 30h_2u_x(x_{I^+}) \\ =& -\frac{h_2^2}{3k_2}\left(35f_2(x_{I^+}) + 8f_2(x_{m+1}) - f_2(x_{m+2})\right) + \frac{2h_2^3}{k_2}(f_2)_x(x_{I^+}) + O\left(h_2^6\right). \end{aligned} \tag{4.34}$$

We then employ the fourth-order Padé scheme at points x_m and x_{m+1} as

$$\frac{k_1\left(u_{m-1}-2u_m+u_{I^-}\right)}{h_1^2}=\frac{1}{12}\left[\left(f_1\right)_{m-1}+10\left(f_1\right)_m+\left(f_1\right)_{I^-}\right]+O\left(h_1^4\right), \tag{4.35}$$

$$\frac{k_2\left(u_{m+2}-2u_{m+1}+u_{I^+}\right)}{h_2^2}=\frac{1}{12}\left[\left(f_2\right)_{m+2}+10\left(f_2\right)_{m+1}+\left(f_2\right)_{I^+}\right]+O\left(h_2^4\right). \tag{4.36}$$

After dropping the truncation errors in Eqs. (4.33)-(4.36) and coupling with the interfacial condition Eqs. (4.26)-(4.27), the following six equations are obtained.

$$u_{I^+}-u_{I^-}=a, \tag{4.37}$$

$$k_2\left(u_x\right)_{I^+}-k_1\left(u_x\right)_{I^-}=b, \tag{4.38}$$

$$u_{m-1}-32u_m+31u_{I^-}-30h_1\left(u_x\right)_{I^-}=c_1, \tag{4.39}$$

$$u_{m+2}-32u_{m+1}+31u_{I^+}+30h_2\left(u_x\right)_{I^+}=c_2, \tag{4.40}$$

$$u_{m-1}-2u_m+u_{I^-}=c_3, \tag{4.41}$$

$$u_{m+2}-2u_{m+1}+u_{I^+}=c_4, \tag{4.42}$$

where $c_1=-\frac{h_1^2}{3k_1}\left[35\left(f_1\right)_{I^-}+8\left(f_1\right)_m-\left(f_1\right)_{m-1}-6h_1\left(\left(f_1\right)_x\right)_{I^-}\right]$,

$c_2=-\frac{h_2^2}{3k_2}[35\left(f_2\right)_{I^+}+8\left(f_2\right)_{m+1}-\left(f_2\right)_{m+2}+6h_2\left(\left(f_2\right)_x\right)_{I^+}]$,

$c_3=\frac{h_1^2}{12k_1}\left[\left(f_1\right)_{m-1}+10\left(f_1\right)_m+\left(f_1\right)_{I^-}\right]$, $c_4=\frac{h_2^2}{12k_2}\left[\left(f_2\right)_{m+2}+10\left(f_2\right)_{m+1}+\left(f_2\right)_{I^+}\right]$.

Subtracting Eq. (4.41) from Eq. (4.42) and using Eq. (4.37), we obtain

$$u_{m+2}-2u_{m+1}+2u_m-u_{m-1}=c_4-c_3-a. \tag{4.43}$$

Multiplying Eq. (4.41) by 31 and subtracting Eq. (4.39), we have

$$30u_{m-1}-30u_m+30h_1\left(u_x\right)_{I^-}=31c_3-c_1. \tag{4.44}$$

Similarly, multiplying Eq. (4.42) by 31 and subtracting Eq. (4.40) gives

$$30u_{m+2}-30u_{m+1}-30h_2\left(u_x\right)_{I^+}=31c_4-c_2. \tag{4.45}$$

Multiplying Eq. (4.44) and Eq. (4.45) by k_1h_2 and k_2h_1, respectively, and adding them together, we obtain

$$\begin{aligned}
&30k_1h_2u_{m-1} - 30k_1h_2u_m + 30k_2h_1u_{m+2} \\
&- 30k_2h_1u_{m+1} - 30h_1h_2\left[k_2\left(u_x\right)_{I^+} - k_1\left(u_x\right)_{I^-}\right] \\
=&31k_2h_1c_4 + 31k_1h_2c_3 - k_2h_1c_2 - k_1h_2c_1. \qquad (4.46)
\end{aligned}$$

Then applying Eq. (4.38) to Eq. (4.46) yields

$$\begin{aligned}
&30k_1h_2u_{m-1} - 30k_1h_2u_m + 30k_2h_1u_{m+2} - 30k_2h_1u_{m+1} \\
=&31k_2h_1c_4 + 31k_1h_2c_3 - k_2h_1c_2 - k_1h_2c_1 + 30h_1h_2b. \qquad (4.47)
\end{aligned}$$

Multiplying Eq. (4.43) by $30k_2h_1$, then subtracting Eq. (4.47), we obtain

$$\begin{aligned}
&30\left[\left(-k_2h_1\right)u_{m+1} + \left(2k_2h_1 + k_1h_2\right)u_m - \left(k_2h_1 + k_1h_2\right)u_{m-1}\right] \\
=&\left(-k_2h_1\right)c_4 - \left(30k_2h_1 + 31k_1h_2\right)c_3 + k_2h_1c_2 + k_1h_2c_1 - 30h_1h_2b - 30k_2h_1a. \qquad (4.48)
\end{aligned}$$

Dividing by $-15\left(k_1h_2 + 2k_2h_1\right)$ gives

$$\left[\left(1 + \frac{k_1h_2}{k_1h_2 + 2k_2h_1}\right)u_{m-1} - 2u_m + \left(1 - \frac{k_1h_2}{k_1h_2 + 2k_2h_1}\right)u_{m+1}\right] = c_5, \qquad (4.49)$$

where $c_5 = \frac{1}{15(k_1h_2+2k_2h_1)}[k_2h_1c_4 + \left(30k_2h_1 + 31k_1h_2\right)c_3 - k_2h_1c_2 - k_1h_2c_1 + 30h_1h_2b + 30k_2h_1a]$. Similarly, multiplying Eq. (4.43) by $30k_1h_2$, and adding it to Eq. (4.48), then dividing by $15\left(2k_1h_2 + k_2h_1\right)$, we obtain

$$\left[\left(1 - \frac{k_2h_1}{2k_1h_2 + k_2h_1}\right)u_m - 2u_{m+1} + \left(1 + \frac{k_2h_1}{2k_1h_2 + k_2h_1}\right)u_{m+2}\right] = c_6, \qquad (4.50)$$

where $c_6 = \frac{1}{15(2k_1h_2+k_2h_1)}[\left(30k_1h_2 + 31k_2h_1\right)c_4 + k_1h_2c_3 - k_2h_1c_2 - k_1h_2c_1 + 30h_1h_2b - 30k_1h_2a]$.

If Eqs. (4.19a)-(4.19b) are used at the interface, we can obtain similar equations to Eqs. (4.49)-(4.50) as

$$\left[\left(1+\frac{k_1h_2}{k_1h_2+2k_2h_1}\right)u_{m-1}-2u_m+\left(1-\frac{k_1h_2}{k_1h_2+2k_2h_1}\right)u_{m+1}\right]=c_7, \tag{4.51}$$

$$\left[\left(1-\frac{k_2h_1}{2k_1h_2+k_2h_1}\right)u_m-2u_{m+1}+\left(1+\frac{k_2h_1}{2k_1h_2+k_2h_1}\right)u_{m+2}\right]=c_8, \tag{4.52}$$

where $c_7=\frac{1}{7(k_1h_2+2k_2h_1)}[k_2h_1c_4+(14k_2h_1+15k_1h_2)c_3-k_2h_1c_2-k_1h_2c_1+14h_1h_2b+14k_2h_1a]$, $c_8=\frac{1}{7(2k_1h_2+k_2h_1)}\left[(14k_1h_2+15k_2h_1)\,c_4+k_1h_2c_3-k_2h_1c_2-k_1h_2c_1+14h_1h_2b-14k_1h_2a\right]$. Here, $c_1=-\frac{h_1^2}{3k_1}\left[18\,(f_1)_{I^-}-4h_1\,((f_1)_x)_{I^-}\right]$, $c_2=-\frac{h_2^2}{3k_2}[18\,(f_2)_{I^+}+4h_2\,((f_2)_x)_{I^+}]$.

If Eqs. (4.20a)-(4.20b) are used at the interface, we have similar equations to Eqs. (4.49)-(4.50) as

$$\left[\left(1+\frac{k_1h_2}{k_1h_2+2k_2h_1}\right)u_{m-1}-2u_m+\left(1-\frac{k_1h_2}{k_1h_2+2k_2h_1}\right)u_{m+1}\right]=c_9, \tag{4.53}$$

$$\left[\left(1-\frac{k_2h_1}{2k_1h_2+k_2h_1}\right)u_m-2u_{m+1}+\left(1+\frac{k_2h_1}{2k_1h_2+k_2h_1}\right)u_{m+2}\right]=c_{10}, \tag{4.54}$$

where $c_9=\frac{2}{k_1h_2+2k_2h_1}\left[(k_2h_1+k_1h_2)\,c_3-k_2h_1c_2-k_1h_2c_1+h_1h_2b+k_2h_1a\right]$, $c_{10}=\frac{2}{2k_1h_2+k_2h_1}\left[(k_1h_2+k_2h_1)\,c_4-k_2h_1c_2-k_1h_2c_1+h_1h_2b-k_1h_2a\right]$. Here, $c_1=-\frac{h_1^2}{12k_1}\left[5\,(f_1)_{I^-}+(f_1)_m-h_1\,((f_1)_x)_{I^-}\right]$, $c_2=-\frac{h_2^2}{12k_2}[5\,(f_2)_{I^+}+(f_2)_{m+1}+h_2\,((f_2)_x)_{I^+}]$.

Eqs. (4.30)-(4.31), Eq. (4.32) and Eqs. (4.49)-(4.50) (or Eqs. (4.51)-(4.52), or Eqs. (4.53)-(4.54)) together form a higher-order accurate finite difference scheme for the heat conduction model in steady-state with Dirichlet boundary. We can rewrite the scheme in matrix form as

$$A_D\vec{u}=\vec{d}_D, \tag{4.55}$$

where $\vec{u}=[u_1,u_2,...,u_{m-2},u_{m-1},u_m,u_{m+1},u_{m+2},u_{m+3},...,u_{M-2},u_{M-1}]^T$,

$$A_D = \begin{bmatrix}
-2 & 1 & & & & & & & & & & \\
1 & -2 & 1 & & & & & & & & & \\
& \ddots & \ddots & \ddots & & & & & & & & \\
& & 1 & -2 & 1 & & & & & & & \\
& & & \frac{2(k_1h_2+k_2h_1)}{2k_2h_1+k_1h_2} & -2 & \frac{2k_2h_1}{2k_2h_1+k_1h_2} & & & & & & \\
& & & & \frac{2k_1h_2}{2k_1h_2+k_2h_1} & -2 & \frac{2(k_1h_2+k_2h_1)}{2k_1h_2+k_2h_1} & & & & & \\
& & & & & 1 & -2 & 1 & & & & \\
& & & & & & \ddots & \ddots & \ddots & & & \\
& & & & & & & & 1 & -2 & 1 & \\
& & & & & & & & & 1 & -2
\end{bmatrix}$$

$$\text{and } \vec{d}_D = \begin{bmatrix}
\frac{h_1^2}{12k_1}\left[(f_1)_0 + 10\,(f_1)_1 + (f_1)_2\right] - u_0 \\
\frac{h_1^2}{12k_1}\left[(f_1)_1 + 10\,(f_1)_2 + (f_1)_3\right] \\
\frac{h_1^2}{12k_1}\left[(f_1)_2 + 10\,(f_1)_3 + (f_1)_4\right] \\
\vdots \\
\frac{h_1^2}{12k_1}\left[(f_1)_{m-2} + 10\,(f_1)_{m-1} + (f_1)_m\right] \\
c_5 \text{ (or } c_7 \text{ or } c_9) \\
c_6 \text{ (or } c_8 \text{ or } c_{10}) \\
\frac{h_2^2}{12k_2}\left[(f_2)_{m+1} + 10\,(f_2)_{m+2} + (f_2)_{m+3}\right] \\
\frac{h_2^2}{12k_2}\left[(f_2)_{m+2} + 10\,(f_2)_{m+3} + (f_2)_{m+4}\right] \\
\vdots \\
\frac{h_2^2}{12k_2}\left[(f_2)_{M-4} + 10\,(f_2)_{M-3} + (f_2)_{M-2}\right] \\
\frac{h_2^2}{12k_2}\left[(f_2)_{M-3} + 10\,(f_2)_{M-2} + (f_2)_{M-1}\right] \\
\frac{h_2^2}{12k_2}\left[(f_2)_{M-2} + 10\,(f_2)_{M-1} + (f_2)_M\right] - u_M
\end{bmatrix}.$$

Note that A_D is a tridiagonal matrix, so one can use the Thomas algorithm to obtain the solution easily. Once the values of u_{m-1}, u_m, u_{m+1} and u_{m+2} are obtained, the values of u_{I^-}, u_{I^+}, $(u_x)_{I^-}$ and $(u_x)_{I^+}$ can be easily obtained by using Eqs. (4.37)-(4.42).

It should be pointed out that the third-order derivatives at interface, $(u_{x^3})_{I^-}$ and $(u_{x^3})_{I^+}$, have been changed to some known values in the derivation to obtain Eqs. (4.33)-(4.34) and the first-order derivatives at interface, $(u_x)_{I^-}$ and $(u_x)_{I^+}$, have been deleted in the derivation to obtain Eqs (4.49)-(4.50).

Furthermore, $(u_x)_{I^-}$ and $(u_x)_{I^+}$ have not been discretized in our derivations for the scheme at interface. We name this idea the gradient preserved method (GPM). As will be seen in next chapter, this idea can also be used for the Neumann boundary and Robin boundary, where $(u_x)_0$ and $(u_x)_M$ exist. The GPM can avoid the troublesome arising from u_x while it is at the interface or on the boundary.

4.3 Analysis of the Scheme for Steady State Heat Conduction Model with Dirichlet Boundary

In this section, we will give the theoretical analysis for solvability, stability and convergence of the proposed compact finite difference scheme for the steady-state heat conduction model with the Dirichlet boundary.

It can be seen that the coefficient matrix A_D is tridiagonal and satisfy conditions: (1) $|a_1| > |c_1| > 0$, (2) $|a_j| \geq |b_j| + |c_j|$, $2 \leq j \leq M-2$, (3) $|a_{M-1}| > |c_{M-1}| > 0$. Based on the lemma on page 528 of Atkinson's book [97], the inverse matrix A_D^{-1} exists,

which implies that the solution is unique, and the solution can be obtained using the Thomas algorithm.

To analyze the stability and convergence, we rewrite the scheme as follow:

$$-u_{j-1}+2u_j-u_{j+1}=h_1^2 g_j,\quad j=1,...,m-1, \tag{4.56}$$

$$\begin{aligned}&\frac{1}{k_1h_2+k_2h_1}\left[-(k_2h_1+k_1h_2)u_{m-1}+(k_2h_1+k_1h_2)u_m+k_2h_1u_m-k_2h_1u_{m+1}\right]\\ &=\left(h_1^2+h_2^2\right)g_m,\end{aligned} \tag{4.57}$$

$$\begin{aligned}&\frac{1}{k_1h_2+k_2h_1}\left[-k_1h_2u_m+k_1h_2u_{m+1}+(k_1h_2+k_2h_1)u_{m+1}-(k_1h_2+k_2h_1)u_{m+2}\right]\\ &=\left(h_1^2+h_2^2\right)g_{m+1},\end{aligned} \tag{4.58}$$

$$-u_{j-1}+2u_j-u_{j+1}=h_2^2 g_j,\quad j=m+2,...,M-1, \tag{4.59}$$

where u_0, $u_N=0$, g is a function of f_1 or f_2.

Multiplying Eqs. (4.56)-(4.59) by $\frac{1}{k_2h_1}u_j$ $(j=1,...,m-1)$, $\frac{1}{k_2h_1}u_m$, $\frac{1}{k_1h_2}u_{m+1}$ and $\frac{1}{k_1h_2}u_j$ $(j=m+2,...,M-1)$, respectively, and summing them together gives

$$\begin{aligned}&\frac{1}{k_2h_1}\left[u_1^2+(u_1-u_2)^2+\cdots+(u_{m-2}-u_{m-1})^2+u_{m-1}^2-u_{m-1}u_m\right]\\ &+\frac{1}{(k_1h_2+k_2h_1)k_2h_1}\left[-(k_2h_1+k_1h_2)u_{m-1}u_m+(k_2h_1+k_1h_2)u_m^2\right.\\ &\left.+k_2h_1u_m^2-k_2h_1u_mu_{m+1}\right]\\ &+\frac{1}{(k_1h_2+k_2h_1)k_1h_2}\left[-k_1h_2u_mu_{m+1}+k_1h_2u_{m+1}^2+(k_1h_2+k_2h_1)u_{m+1}^2\right.\\ &\left.-(k_1h_2+k_2h_1)u_{m+1}u_{m+2}\right]\\ &+\frac{1}{k_1h_2}\left[-u_{m+1}u_{m+2}+u_{m+1}^2+(u_{m+1}-u_{m+2})^2\cdots+(u_{M-2}-u_{M-1})^2+u_{M-1}^2\right]\\ &=\frac{1}{k_2h_1}\sum_{j=1}^{m}h_1^2g_ju_j+\frac{1}{k_1h_2}\sum_{j=m+1}^{M-1}h_2^2g_ju_j,\end{aligned} \tag{4.60}$$

The above equation can be simplified to

$$\begin{aligned}&\frac{1}{k_2}h_1\sum_{j=1}^{m-1}\left(\delta_x u_{j-\frac{1}{2}}\right)^2+\frac{k_0+1}{k_1k_0+k_2}\left(h_1+h_2\right)\left(\delta_x u_{m+\frac{1}{2}}\right)^2+\frac{1}{k_1}h_2\sum_{j=m+2}^{M-1}\left(\delta_x u_{j+\frac{1}{2}}\right)^2\\ =&\frac{1}{k_2h_1}\sum_{j=1}^{m}h_1^2g_ju_j+\frac{1}{k_1h_2}\sum_{j=m+1}^{M-1}h_2^2g_ju_j,\end{aligned}\tag{4.61}$$

where $k_0=\frac{h_1}{h_2}$, $\delta_x u_{j-\frac{1}{2}}=\frac{u_j-u_{j-1}}{h_1}$, $j=1,...,m-1$; $\delta_x u_{m+\frac{1}{2}}=\frac{2(u_{m+1}-u_m)}{h_1+h_2}$; $\delta_x u_{j+\frac{1}{2}}=\frac{u_{j+1}-u_j}{h_2}$, $j=m+2,...,M-1$. Denoting $|u|_1^2=h_1\sum_{j=1}^{m-1}\left(\delta_x u_{j-\frac{1}{2}}\right)^2+\left(h_1+h_2\right)\left(\delta_x u_{m+\frac{1}{2}}\right)^2$ $+h_2\sum_{j=m+2}^{M-1}\left(\delta_x u_{j+\frac{1}{2}}\right)^2$, we obtain the left-hand-side (LHS) of Eq. (4.61) as

$$\begin{aligned}LHS\geq&\min\left\{\frac{1}{k_2},\frac{k_0+1}{k_1k_0+k_2},\frac{1}{k_1}\right\}|u|_1^2\\ \equiv&\varepsilon_1|u|_1^2,\end{aligned}\tag{4.62}$$

where $\varepsilon_1=\min\left\{\frac{1}{k_2},\frac{k_0+1}{k_1k_0+k_2},\frac{1}{k_1}\right\}$. Denoting $\|u\|^2=h_1\sum_{j=1}^{m-1}u_j^2+h_2\sum_{j=m+1}^{M-1}u_j^2$, and using the Young's inequality, $ab\leq\epsilon a^2+\frac{1}{4\epsilon}b^2$, we obtain the right-hand-side (RHS) of Eq. (4.61) as

$$\begin{aligned}RHS\leq&\frac{1}{k_2}h_1\sum_{j=1}^{m}g_ju_j+\frac{1}{k_1}h_2\sum_{j=m+1}^{M-1}g_ju_j\\ \leq&\frac{1}{k_2}h_1\sum_{j=1}^{m}|g_ju_j|+\frac{1}{k_1}h_2\sum_{j=m+1}^{M-1}|g_ju_j|\\ \leq&\max\left\{\frac{1}{k_2},\frac{1}{k_1}\right\}\left[\sqrt{h_1\sum_{j=1}^{m}g_j^2}\cdot\sqrt{h_1\sum_{j=1}^{m}u_j^2}+\sqrt{h_2\sum_{j=m+1}^{M-1}g_j^2}\cdot\sqrt{h_2\sum_{j=m+1}^{M-1}u_j^2}\right]\\ \leq&\varepsilon_2\left(\epsilon h_1\sum_{j=1}^{m-1}u_j^2+\epsilon h_2\sum_{j=m+1}^{M-1}u_j^2+\frac{1}{4\epsilon}h_1\sum_{j=1}^{m-1}g_j^2+\frac{1}{4\epsilon}h_2\sum_{j=m+1}^{M-1}g_j^2\right)\\ \leq&\varepsilon_2\left(\epsilon\|u\|^2+\frac{1}{4\epsilon}\|g\|^2\right)\\ \leq&\varepsilon_2\left(\epsilon|u|_1^2+\frac{1}{4\epsilon}\|g\|^2\right),\end{aligned}\tag{4.63}$$

where $\varepsilon_2 = \max\left\{\frac{1}{k_2}, \frac{1}{k_1}\right\}$. Here, the fact, $\|u\|^2 < |u|_1^2$, has been used. Combining Eqs. (4.62)-(4.63) together yields

$$\begin{aligned}
\varepsilon_1 |u|_1^2 \leq & \varepsilon_2 \left(\epsilon |u|_1^2 + \frac{1}{4\epsilon} \|g\|^2\right) \\
\left(\frac{\varepsilon_1}{\varepsilon_2} - \epsilon\right) |u|_1^2 \leq & \frac{1}{4\epsilon} \|g\|^2 \\
|u|_1^2 \leq & \frac{2\varepsilon_1^2}{\varepsilon_2^2} \|g\|^2 \\
= & \varepsilon_3 \|g\|^2 .
\end{aligned} \tag{4.64}$$

Here, we have used $\epsilon = \frac{\varepsilon_1}{2\varepsilon_2}$ and $\varepsilon_3 = \frac{2\varepsilon_1^2}{\varepsilon_2^2}$.

From the above priori estimate, we now prove the stability and convergence of the scheme.

Theorem 4.3. *Assume that* $\left\{u_j^{(1)}\right\}$ *and* $\left\{u_j^{(2)}\right\}$ *are the numerical solutions obtained based on scheme Eqs. (4.30)-(4.32), and Eqs. (4.49)-(4.50) (or Eqs. (4.51)-(4.52), or Eqs. (4.53)-(4.54)) with the same boundary and interfacial conditions but different values of* $f_1^{(1)}(x)$, $f_2^{(1)}(x)$, $f_1^{(2)}(x)$, $f_2^{(2)}(x)$. *Let* $u = u^{(2)} - u^{(1)}$, $f_1(x) = f_1^{(2)}(x) - f_1^{(1)}(x)$, $f_2(x) = f_2^{(2)}(x) - f_2^{(1)}(x)$. *Then it holds*

$$|u|_1^2 \leq c\left(h_1 \sum_{j=1}^{m-1} (f_1)_j^2 + h_2 \sum_{j=m+1}^{M-1} (f_2)_j^2\right), \tag{4.65}$$

where c *is a constant, implying that the scheme is stable. It should be pointed out that the above estimate is a discrete analogue of Eq. (3.19) in Chapter 3.*

Theorem 4.4. *Assume that* $u(x_j)$ *and* u_j *are the exact solution of model Eqs. (4.24)-(4.28) and numerical solution of scheme Eqs. (4.30)-(4.32), and Eqs. (4.49)-(4.50) (or Eqs. (4.51)-(4.52), or Eqs. (4.53)-(4.54)). Let* $\epsilon = u(x_j) - u_j$.

Then it holds

$$|\epsilon|_1 \leq c\left(h_1^4 + h_2^4\right), \tag{4.66}$$

where c is a constant.

Proof. It can be seen that $\epsilon(x_j)$ satisfies

$$-\epsilon_{j-1} + 2\epsilon_j - \epsilon_{j+1} = h_1^2 R_j, \quad j = 1, ..., m-1, \tag{4.67}$$

$$\begin{aligned}&\frac{1}{k_1h_2 + k_2h_1}[-(k_2h_1 + k_1h_2)\epsilon_{m-1} + (k_2h_1 + k_1h_2)\epsilon_m + k_2h_1\varepsilon_m - k_2h_1\epsilon_{m+1}]\\ &= \left(h_1^2 + h_2^2\right) R_m,\end{aligned} \tag{4.68}$$

$$\begin{aligned}&\frac{1}{k_1h_2 + k_2h_1}\left[-k_1h_2\epsilon_m + k_1h_2\epsilon_{m+1} + (k_1h_2 + k_2h_1)\epsilon_{m+1} - (k_1h_2 + k_2h_1)\epsilon_{m+2}\right]\\ &= \left(h_1^2 + h_2^2\right) R_{m+1},\end{aligned} \tag{4.69}$$

$$-\epsilon_{j-1} + 2\epsilon_j - \epsilon_{j+1} = h_2^2 R_j, \quad j = m+2, ..., M-1, \tag{4.70}$$

where R_j is $O(h_1^4)$ when $1 \leq j \leq m$, $O(h_2^4)$ when $m+1 \leq j \leq M-1$. From the priori estimate, we obtain

$$|\epsilon|_1^2 \leq c\left(h_1 \sum_{j=1}^{m-1} (R_1)_j^2 + h_2 \sum_{j=m+1}^{M-1} (R_2)_j^2\right) \leq c\left(h_1^4 + h_2^4\right)^2. \tag{4.71}$$

4.4 Conclusion

In this chapter, we have proposed three higher-order compact finite difference schemes for solving the steady-state heat conduction model with the Dirichlet boundary in one dimensional double-layered solid structures. In particular, by using the GPM, we have proposed a kind of new third-order and fourth-order compact schemes at the interface. The overall scheme is a tridiagonal linear system, which can be efficiently solved using the Thomas algorithm. Furthermore, we have obtained a

priori estimate for the compact finite difference scheme, which is the discrete analogue of the energy estimate of the steady-state heat conduction model. Based on this priori estimate, the compact scheme is analyzed to be unconditionally stable and convergent with $O\left(h_1^4 + h_2^4\right)$. In next chapter, we will give the schemes for steady-state heat conduction model with Neumann boundary and Robin boundary, and the schemes for unsteady-state heat conduction model and nanoscale heat conduction model. As will be seen, we will keep using the generalized compact finite difference method on boundary and at interface, and using the idea of GPM to derive those schemes.

CHAPTER 5

NUMERICAL METHODS: PART II — SCHEMES FOR THE DOUBLE-LAYERED HEAT CONDUCTION MODELS

In this chapter, using the compact finite difference method and the gradient preserved method, a kind of higher-order compact finite difference schemes for aforementioned three mathematical models will be proposed. In particular, we will develop fourth-order compact schemes at the interface using only three-points in space.

5.1 Schemes for Steady State Heat Conduction Model

To develop higher-order accurate finite difference schemes for solving the elliptic problem in Eqs. (3.1)-(3.5), we first design a one-dimensional mesh and denote grid sizes to be $h_1 = l/m$, $h_2 = (L-l)/(M-m)$, respectively, where m, M $(m < M)$ are positive integers, as shown in Figure 5.1. Grid points in the mesh are denoted as $x_j = jh_1$, $0 \le j \le m$; $x_j = l + (j-m)\,h_2$, $m+1 \le j \le M$ and $\Omega_h = \{x_j | 0 \le j \le M\}$, where the interface is located at grid point $x_I = (m+1)\,h_1 = l$.

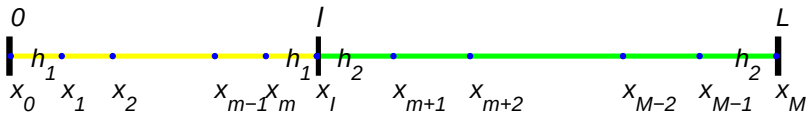

Figure 5.1: One-dimensional mesh for steady-state heat conduction model.

Denote u_j as the approximation of $u(x_j)$, and so on for others. We now develop a fourth-order compact finite difference scheme using three-points in space. We only consider the Neumann boundary and the Robin boundary here as the scheme for the Dirichlet boundary has been given in previous chapter.

For the interior points, $x_1 \le x_j \le x_{m-1}$ and $x_{m+2} \le x_j \le x_{M-1}$, the fourth-order Padé scheme gives

$$\frac{k_1(u_{j-1}-2u_j+u_{j+1})}{h_1^2} = \frac{1}{12}\left[(f_1)_{j-1}+10\,(f_1)_j+(f_1)_{j+1}\right], \quad 1 \le j \le m-1, \tag{5.1}$$

$$\frac{k_2(u_{j-1}-2u_j+u_{j+1})}{h_2^2} = \frac{1}{12}\left[(f_2)_{j-1}+10\,(f_2)_j+(f_2)_{j+1}\right], \quad m+2 \le j \le M-1. \tag{5.2}$$

For Neumann boundary condition, $u_x(0) = \phi_1$, Eq. (4.3a) yields

$$\begin{aligned} u_x(x_0) = &-\frac{31u(x_0)-32u(x_1)+u(x_2)}{30h_1} \\ &-\frac{h_1}{90}[35u_{xx}(x_0)+8u_{xx}(x_1)-u_{xx}(x_2)] \\ &-\frac{h_1^2}{15}u_{x^3}(x_0) + O\left(h_1^5\right). \end{aligned} \tag{5.3}$$

From Eq. (3.1), we have $u_{xx}(x_0) = \frac{f_1(x_0)}{k_1}$, $u_{xx}(x_1) = \frac{f_1(x_1)}{k_1}$, $u_{xx}(x_2) = \frac{f_1(x_2)}{k_1}$ and $u_{x^3}(x_0) = \frac{(f_1)_x(x_0)}{k_1}$. Substituting them into Eq. (5.3) gives

$$\begin{aligned} u_x(x_0) = &-\frac{31u(x_0)-32u(x_1)+u(x_2)}{30h_1} \\ &-\frac{h_1}{90k_1}[35f_1(x_0)+8f_1(x_1)-f_1(x_2)] \\ &-\frac{h_1^2}{15k_1}(f_1)_x(x_0) + O\left(h_1^5\right). \end{aligned} \tag{5.4}$$

With $u_x(0) = \phi_1$, after dropping the truncation error in Eqs. (5.4), we obtain

$$-31u_0+32u_1-u_2 = 30h_1\phi_1 + \frac{h_1^2}{3k_1}\left[35\,(f_1)_0+8\,(f_1)_1-(f_1)_2\right] + \frac{2h_1^3}{k_1}\left((f_1)_x\right)_0. \tag{5.5}$$

On the other hand, when $j = 1$, Eq. (5.1) gives

$$u_0 - 2u_1 + u_2 = \frac{h_1^2}{12k_1}\left[(f_1)_0 + 10\,(f_1)_1 + (f_1)_2\right]. \tag{5.6}$$

Adding Eq. (5.5) and Eq. (5.6) together leads to a fourth-order scheme as

$$\begin{aligned} &-30u_0 + 30u_1 \\ =&-30h_1\phi_1 + \frac{h_1^2}{12k_1}\left[141\,(f_1)_0 + 42\,(f_1)_1 - 3\,(f_1)_2\right] + \frac{2h_1^3}{k_1}\left((f_1)_x\right)_0, \end{aligned} \tag{5.7}$$

Similarly, from Eq. (3.2), we have $u_{xx}\,(x_M) = \frac{f_2(x_M)}{k_2}$, $u_{xx}\,(x_{M-1}) = \frac{f_2(x_{M-1})}{k_2}$, $u_{xx}\,(x_{M-2}) = \frac{f_2(x_{M-2})}{k_2}$ and $u_{x^3}\,(x_M) = \frac{(f_2)_x(x_M)}{k_2}$. By using Eq. (4.3b), we obtain

$$\begin{aligned} u_x\,(x_M) =&\frac{31u\,(x_M) - 32u\,(x_{M-1}) + u\,(x_{M-2})}{30h_2} \\ &+\frac{h_2}{90k_2}\left(35f_2\,(x_M)+8f_2\,(x_{M-1})-f_2(x_{M-2})\right)-\frac{h_2^2}{15k_2}(f_2)_x(x_M)+O\left(h_2^5\right). \end{aligned} \tag{5.8}$$

Dropping the truncation error in Eq. (5.8) and using $u_x\,(x_M) = \phi_2$ gives

$$\begin{aligned} &-31u_M + 32u_{M-1} - u_{M-2} \\ =&-30h_2\phi_2+\frac{h_2^2}{3k_2}\left[35\,(f_2)_M+8\,(f_2)_{M-1}-(f_2)_{M-2}\right]-\frac{2h_2^3}{k_2}\left((f_2)_x\right)_M. \end{aligned} \tag{5.9}$$

On the other hand, from Eq. (5.2), when $j = M - 1$, we have

$$u_{M-2} - 2u_{M-1} + u_M = \frac{h_2^2}{12k_2}\left[(f_2)_{M-2} + 10\,(f_2)_{M-1}\,(f_2)_M\right]. \tag{5.10}$$

Adding Eq. (5.9) and Eq. (5.10) together gives a fourth-order scheme as

$$\begin{aligned} &30u_{M-1} - 30u_M \\ =&-30h_2\phi_2 + \frac{h_2^2}{12k_2}\left[-3\,(f_2)_{M-2} + 42\,(f_2)_{M-1} + 141\,(f_2)_M\right] - \frac{2h_2^3}{k_2}\left((f_2)_x\right)_M. \end{aligned} \tag{5.11}$$

For Robin boundary condition, Eq. (3.5c), one may simply replace ϕ_1 and ϕ_2 in Eq. (5.7) and Eq. (5.11) with $\frac{\phi_1-\gamma_1u_0}{-\alpha_1}$ and $\frac{\phi_2-\gamma_2u_M}{\alpha_2}$, respectively. This gives a

fourth-order scheme as

$$\begin{aligned}
&-30\left(1+\frac{h_1\gamma_1}{\alpha_1}\right)u_0+30u_1\\
=&-30h_1\frac{\phi_1}{\alpha_1}+\frac{h_1^2}{12k_1}\left[141\left(f_1\right)_0+42\left(f_1\right)_1-3\left(f_1\right)_2\right]+\frac{2h_1^3}{k_1}\left(\left(f_1\right)_x\right)_0, \qquad (5.12)\\
&30u_{M-1}-30\left(1+\frac{h_2\gamma_2}{\alpha_2}\right)u_M\\
=&-30h_2\frac{\phi_2}{a_2}+\frac{h_2^2}{12k_2}\left[-3\left(f_2\right)_{M-2}+42\left(f_2\right)_{M-1}+141\left(f_2\right)_M\right]-\frac{2h_2^3}{k_2}\left(\left(f_2\right)_x\right)_M. \qquad (5.13)
\end{aligned}$$

At the interface, we already had the scheme, which is either the fourth-order scheme, Eqs. (4.49)-(4.50) or the third-order scheme, Eqs. (4.51)-(4.52) or Eqs. (4.53)-(4.54).

Thus, Eqs. (5.1)-(5.2), Eqs. (5.7) and (5.11), and Eqs. (4.49)-(4.50) together form a higher-order accurate finite difference scheme for the heat conduction model in steady-state with Dirichlet boundary. The scheme can be rewritten in matrix form as

$$A_N\vec{u}=\vec{d}_N, \qquad (5.14)$$

where $\vec{u}=\left[u_0,u_1,u_2,...,u_{m-2},u_{m-1},u_m,u_{m+1},u_{m+2},u_{m+3},...,u_{M-2},u_{M-1},u_M\right]^T$,

$$A_N = \begin{bmatrix}
-30 & 30 & & & & & & & & & & & \\
1 & -2 & 1 & & & & & & & & & & \\
& \ddots & \ddots & \ddots & & & & & & & & & \\
& & 1 & -2 & 1 & & & & & & & & \\
& & & \frac{2(k_1h_2+k_2h_1)}{2k_2h_1+k_1h_2} & -2 & \frac{2k_2h_1}{2k_2h_1+k_1h_2} & & & & & & & \\
& & & & \frac{2k_1h_2}{2k_1h_2+k_2h_1} & -2 & \frac{2(k_1h_2+k_2h_1)}{2k_1h_2+k_2h_1} & & & & & & \\
& & & & & 1 & -2 & 1 & & & & & \\
& & & & & & \ddots & \ddots & \ddots & & & & \\
& & & & & & & & & 1 & -2 & 1 & \\
& & & & & & & & & & 30 & -30 &
\end{bmatrix}$$

$$\text{and } \vec{d}_N = \begin{bmatrix}
30h_1\phi_1 + \frac{h_1^2}{12k_1}\left[141\left(f_1\right)_0 + 42\left(f_1\right)_1 - 3\left(f_1\right)_2\right] + \frac{2h_1^3}{k_1}\left(\left(f_1\right)_x\right)_0 \\
\frac{h_1^2}{12k_1}\left[\left(f_1\right)_0 + 10\left(f_1\right)_1 + \left(f_1\right)_2\right] \\
\frac{h_1^2}{12k_1}\left[\left(f_1\right)_1 + 10\left(f_1\right)_2 + \left(f_1\right)_3\right] \\
\vdots \\
\frac{h_1^2}{12k_1}\left[\left(f_1\right)_{m-2} + 10\left(f_1\right)_{m-1} + \left(f_1\right)_m\right] \\
c_5 \\
c_6 \\
\frac{h_2^2}{12k_2}\left[\left(f_2\right)_{m+1} + 10\left(f_2\right)_{m+2} + \left(f_2\right)_{m+3}\right] \\
\frac{h_2^2}{12k_2}\left[\left(f_2\right)_{m+2} + 10\left(f_2\right)_{m+3} + \left(f_2\right)_{m+4}\right] \\
\vdots \\
\frac{h_2^2}{12k_2}\left[\left(f_2\right)_{M-3} + 10\left(f_2\right)_{M-2} + \left(f_2\right)_{M-1}\right] \\
\frac{h_2^2}{12k_2}\left[\left(f_2\right)_{M-2} + 10\left(f_2\right)_{M-1} + \left(f_2\right)_M\right] \\
-30h_2\phi_2 + \frac{h_2^2}{12k_2}\left[-3\left(f_2\right)_{M-2} + 42\left(f_2\right)_{M-1} + 141\left(f_2\right)_M\right] - \frac{2h_2^3}{k_2}\left(\left(f_2\right)_x\right)_M
\end{bmatrix},$$

where c_5, c_6 are given in Eqs. (4.49)-(4.50). By Gauss elimination, we can obtain the determinant of A_N, which is zero. Hence, A_N is singular. This is a kind of tricky and has to be careful when computing. To solve the numerical solution uniquely, we fix

$$u_0 = 0. \tag{5.15}$$

Same as the Dirichlet boundary case, the values of u_{I^-}, u_{I^+}, $(u_x)_{I^-}$ and $(u_x)_{I^+}$ can be obtained by using Eqs. (4.37)-(4.42).

Eqs. (5.1)-(5.2), Eqs. (5.7) and (5.11), and Eqs. (4.49)-(4.50) together form a higher-order accurate finite difference scheme for the heat conduction model in steady state with Robin boundary. The scheme can be rewritten in matrix form as

$$A_R\vec{u} = \vec{d}_R, \tag{5.16}$$

where $\vec{u} = [u_0, u_1, u_2, ..., u_{m-2}, u_{m-1}, u_m, u_{m+1}, u_{m+2}, u_{m+3,}..., u_{M-2}, u_{M-1}, u_M]^T$,

$$A_R = \begin{bmatrix}
-30\left(1+\frac{h_1\gamma_1}{\alpha_1}\right) & 30 & & & & & & & & & & & \\
1 & -2 & 1 & & & & & & & & & & \\
& \ddots & \ddots & \ddots & & & & & & & & & \\
& & 1 & -2 & 1 & & & & & & & & \\
& & & \frac{2(k_1h_2+k_2h_1)}{2k_2h_1+k_1h_2} & -2 & \frac{2k_2h_1}{2k_2h_1+k_1h_2} & & & & & & & \\
& & & & \frac{2k_1h_2}{2k_1h_2+k_2h_1} & -2 & \frac{2(k_1h_2+k_2h_1)}{2k_1h_2+k_2h_1} & & & & & & \\
& & & & & 1 & -2 & 1 & & & & & \\
& & & & & & \ddots & \ddots & \ddots & & & & \\
& & & & & & & 1 & -2 & 1 & & & \\
& & & & & & & & 30 & -30\left(1+\frac{h_2\gamma_2}{\alpha_2}\right)
\end{bmatrix}$$

$$\text{and } \vec{d}_R = \begin{bmatrix} -30h_1\frac{\phi_1}{\alpha_1} + \frac{h_1^2}{12k_1}\left[141\left(f_1\right)_0 + 42\left(f_1\right)_1 - 3\left(f_1\right)_2\right] + \frac{2h_1^3}{k_1}\left(\left(f_1\right)_x\right)_0 \\ \frac{h_1^2}{12k_1}\left[\left(f_1\right)_1 + 10\left(f_1\right)_2 + \left(f_1\right)_3\right] \\ \frac{h_1^2}{12k_1}\left[\left(f_1\right)_2 + 10\left(f_1\right)_3 + \left(f_1\right)_4\right] \\ \vdots \\ \frac{h_1^2}{12k_1}\left[\left(f_1\right)_{m-2} + 10\left(f_1\right)_{m-1} + \left(f_1\right)_m\right] \\ c_5 \\ c_6 \\ \frac{h_2^2}{12k_2}\left[\left(f_2\right)_{m+1} + 10\left(f_2\right)_{m+2} + \left(f_2\right)_{m+3}\right] \\ \frac{h_2^2}{12k_2}\left[\left(f_2\right)_{m+2} + 10\left(f_2\right)_{m+3} + \left(f_2\right)_{m+4}\right] \\ \vdots \\ \frac{h_2^2}{12k_2}\left[\left(f_2\right)_{M-4} + 10\left(f_2\right)_{M-3} + \left(f_2\right)_{M-2}\right] \\ \frac{h_2^2}{12k_2}\left[\left(f_2\right)_{M-3} + 10\left(f_2\right)_{M-2} + \left(f_2\right)_{M-1}\right] \\ -30h_2\frac{\phi_2}{a_2} + \frac{h_2^2}{12k_2}\left[-3\left(f_2\right)_{M-2} + 42\left(f_2\right)_{M-1} + 141\left(f_2\right)_M\right] - \frac{2h_2^3}{k_2}\left(\left(f_2\right)_x\right)_M \end{bmatrix}.$$

Again, A_R is a tridiagonal matrix, so one can use the Thomas algorithm to obtain the solution efficiently. Once the values of u_{m-1}, u_m, u_{m+1} and u_{m+2} are obtained, the values of u_{I^-}, u_{I^+}, $(u_x)_{I^-}$ and $(u_x)_{I^+}$ can be easily obtained by using Eqs. (4.37)-(4.42).

5.2 Schemes for Unsteady State Heat Conduction Model

To develop higher-order accurate finite difference schemes for solving the heat conduction problem in Eqs. (3.19)-(3.24), we first design a mesh, as shown in Figure 5.2, where grid sizes and time step are $h_1 = l/m$, $h_2 = (L-l)/(M-m)$, $\Delta t = T/N$, respectively, and m, M $(m < M)$ and N are positive integers. Grid points in the

mesh are denoted as $x_j = jh_1,\ 0 \le j \le m;\ x_j = l + (j-m)\,h_2,\ m+1 \le j \le M;$ $t_n = n\Delta t,\ 0 \le n \le N$ and $\Omega_h = \{x_j | 0 \le j \le M\}$, $\Omega_{\Delta t} = \{t_n | 0 \le n \le N\}$, where the interface is located at grid point $x_I = (m+1)\,h_1 = l$.

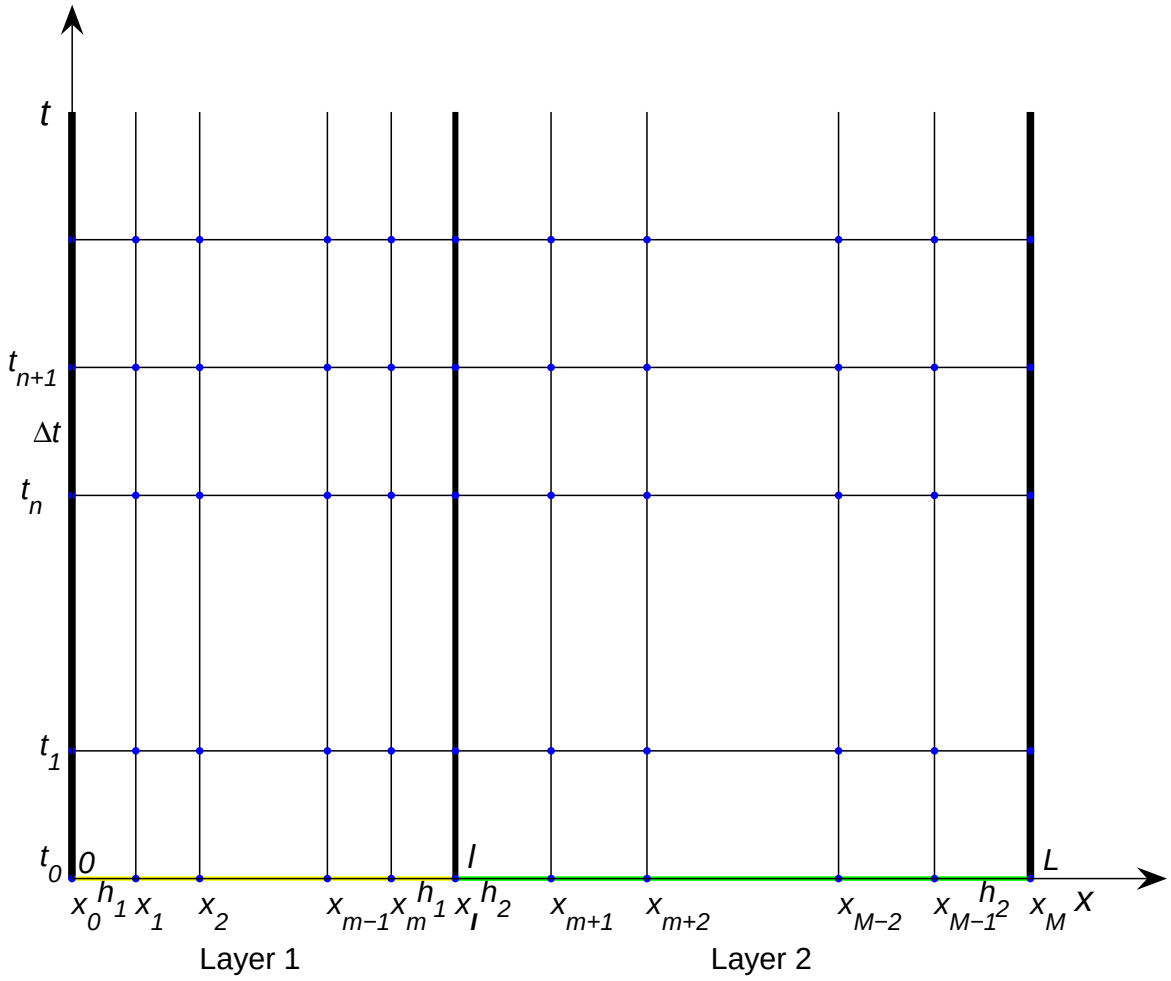

Figure 5.2: Two-dimensional mesh for unsteady-state heat conduction model.

We now develop a higher-order accurate compact finite difference scheme using three-points in space and two-levels in time. Higher-order, third-order or fourth-order always mean the order of accuracy in spatial dimension in this dissertation. Denote u_j^n as the approximation of $u\,(x_j, t_n)$.

For the interior points, $x_1 \leq x_j \leq x_{m-1}$, by the fourth-order Padé scheme, we have

$$\begin{aligned}
&\frac{1}{12}\left[u_{xx}\left(x_{j-1},t\right)+10u_{xx}\left(x_j,t\right)+u_{xx}\left(x_{j+1},t\right)\right]\\
=&\frac{1}{h_1^2}\left[u\left(x_{j-1},t\right)-2u\left(x_j,t\right)+u\left(x_{j+1},t\right)\right]+O\left(h_1^4\right).
\end{aligned} \tag{5.17}$$

Substituting it into Eq. (3.19) gives

$$\begin{aligned}
&\frac{\rho_1 C_1}{12}\left[u_t\left(x_{j-1},t\right)+10u_t\left(x_j,t\right)+u_t\left(x_{j+1},t\right)\right]\\
=&\frac{k_1}{h_1^2}\left[u\left(x_{j-1},t\right)-2u\left(x_j,t\right)+u\left(x_{j+1},t\right)\right]\\
&+\frac{1}{12}\left[f_1\left(x_{j-1},t\right)+10f_1\left(x_j,t\right)+f_1\left(x_{j+1},t\right)\right]+O\left(h_1^4\right).
\end{aligned} \tag{5.18}$$

Using the Crank-Nicolson method, we obtain

$$\begin{aligned}
&\frac{\rho_1 C_1}{12}\left[\frac{u\left(x_{j-1},t_{n+1}\right)-u\left(x_{j-1},t_n\right)}{\Delta t}\right.\\
&+10\frac{u\left(x_j,t_{n+1}\right)-u\left(x_j,t_n\right)}{\Delta t}\\
&\left.+\frac{u\left(x_{j+1},t_{n+1}\right)-u\left(x_{j+1},t_n\right)}{\Delta t}\right]\\
=&\frac{k_1}{2h_1^2}\left[u\left(x_{j-1},t_{n+1}\right)-2u\left(x_j,t_{n+1}\right)+u\left(x_{j+1},t_{n+1}\right)\right]\\
&+\frac{k_1}{2h_1^2}\left[u\left(x_{j-1},t_n\right)-2u\left(x_j,t_n\right)+u\left(x_{j+1},t_n\right)\right]\\
&+\frac{1}{12}\left[f_1\left(x_{j-1},t_{n+\frac{1}{2}}\right)+10f_1\left(x_j,t_{n+\frac{1}{2}}\right)+f_1\left(x_{j+1},t_{n+\frac{1}{2}}\right)\right]+O\left(h_1^4+\Delta t^2\right).
\end{aligned} \tag{5.19}$$

Dropping the truncation error yields a fourth-order compact scheme as

$$\begin{aligned}
&\left(\frac{\rho_1 C_1}{12\Delta t}-\frac{k_1}{2h_1^2}\right)u_{j-1}^{n+1}+\left(\frac{10\rho_1 C_1}{12\Delta t}+\frac{k_1}{h_1^2}\right)u_j^{n+1}+\left(\frac{\rho_1 C_1}{12\Delta t}-\frac{k_1}{2h_1^2}\right)u_{j+1}^{n+1}\\
=&\left(\frac{\rho_1 C_1}{12\Delta t}+\frac{k_1}{2h_1^2}\right)u_{j-1}^{n}+\left(\frac{10\rho_1 C_1}{12\Delta t}-\frac{k_1}{h_1^2}\right)u_j^{n}+\left(\frac{\rho_1 C_1}{12\Delta t}+\frac{k_1}{2h_1^2}\right)u_{j+1}^{n}\\
&+\frac{1}{12}\left[\left(f_1\right)_{j-1}^{n+\frac{1}{2}}+10\left(f_1\right)_j^{n+\frac{1}{2}}+\left(f_1\right)_{j+1}^{n+\frac{1}{2}}\right],\ 1\leq j\leq m-1.
\end{aligned} \tag{5.20}$$

Multiplying both sides by $\frac{12\Delta t}{\rho_1 C_1}$, and letting $\mu_1 = \frac{6k_1\Delta t}{\rho_1 C_1 h_1^2}$, $\lambda_1 = \frac{\Delta t}{\rho_1 C_1}$, we can rewrite the above equation in a simple way as

$$\begin{aligned}
&(1-\mu_1)\,u_{j-1}^{n+1} + (10+2\mu_1)\,u_j^{n+1} + (1-\mu_1)\,u_{j+1}^{n+1} \\
&= (1+\mu_1)\,u_{j-1}^{n} + (10-2\mu_1)\,u_j^{n} + (1+\mu_1)\,u_{j+1}^{n} \\
&\quad + \lambda_1\left[(f_1)_{j-1}^{n+\frac{1}{2}} + 10\,(f_1)_j^{n+\frac{1}{2}} + (f_1)_{j+1}^{n+\frac{1}{2}}\right],\ 1 \le j \le m-1. \qquad (5.21)
\end{aligned}$$

Similarly, for the interior points, $x_{m+2} \le x_j \le x_{M-1}$, a fourth-order compact scheme can be obtained as

$$\begin{aligned}
&\left(\frac{\rho_2 C_2}{12\Delta t} - \frac{k_2}{2h_2^2}\right) u_{j-1}^{n+1} + \left(\frac{10\rho_2 C_2}{12\Delta t} + \frac{k_2}{h_2^2}\right) u_j^{n+1} + \left(\frac{\rho_2 C_2}{12\Delta t} - \frac{k_2}{2h_2^2}\right) u_{j+1}^{n+1} \\
&= \left(\frac{\rho_2 C_2}{12\Delta t} + \frac{k_2}{2h_2^2}\right) u_{j-1}^{n} + \left(\frac{10\rho_2 C_2}{12\Delta t} - \frac{k_2}{h_2^2}\right) u_j^{n} + \left(\frac{\rho_2 C_2}{12\Delta t} + \frac{k_2}{2h_2^2}\right) u_{j+1}^{n} \\
&\quad + \frac{1}{12}\left[(f_2)_{j-1}^{n+\frac{1}{2}} + 10\,(f_2)_j^{n+\frac{1}{2}} + (f_2)_{j+1}^{n+\frac{1}{2}}\right],\ m+2 \le j \le M-1. \qquad (5.22)
\end{aligned}$$

Again, multiplying both sides by $\frac{12\Delta t}{\rho_2 C_2}$, then letting $\mu_2 = \frac{6k_2\Delta t}{\rho_2 C_2 h_2^2}$, $\lambda_2 = \frac{\Delta t}{\rho_2 C_2}$, we obtain a simple form of Eq. (5.22) as

$$\begin{aligned}
&(1-\mu_2)\,u_{j-1}^{n+1} + (10+2\mu_2)\,u_j^{n+1} + (1-\mu_2)\,u_{j+1}^{n+1} \\
&= (1+\mu_2)\,u_{j-1}^{n} + (10-2\mu_2)\,u_j^{n} + (1+\mu_2)\,u_{j+1}^{n} \\
&\quad + \lambda_2\left[(f_2)_{j-1}^{n+\frac{1}{2}} + 10\,(f_2)_j^{n+\frac{1}{2}} + (f_2)_{j+1}^{n+\frac{1}{2}}\right],\ m+2 \le j \le M-1. \qquad (5.23)
\end{aligned}$$

At the boundary points, x_0 and x_M, we simply set

$$u_0^{n+1} = (\phi_1)^{n+1}, \quad u_M^{n+1} = (\phi_2)^{n+1}, \qquad (5.24)$$

for Dirichlet boundary condition, Eq. (3.24a).

For Neumann boundary condition, $u_x(0,t) = \phi_1(t)$, using Eq. (4.2a) and Eq. (4.3a), respectively, we have

$$\begin{aligned} u_x(x_0,t) =& \frac{u(x_1,t) - u(x_0,t)}{h_1} - \frac{h_1}{12}\left(5u_{xx}(x_0,t) + u_{xx}(x_1,t)\right) \\ & - \frac{h_1^2}{12}u_{x^3}(x_0,t) + O\left(h_1^4\right), \end{aligned} \tag{5.25}$$

$$\begin{aligned} u_x(x_0,t) =& -\frac{31u(x_0,t) - 32u(x_1,t) + u(x_2,t)}{30h_1} \\ & - \frac{h_1}{90}\left[35u_{xx}(x_0,t) + 8u_{xx}(x_1,t) - u_{xx}(x_2,t)\right] \\ & - \frac{h_1^2}{15}u_{x^3}(x_0,t) + O\left(h_1^5\right). \end{aligned} \tag{5.26}$$

Eq. (3.19) gives us the following equations:

$$\rho_1 C_1 u_t(x_j,t) = k_1 u_{xx}(x_j,t) + f_1(x_j,t), \quad j = 0,1,2, \tag{5.27a}$$

$$\rho_1 C_1 u_{xt}(x_0,t) = k_1 u_{x^3}(x_0,t) + (f_1)_x(x_0,t). \tag{5.27b}$$

Solving $u_{xx}(x_0,t)$, $u_{xx}(x_1,t)$, $u_{xx}(x_2,t)$ and $u_{x^3}(x_0,t)$, and substituting them into Eq. (5.25) and Eq. (5.26), respectively, we obtain

$$\begin{aligned} u_x(x_0,t) =& \frac{u(x_1,t) - u(x_0,t)}{h_1} - \frac{h_1\rho_1 C_1}{12k_1}\left[5u_t(x_0,t) + u_t(x_1,t)\right] \\ & + \frac{h_1}{12k_1}\left[5f_1(x_0,t) + f_1(x_1,t)\right] \\ & - \frac{h_1^2}{12k_1}\left(\rho_1 C_1 u_{xt}(x_0,t) - (f_1)_x(x_0,t)\right) + O\left(h_1^4\right), \end{aligned} \tag{5.28}$$

$$\begin{aligned} u_x(x_0,t) =& -\frac{31u(x_0,t) - 32u(x_1,t) + u(x_2,t)}{30h_1} \\ & - \frac{h_1\rho_1 C_1}{90k_1}\left[35u_t(x_0,t) + 8u_t(x_1,t) - u_t(x_2,t)\right] \\ & + \frac{h_1}{90k_1}\left(35f_1(x_0,t) + 8f_1(x_1,t) - f_1(x_2,t)\right) \\ & - \frac{h_1^2}{15k_1}\left(\rho_1 C_1 u_{xt}(x_0,t) - (f_1)_x(x_0,t)\right) + O\left(h_1^5\right). \end{aligned} \tag{5.29}$$

Then, the Crank-Nicolson method gives

$$\begin{aligned}
&\frac{(u_x)_0^{n+1}+(u_x)_0^n}{2}\\
=&\frac{u_1^{n+1}-u_0^{n+1}}{2h_1}+\frac{u_1^n-u_0^n}{2h_1}\\
&-\frac{h_1\rho_1 C_1}{12k_1}\left[5\frac{u_0^{n+1}-u_0^n}{\Delta t}+\frac{u_1^{n+1}-u_1^n}{\Delta t}\right]+\frac{h_1}{12k_1}\left[5\left(f_1\right)_0^{n+\frac{1}{2}}+\left(f_1\right)_1^{n+\frac{1}{2}}\right]\\
&-\frac{h_1^2\rho_1 C_1}{12k_1}\frac{(u_x)_0^{n+1}-(u_x)_0^n}{\Delta t}+\frac{h_1^2}{12k_1}\left(\left(f_1\right)_x\right)_0^{n+\frac{1}{2}}+O\left(h_1^4+\Delta t^2\right), \qquad (5.30)
\end{aligned}$$

and

$$\begin{aligned}
&\frac{(u_x)_0^{n+1}+(u_x)_0^n}{2}\\
=&-\frac{31u_0^{n+1}-32u_1^{n+1}+u_2^{n+1}}{60h_1}-\frac{31u_0^n-32u_1^n+u_2^n}{60h_1}\\
&-\frac{h_1\rho_1 C_1}{90k_1}\left(35\frac{u_0^{n+1}-u_0^n}{\Delta t}+8\frac{u_1^{n+1}-u_1^n}{\Delta t}-\frac{u_2^{n+1}-u_2^n}{\Delta t}\right)\\
&+\frac{h_1}{90k_1}\left[35\left(f_1\right)_0^{n+\frac{1}{2}}+8\left(f_1\right)_1^{n+\frac{1}{2}}-\left(f_1\right)_2^{n+\frac{1}{2}}\right]\\
&-\frac{h_1^2\rho_1 C_1}{15k_1}\frac{(u_x)_0^{n+1}-(u_x)_0^n}{\Delta t}+\frac{h_1^2}{15k_1}\left(\left(f_1\right)_x\right)_0^{n+\frac{1}{2}}+O\left(h_1^5+\Delta t^2\right). \qquad (5.31)
\end{aligned}$$

It should be pointed out that we only discretized u_{xt} on the time direction, but kept the space direction without discretization. This means the GPM was used. Dropping the truncation errors and rearranging the terms in Eqs. (5.30)-(5.31) and using $u_x(0,t)=\phi_1(t)$ gives us a third-order scheme and a fourth-order scheme, respectively, as

$$\begin{aligned}
&\left(5+\mu_1\right)u_0^{n+1}+\left(1-\mu_1\right)u_1^{n+1}\\
=&\left(5-\mu_1\right)u_0^n+\left(1+\mu_1\right)u_1^n+\lambda_1\left[5\left(f_1\right)_0^{n+\frac{1}{2}}+\left(f_1\right)_1^{n+\frac{1}{2}}\right]+\lambda_1 h_1\left(\left(f_1\right)_x\right)_0^{n+\frac{1}{2}}\\
&-h_1\left(1+\mu_1\right)\left(\phi_1\right)^{n+1}+h_1\left(1-\mu_1\right)\left(\phi_1\right)^n, \qquad (5.32)
\end{aligned}$$

and

$$\begin{aligned}
&(140+31\mu_1)\,u_0^{n+1}+(32-32\mu_1)\,u_1^{n+1}-(4-\mu_1)\,u_2^{n+1}\\
=&\,(140-31\mu_1)\,u_0^{n}+(32+32\mu_1)\,u_1^{n}-(4+\mu_1)\,u_2^{n}\\
&+4\lambda_1\left[35\,(f_1)_0^{n+\frac{1}{2}}+8\,(f_1)_1^{n+\frac{1}{2}}-(f_1)_2^{n+\frac{1}{2}}\right]+24\lambda_1 h_1\,((f_1)_x)_0^{n+\frac{1}{2}}\\
&-h_1\,(24+30\mu_1)\,(\phi_1)^{n+1}+h_1\,(24-30\mu_1)\,(\phi_1)^{n},
\end{aligned}\tag{5.33}$$

where $\mu_1=\frac{6k_1\Delta t}{\rho_1 C_1 h_1^2}$, $\lambda_1=\frac{\Delta t}{\rho_1 C_1}$. When $j=1$, Eq. (5.21) becomes

$$\begin{aligned}
&(1-\mu_1)\,u_0^{n+1}+(10+2\mu_1)\,u_1^{n+1}+(1-\mu_1)\,u_2^{n+1}\\
=&\,(1+\mu_1)\,u_0^{n}+(10-2\mu_1)\,u_1^{n}+(1+\mu_1)\,u_2^{n}\\
&+\lambda_1\left[(f_1)_0^{n+\frac{1}{2}}+10\,(f_1)_1^{n+\frac{1}{2}}+(f_1)_2^{n+\frac{1}{2}}\right].
\end{aligned}\tag{5.34}$$

Multiplying Eq. (5.33) and Eq. (5.34) by $(1-\mu_1)$ and $(4-\mu_1)$, respectively, then adding them together, after simplification, we obtain

$$\begin{aligned}
&\left(144-114\mu_1-30\mu_1^2\right)u_0^{n+1}+\left(72-66\mu_1+30\mu_1^2\right)u_1^{n+1}\\
=&\left(144-168\mu_1+30\mu_1^2\right)u_0^{n}+\left(72-18\mu_1-30\mu_1^2\right)u_1^{n}+6\mu_1 u_2^{n}\\
&+\lambda_1\,(144-141\mu_1)\,(f_1)_0^{n+\frac{1}{2}}+\lambda_1\,(72-42\mu_1)\,(f_1)_1^{n+\frac{1}{2}}+3\lambda_1\mu_1\,(f_1)_2^{n+\frac{1}{2}}\\
&+24h_1\lambda_1\,(1-\mu_1)\,((f_1)_x)_0^{n+\frac{1}{2}}-h_1\,(1-\mu_1)\,(24+30\mu_1)\,(\phi_1)^{n+1}\\
&+h_1\,(1-\mu_1)\,(24+30\mu_1)\,(\phi_1)^{n},
\end{aligned}\tag{5.35}$$

As we can see from Eq. (5.35), $|144-114\mu_1-30\mu_1^2|>|72-66\mu_1+30\mu_1^2|$ is not true for some values of the parameter, such as $\mu_1=1$. Hence, the third-order scheme, Eq. (5.32), will be used for Neumann boundary condition, $u_x\,(0,t)=\phi_1\,(t)$. Similarly, for the other side of the Neumann boundary condition, $u_x\,(L,t)=\phi_2\,(t)$, by Eq. (4.2b),

we have

$$\begin{aligned} u_x(L,t) =& \frac{u(x_M,t)-u(x_{M-1},t)}{h_2} \\ &+ \frac{h_2}{12}\left[5u_{xx}(x_M,t)+u_{xx}(x_{M-1},t)\right] \\ &- \frac{h_2^2}{12}u_{x^3}(x_M,t)+O\left(h_2^4\right). \end{aligned} \tag{5.36}$$

Using the similar argument, we obtain a third-order scheme as

$$\begin{aligned} &(1-\mu_2)\,u_{M-1}^{n+1}+(5+\mu_2)\,u_M^{n+1} \\ =&(1+\mu_2)\,u_{M-1}^{n}+(5-\mu_2)\,u_M^{n}+\lambda_2\left[(f_2)_{M-1}^{n+\frac{1}{2}}+5\,(f_2)_M^{n+\frac{1}{2}}\right] \\ &-h_2\lambda_2\left((f_2)_x\right)_M^{n+\frac{1}{2}}+h_2(\mu_2+1)\,(\phi_2)^{n+1}-(1-\mu_2)\,(\phi_2)^n, \end{aligned} \tag{5.37}$$

where $\mu_2=\frac{k_2\Delta t}{\rho_2 C_2 h_2^2}$, $\lambda_2=\frac{\Delta t}{\rho_2 C_2}$.

For Robin boundary condition, Eq. (3.24c), we replace $(\phi_1)^{n+1}$, $(\phi_1)^n$, $(\phi_2)^{n+1}$ and $(\phi_2)^n$ by $\frac{(\phi_1)^{n+1}}{-\alpha_1}+\frac{\gamma_1}{\alpha_1}u_0^{n+1}$, $\frac{(\phi_1)^n}{-\alpha_1}+\frac{\gamma_1}{\alpha_1}u_0^n$, $\frac{(\phi_2)^{n+1}}{\alpha_2}-\frac{\gamma_2}{\alpha_2}u_M^{n+1}$ and $\frac{(\phi_2)^n}{\alpha_2}-\frac{\gamma_2}{\alpha_2}u_M^n$, respectively, in Eq. (5.32) and Eq. (5.37), and obtain a third-order scheme as

$$\begin{aligned} &\left[5+\mu_1+\frac{\gamma_1}{\alpha_1}h_1(1+\mu_1)\right]u_0^{n+1}+(1-\mu_1)\,u_1^{n+1} \\ =&\left[5-\mu_1+\frac{\gamma_1}{\alpha_1}h_1(1-\mu_1)\right]u_0^{n}+(1+\mu_1)\,u_1^{n}+\lambda_1\left[5\,(f_1)_0^{n+\frac{1}{2}}+(f_1)_1^{n+\frac{1}{2}}\right] \\ &+h_1\lambda_1\left((f_1)_x\right)_0^{n+\frac{1}{2}}+\frac{1}{\alpha_1}h_1(1+\mu_1)\,(\phi_1)^{n+1}-\frac{1}{\alpha_1}h_1(1-\mu_1)\,(\phi_1)^n, \end{aligned} \tag{5.38}$$

$$\begin{aligned} &(1-\mu_2)\,u_{M-1}^{n+1}+\left[5+\mu_2+\frac{\gamma_2}{\alpha_2}h_2(1+\mu_2)\right]u_M^{n+1} \\ =&(1+\mu_2)\,u_{M-1}^{n}+\left(5-\mu_2+\frac{\gamma_2}{\alpha_2}h_2(1-\mu_2)\right)u_M^{n} \\ &+\frac{1}{12}\left[(f_2)_{M-1}^{n+\frac{1}{2}}+5\,(f_2)_M^{n+\frac{1}{2}}\right]-\frac{h_2}{12}\left((f_2)_x\right)_M^{n+\frac{1}{2}} \\ &+\frac{1}{\alpha_2}h_2(1+\mu_2)\,(\phi_2)^{n+1}-\frac{1}{\alpha_2}h_2(1-\mu_2)\,(\phi_2)^n. \end{aligned} \tag{5.39}$$

At grid points around interface x_I, we have the similar equations to Eqs. (4.37)-(4.42) as

$$u_{I^+}(t) - u_{I^-}(t) = a(t), \tag{5.40}$$

$$k_2 (u_x)_{I^+}(t) - k_1 (u_x)_{I^-}(t) = b(t), \tag{5.41}$$

$$u(x_{m-1}, t) - 32u(x_m, t) + 31u_{I^-}(t) - 30h_1 (u_x)_{I^-}(t) = c_1(t), \tag{5.42}$$

$$u(x_m, t) - 32u(x_{m+1}, t) + 31u_{I^+}(t) + 30h_2 (u_x)_{I^+}(t) = c_2(t), \tag{5.43}$$

$$u(x_{m-1}, t) - 2u(x_m, t) + u_{I^-}(t) = c_3(t), \tag{5.44}$$

$$u(x_{m+2}, t) - 2u(x_{m+1}, t) + u_{I^+}(t) = c_4(t), \tag{5.45}$$

where $c_1(t) = -\frac{h_1^2}{3k_1}[35(\rho_1 C_1 u_t(t) - f_1(t))_{I^-} + 8(\rho_1 C_1 u_t(t) - f_1(t))_m$

$$-(\rho_1 C_1 u_t(t) - f_1(t))_{m-1} - 6h_1(\rho_1 C_1 u_{xt}(t) - (f_1)_x(t))_{I^-}],$$

$c_2(t) = -\frac{h_2^2}{3k_2}[35(\rho_2 C_2 u_t(t) - f_2(t))_{I^+} + 8(\rho_2 C_2 u_t(t) - f_2(t))_{m+1}$

$$-(\rho_2 C_2 u_t(t) - f_2(t))_{m+2} + 6h_2(\rho_2 C_2 u_{xt}(t) - (f_2)_x(t))_{I^+}],$$

$c_3(t) = \frac{h_1^2}{12k_1}\left[(\rho_1 C_1 u_t(t) - f_1(t))_{m-1} + 10(\rho_1 C_1 u_t(t) - f_1(t))_m + (\rho_1 C_1 u_t(t) - f_1(t))_{I^-}\right],$

$c_4(t) = \frac{h_2^2}{12k_2}\left[(\rho_2 C_2 u_t(t) - f_2(t))_{m+2} + 10(\rho_2 C_2 u_t(t) - f_2(t))_{m+1} + (\rho_2 C_2 u_t(t) - f_2(t))_{I^+}\right].$

Using the Crank-Nicolson method, Eqs. (5.40)-(5.45) become

$$\frac{u_{I^+}^{n+1} + u_{I^+}^n}{2} - \frac{u_{I^-}^{n+1} + u_{I^-}^n}{2} = a^{n+\frac{1}{2}}, \tag{5.46}$$

$$\frac{k_2 (u_x)_{I^+}^{n+1} + k_2 (u_x)_{I^+}^n}{2} - \frac{k_1 (u_x)_{I^-}^{n+1} + k_1 (u_x)_{I^-}^n}{2} = b^{n+\frac{1}{2}}, \tag{5.47}$$

$$\begin{aligned}
&\frac{u_{m-1}^{n+1} + u_{m-1}^n}{2} - \frac{32(u_m^{n+1} + u_m^n)}{2} + \frac{31\left(u_{I^-}^{n+1} + u_{I^-}^n\right)}{2} - \frac{30h_1\left((u_x)_{I^-}^{n+1} + (u_x)_{I^-}^n\right)}{2} \\
=&\frac{h_1^2}{3k_1}\left[\frac{\rho_1 C_1\left(u_{m-1}^{n+1} - u_{m-1}^n\right)}{\Delta t} - (f_1)_{m-1}^{n+\frac{1}{2}}\right] - \frac{8h_1^2}{3k_1}\left[\frac{\rho_1 C_1 (u_m^{n+1} - u_m^n)}{\Delta t} - (f_1)_m^{n+\frac{1}{2}}\right] \\
&-\frac{35h_1^2}{3k_1}\left[\frac{\rho_1 C_1\left(u_{I^-}^{n+1} - u_{I^-}^n\right)}{\Delta t} - (f_1)_{I^-}^{n+\frac{1}{2}}\right] + \frac{2h_1^2}{k_1}\left[\frac{\rho_1 C_1\left((u_x)_{I^-}^{n+1} - (u_x)_{I^-}^n\right)}{\Delta t} - ((f_1)_x)_{I^-}^{n+\frac{1}{2}}\right],
\end{aligned} \tag{5.48}$$

and

$$\begin{aligned}
&\frac{u_{m+2}^{n+1}+u_{m+2}^{n}}{2}-\frac{32\left(u_{m+1}^{n+1}+u_{m+1}^{n}\right)}{2}+\frac{31\left(u_{I^+}^{n+1}+u_{I^+}^{n}\right)}{2}+\frac{30h_2\left((u_x)_{I^+}^{n+1}+(u_x)_{I^+}^{n}\right)}{2}\\
=&\frac{h_2^2}{3k_2}\left[\frac{\rho_2C_2\left(u_{m+2}^{n+1}-u_{m+2}^{n}\right)}{\Delta t}-(f_2)_{m+2}^{n+\frac{1}{2}}\right]-\frac{8h_2^2}{3k_2}\left[\frac{\rho_2C_2\left(u_{m+1}^{n+1}-u_{m+1}^{n}\right)}{\Delta t}-(f_2)_{m+1}^{n+\frac{1}{2}}\right]\\
&-\frac{35h_2^2}{3k_2}\left[\frac{\rho_2C_2\left(u_{I^+}^{n+1}-u_{I^+}^{n}\right)}{\Delta t}-(f_2)_{I+}^{n+\frac{1}{2}}\right]-\frac{2h_2^2}{k_2}\left[\frac{\rho_2C_2\left((u_x)_{I^+}^{n+1}-(u_x)_{I^+}^{n}\right)}{\Delta t}-\left((f_2)_x\right)_{I^+}^{n+\frac{1}{2}}\right], \quad (5.49)\\
&\frac{u_{m-1}^{n+1}+u_{m-1}^{n}}{2}-2\frac{u_{m}^{n+1}+u_{m}^{n}}{2}+\frac{u_{I^-}^{n+1}+u_{I^-}^{n}}{2}\\
=&\frac{h_1^2\rho_1C_1}{12k_1\Delta t}\left(u_{m-1}^{n+1}-u_{m-1}^{n}\right)-\frac{h_1^2}{12k_1}\left(f_1\right)_{m-1}^{n+\frac{1}{2}}+\frac{10h_1^2\rho_1C_1}{12k_1\Delta t}\left(u_{m}^{n+1}-u_{m}^{n}\right)\\
&-\frac{10h_1^2}{12k_1}\left(f_1\right)_{m}^{n+\frac{1}{2}}+\frac{h_1^2\rho_1C_1}{12k_1\Delta t}\left(u_{I^-}^{n+1}-u_{I^-}^{n}\right)-\frac{h_1^2}{12k_1}\left(f_1\right)_{I^-}^{n+\frac{1}{2}}, \quad (5.50)\\
&\frac{u_{m+2}^{n+1}+u_{m+2}^{n}}{2}-2\frac{u_{m+1}^{n+1}+u_{m+1}^{n}}{2}+\frac{u_{I^+}^{n+1}+u_{I^+}^{n+1}}{2}\\
=&\frac{h_2^2\rho_2C_2}{12k_2\Delta t}\left(u_{m+2}^{n+1}-u_{m+2}^{n}\right)-\frac{h_2^2}{12k_2}\left(f_2\right)_{m+2}^{n+\frac{1}{2}}+\frac{10h_2^2\rho_2C_2}{12k_2\Delta t}\left(u_{m+1}^{n+1}-u_{m+1}^{n}\right)\\
&-\frac{10h_2^2}{12k_2}\left(f_2\right)_{m+1}^{n+\frac{1}{2}}+\frac{h_2^2\rho_2C_2}{12k_2\Delta t}\left(u_{I^+}^{n+1}-u_{I^+}^{n}\right)-\frac{h_2^2}{12k_2}\left(f_2\right)_{I^+}^{n+\frac{1}{2}}. \quad (5.51)
\end{aligned}$$

Thus, we obtain a system of 6 equations with 8 unknowns at time level $n+1$, $\left\{u_{m-1}^{n+1},u_{m}^{n+1},u_{m+1}^{n+1},u_{m+2}^{n+1},u_{I^-}^{n+1},u_{I^+}^{n+1},(u_x)_{I^-}^{n+1},(u_x)_{I^+}^{n+1}\right\}$. That is

$$u_{I^+}^{n+1}-u_{I^-}^{n+1}=a_n, \quad (5.52)$$

$$k_2\left(u_x\right)_{I^+}^{n+1}-k_1\left(u_x\right)_{I^-}^{n+1}=b_n, \quad (5.53)$$

$$c_{11}\cdot u_{m-1}^{n+1}+c_{12}\cdot u_{m}^{n+1}+c_{13}\cdot u_{I^-}^{n+1}+c_{14}\cdot(u_x)_{I^-}^{n+1}=c_{1n}, \quad (5.54)$$

$$c_{21}\cdot u_{m+2}^{n+1}+c_{22}\cdot u_{m+1}^{n+1}+c_{23}\cdot u_{I^+}^{n+1}+c_{24}\cdot(u_x)_{I^+}^{n+1}=c_{2n}, \quad (5.55)$$

$$c_{31}\cdot u_{m-1}^{n+1}+c_{32}\cdot u_{m}^{n+1}+c_{33}\cdot u_{I^-}^{n+1}=c_{3n}, \quad (5.56)$$

$$c_{41}\cdot u_{m+2}^{n+1}+c_{42}\cdot u_{m+1}^{n+1}+c_{43}\cdot u_{I^+}^{n+1}=c_{4n}, \quad (5.57)$$

where $a_n=2a^{n+\frac{1}{2}}-\left(u_{I^+}-u_{I^-}\right)$, $b_n=2b^{n+\frac{1}{2}}-\left(k_2\left(u_x\right)_{I^+}-k_1\left(u_x\right)_{I^-}\right)$,

$c_{11}=12-3\mu_1$, $c_{12}=-\left(96-96\mu_1\right)$, $c_{13}=-\left(420+93\mu_1\right)$, $c_{14}=h_1\left(72+90\mu_1\right)$,

$$c_{1n} = (12+3\mu_1)\,u_{m-1}^n - (96+96\mu_1)\,u_m^n - (420-93\mu_1)\,u_{I^-}^n + h_1\,(72-90\mu_1)\,(u_x)_{I^-}^n$$
$$+2\lambda_1\,(f_1)_{m-1}^{n+\frac{1}{2}} - 16\lambda_1\,(f_1)_m^{n+\frac{1}{2}} - 70\lambda_1\,(f_1)_{I^-}^{n+\frac{1}{2}} + 12\lambda_1 h_1\,((f_1)_x)_{I^-}^{n+\frac{1}{2}};$$

$$c_{21} = 12-3\mu_2,\ c_{22} = -\,(96-96\mu_2)\,,\ c_{23} = -\,(420+93\mu_2)\,,\ c_{24} = -h_2\,(72+90\mu_2)\,,$$

$$c_{2n} = (12+3\mu_2)\,u_{m+2}^n - (96+96\mu_2)\,u_{m+1}^n - (420-93\mu_2)\,u_{I^+}^n - h_2\,(72-90\mu_2)\,(u_x)_{I^+}^n$$
$$+2\lambda_2\,(f_2)_{m-1}^{n+\frac{1}{2}} - 16\lambda_2\,(f_2)_m^{n+\frac{1}{2}} - 70\lambda_2\,(f_2)_{I^-}^{n+\frac{1}{2}} + 12\lambda_2 h_2\,((f_2)_x)_{I^-}^{n+\frac{1}{2}};$$

$$c_{31} = 1-\mu_1,\ c_{32} = 10+2\mu_1,\ c_{33} = c_{31} = 1-\mu_1,$$

$$c_{3n} = (1+\mu_1)\,u_{m-1}^n + (10-2\mu_1)\,u_m^n + (1+\mu_1)\,u_{I^-}^n + \lambda_1(f_1)_{m-1}^{n+\frac{1}{2}} + 10\lambda_1(f_1)_m^{n+\frac{1}{2}} + \lambda_1(f_1)_{I^-}^{n+\frac{1}{2}};$$

$$c_{41} = 1-\mu_2,\ c_{42} = 10+2\mu_2,\ c_{43} = c_{41} = 1-\mu_2,$$

$$c_{4n} = (1+\mu_2)\,u_{m+2}^n + (10-2\mu_2)\,u_{m+1}^n + (1+\mu_2)\,u_{I^+}^n + \lambda_2(f_2)_{m+2}^{n+\frac{1}{2}} + 10\lambda_2(f_2)_{m+1}^{n+\frac{1}{2}} + \lambda_2(f_2)_{I^+}^{n+\frac{1}{2}}.$$

Using a similar augment as in the steady-state case, we can delete $u_{I^-}^{n+1}$, $u_{I^+}^{n+1}$, $(u_x)_{I^-}^{n+1}$, $(u_x)_{I^+}^{n+1}$ in the above equations and obtain two equations as follows:

$$c_{51}\cdot u_{m-1}^{n+1} + c_{52}\cdot u_m^{n+1} + c_{53}\cdot u_{m+1}^{n+1} = c_{5n}, \tag{5.58}$$

$$c_{61}\cdot u_m^{n+1} + c_{62}\cdot u_{m+1}^{n+1} + c_{63}\cdot u_{m+2}^{n+1} = c_{6n}, \tag{5.59}$$

where $c_{51} = k_1 c_{24} c_{41}\,(c_{13}c_{31} - c_{11}c_{33}) - k_2 c_{14} c_{31}\,(c_{23}c_{41} - c_{21}c_{43})\,,$

$c_{52} = k_1 c_{24} c_{41}(c_{13}c_{32} - c_{12}c_{33}) - k_2 c_{14} c_{32}(c_{23}c_{41} - c_{21}c_{43}),\ c_{53} = k_2 c_{14} c_{33}(c_{22}c_{41} - c_{21}c_{42})\,,$

$c_{5n} = -k_1 c_{24} c_{33} c_{41} c_{1n} + k_2 c_{14} c_{33} c_{41} c_{2n} + [k_1 c_{24} c_{13} c_{41} - k_2 c_{14}\,(c_{23}c_{41} - c_{21}c_{43})]c_{3n}$
$-k_2 c_{14} c_{21} c_{33} c_{4n} + k_2 c_{14} c_{33}(c_{21}c_{43} - c_{23}c_{41})a_n - c_{14} c_{24} c_{33} c_{41} b_n;$

$c_{61} = k_1 c_{24} c_{43}(c_{12}c_{31} - c_{11}c_{32}),\ c_{62} = k_2 c_{14} c_{31}(c_{23}c_{42} - c_{22}c_{43}) - k_1 c_{24} c_{42}(c_{13}c_{31} - c_{11}c_{33})\,,$

$c_{63} = k_2 c_{14} c_{31}\,(c_{23}c_{41} - c_{21}c_{43}) - k_1 c_{24} c_{41}\,(c_{13}c_{31} - c_{11}c_{33})\,,$

$c_{6n} = k_1 c_{24} c_{31} c_{43} c_{1n} - k_2 c_{14} c_{31} c_{43} c_{2n} + \left[\frac{k_1 c_{24} c_{13} c_{31} c_{43}}{-c_{33}} - k_1 c_{24} c_{43}\left(c_{11} + \frac{c_{13}c_{31}}{-c_{33}}\right)\right] c_{3n}$
$+\left[k_2 c_{14} c_{23} c_{31} + k_1 c_{24} c_{33}\left(c_{11} + \frac{c_{13}c_{31}}{-c_{33}}\right)\right] c_{4n}$
$-k_1 c_{24} c_{33} c_{43}\left(c_{11} + \frac{c_{13}c_{31}}{-c_{33}}\right) a_n + c_{14} c_{24} c_{31} c_{43} b_n.$

We have treated u_x as an unknown without discretization in the above derivation based on the GPM.

Thus, Eqs. (5.21) and (5.23), Eq. (5.24), and Eqs. (5.58)-(5.59) together form a higher-order accurate finite difference scheme for the heat conduction model in unsteady-state case with Dirichlet boundary. The scheme can be rewritten in matrix form as

$$A_D \vec{u}^{n+1} = \vec{d}_D, \tag{5.60}$$

where $\vec{u}^{n+1} = \left[u_1^{n+1}, u_2^{n+1}, ..., u_{m-2}^{n+1}, u_{m-1}^{n+1}, u_m^{n+1}, u_{m+1}^{n+1}, u_{m+2}^{n+1}, u_{m+3,}^{n+1}..., u_{M-2}^{n+1}, u_{M-1}^{n+1}\right]^T$,

$$A_D = \begin{bmatrix}
10+2\mu_1 & 1-\mu_1 & & & & & & & & & & & \\
1-\mu_1 & 10+2\mu_1 & 1-\mu_1 & & & & & & & & & & \\
 & \ddots & \ddots & \ddots & & & & & & & & & \\
 & & 1-\mu_1 & 10+2\mu_1 & 1-\mu_1 & & & & & & & & \\
 & & & c_{51} & c_{52} & c_{53} & & & & & & & \\
 & & & & c_{61} & c_{62} & c_{63} & & & & & & \\
 & & & & & 1-\mu_2 & 10+2\mu_2 & 1-\mu_2 & & & & & \\
 & & & & & & \ddots & \ddots & \ddots & & & & \\
 & & & & & & & & 1-\mu_2 & 10+2\mu_2 & 1-\mu_2 & & \\
 & & & & & & & & & 1-\mu_2 & 10+2\mu_2 & 1-\mu_2 & \\
 & & & & & & & & & & 1-\mu_2 & 10+2\mu_2
\end{bmatrix}$$

$$\text{and } \vec{d}_D = \begin{bmatrix} (1+\mu_1)u_0^n+(10-2\mu_1)u_1^n+(1+\mu_1)u_2^n+(F_1)_1^{n+\frac{1}{2}}-(1-\mu_1)u_0^{n+1} \\ (1+\mu_1)u_1^n+(10-2\mu_1)u_2^n+(1+\mu_1)u_3^n+(F_1)_2^{n+\frac{1}{2}} \\ (1+\mu_1)u_2^n+(10-2\mu_1)u_3^n+(1+\mu_1)u_4^n+(F_1)_3^{n+\frac{1}{2}} \\ \vdots \\ (1+\mu_1)u_{m-2}^n+(10-2\mu_1)u_{m-1}^n+(1+\mu_1)u_m^n+(F_1)_{m-1}^{n+\frac{1}{2}} \\ c_{5n} \\ c_{6n} \\ (1+\mu_2)u_{m+1}^n+(10-2\mu_2)u_{m+2}^n+(1+\mu_2)u_{m+3}^n+(F_2)_{m+2}^{n+\frac{1}{2}} \\ (1+\mu_2)u_{m+2}^n+(10-2\mu_2)u_{m+3}^n+(1+\mu_2)u_{m+4}^n+(F_2)_{m+3}^{n+\frac{1}{2}} \\ \vdots \\ (1+\mu_2)u_{M-4}^n+(10-2\mu_2)u_{M-3}^n+(1+\mu_2)u_{M-2}^n+(F_2)_{M-3}^{n+\frac{1}{2}} \\ (1+\mu_2)u_{M-3}^n+(10-2\mu_2)u_{M-2}^n+(1+\mu_2)u_{M-1}^n+(F_2)_{M-2}^{n+\frac{1}{2}} \\ (1+\mu_2)u_{M-2}^n+(10-2\mu_2)u_{M-1}^n+(1+\mu_2)u_M^n+(F_2)_{M-1}^{n+\frac{1}{2}}-(1-\mu_2)u_M^{n+1} \end{bmatrix},$$

where $(F_1)_j^{n+\frac{1}{2}} = (f_1)_{j-1}^{n+\frac{1}{2}} + 10\,(f_1)_j^{n+\frac{1}{2}} + (f_1)_{j+1}^{n+\frac{1}{2}}$, $1 \le j \le m-1$; $(F_2)_j^{n+\frac{1}{2}} = (f_2)_{j-1}^{n+\frac{1}{2}} + 10\,(f_2)_j^{n+\frac{1}{2}} + (f_2)_{j+1}^{n+\frac{1}{2}}$, $m+1 \le j \le M-1$. Note that A_D is a tridiagonal matrix, one can use the Thomas algorithm to obtain the solution efficiently. Once the values of u_{m-1}^{n+1}, u_m^{n+1}, u_{m+1}^{n+1} and u_{m+2}^{n+1} are obtained, the values of $u_{I^-}^{n+1}$, $u_{I^+}^{n+1}$, $(u_x)_{I^-}^{n+1}$ and $(u_x)_{I^+}^{n+1}$ can be easily obtained by using Eqs. (5.52)-(5.57).

Eqs. (5.21) and (5.23), Eqs. (5.32) and (5.37), and Eqs. (5.58)-(5.59) together form a higher-order accurate finite difference scheme for the heat conduction model in unsteady-state case with Neumann boundary. We can rewrite the scheme in matrix form as

$$A_N \vec{u}^{n+1} = \vec{d}_N, \tag{5.61}$$

where $\vec{u}^{n+1} = \left[u_0^{n+1}, u_1^{n+1}, u_2^{n+1}, ..., u_{m-1}^{n+1}, u_m^{n+1}, u_{m+1}^{n+1}, u_{m+2}^{n+1}, ..., u_{M-2}^{n+1}, u_{M-1}^{n+1}, u_M^{n+1}\right]^T$,

$$A_N=\begin{bmatrix}
5+\mu_1 & 1-\mu_1 & & & & & & & & & & \\
1-\mu_1 & 10+2\mu_1 & 1-\mu_1 & & & & & & & & & \\
 & \ddots & \ddots & \ddots & & & & & & & & \\
 & & 1-\mu_1 & 10+2\mu_1 & 1-\mu_1 & & & & & & & \\
 & & & c_{51} & c_{52} & c_{53} & & & & & & \\
 & & & c_{61} & c_{62} & c_{63} & & & & & & \\
 & & & & 1-\mu_2 & 10+2\mu_2 & 1-\mu_2 & & & & & \\
 & & & & & \ddots & \ddots & \ddots & & & & \\
 & & & & & & & 1-\mu_2 & 10+2\mu_2 & 1-\mu_2 & & \\
 & & & & & & & & 1-\mu_2 & 5+\mu_2 &
\end{bmatrix}$$

and $\vec{d}_N=$

$$\begin{bmatrix}
(5-\mu_1)\,u_0^n+(1+\mu_1)u_1^n+(LF)^{n+\frac{1}{2}}+(L\Phi)^n \\
(1+\mu_1)u_0^n+(10-2\mu_1)u_1^n+(1+\mu_1)u_2^n+(MF_1)_1^{n+\frac{1}{2}} \\
(1+\mu_1)u_1^n+(10-2\mu_1)u_2^n+(1+\mu_1)u_3^n+(MF_1)_2^{n+\frac{1}{2}} \\
\vdots \\
(1+\mu_1)u_{m-2}^n+(10-2\mu_1)u_{m-1}^n+(1+\mu_1)u_m^n+(MF_1)_{m-1}^{n+\frac{1}{2}} \\
c_{5n} \\
c_{6n} \\
(1+\mu_2)u_{m+1}^n+(10-2\mu_2)u_{m+2}^n+(1+\mu_2)u_{m+3}^n+(MF_2)_{m+2}^{n+\frac{1}{2}} \\
(1+\mu_2)u_{m+2}^n+(10-2\mu_2)u_{m+3}^n+(1+\mu_2)u_{m+4}^n+(MF_2)_{m+3}^{n+\frac{1}{2}} \\
\vdots \\
(1+\mu_2)u_{M-3}^n+(10-2\mu_2)u_{M-2}^n+(1+\mu_2)u_{M-1}^n+(MF_2)_{M-2}^{n+\frac{1}{2}} \\
(1+\mu_2)u_{M-2}^n+(10-2\mu_2)u_{M-1}^n+(1+\mu_2)u_M^n+(MF_2)_{M-1}^{n+\frac{1}{2}} \\
(1+\mu_2)u_{M-1}^n+(5-\mu_2)u_M^n+(RF)^{n+\frac{1}{2}}+(R\Phi)^n
\end{bmatrix},$$

where $(LF)^{n+\frac{1}{2}} = \frac{\Delta t}{\rho_1 C_1}\left[5\left(f_1\right)_0^{n+\frac{1}{2}} + \left(f_1\right)_1^{n+\frac{1}{2}} + h_1\left(\left(f_1\right)_x\right)_0^{n+\frac{1}{2}}\right]$,

$(L\Phi)^n = -h_1\left[\left(1+\mu_1\right)\left(\phi_1\right)^{n+1} + \left(1-\mu_1\right)\left(\phi_1\right)^n\right]$,

$(RF)^{n+\frac{1}{2}} = \frac{\Delta t}{\rho_2 C_2}\left[5\left(f_2\right)_{M-1}^{n+\frac{1}{2}} + \left(f_2\right)_M^{n+\frac{1}{2}} - h_2\left(\left(f_2\right)_x\right)_M^{n+\frac{1}{2}}\right]$,

$(R\Phi)^n = h_2\left[\left(1+\mu_2\right)\left(\phi_2\right)^{n+1} - \left(1-\mu_2\right)\left(\phi_2\right)^n\right]$. Once the values of u_{m-1}^{n+1}, u_m^{n+1}, u_{m+1}^{n+1} and u_{m+2}^{n+1} are obtained, the values of $u_{I^-}^{n+1}$, $u_{I^+}^{n+1}$, $(u_x)_{I^-}^{n+1}$ and $(u_x)_{I^+}^{n+1}$ can be easily obtained by using Eqs. (5.52)-(5.57).

Eqs. (5.21) and (5.23), Eqs. (5.38)-(5.39), and Eqs. (5.58)-(5.59) together form a higher-order accurate finite difference scheme for the heat conduction model in unsteady-state case with Robin boundary condition. The scheme can be rewritten in matrix form as

$$A_R \vec{u}^{n+1} = \vec{d}_R, \tag{5.62}$$

where $\vec{u}^{n+1} = \left[u_0^{n+1}, u_1^{n+1}, u_2^{n+1}, ..., u_{m-1}^{n+1}, u_m^{n+1}, u_{m+1}^{n+1}, u_{m+2}^{n+1}..., u_{M-2}^{n+1}, u_{M-1}^{n+1}, u_M^{n+1}\right]^T$,

$$A_R = \begin{bmatrix}
5+\mu_1+\frac{\gamma_1}{\alpha_1}h_1(1+\mu_1) & 1-\mu_1 & & & & & & & & & \\
1-\mu_1 & 10+2\mu_1 & 1-\mu_1 & & & & & & & & \\
 & \ddots & \ddots & \ddots & & & & & & & \\
 & & 1-\mu_1 & 10+2\mu_1 & 1-\mu_1 & & & & & & \\
 & & & c_{51} & c_{52} & c_{53} & & & & & \\
 & & & c_{61} & c_{62} & c_{63} & & & & & \\
 & & & & 1-\mu_2 & 10+2\mu_2 & 1-\mu_2 & & & & \\
 & & & & & \ddots & \ddots & \ddots & & & \\
 & & & & & & 1-\mu_2 & 10+2\mu_2 & 1-\mu_2 & & \\
 & & & & & & & 1-\mu_2 & 5+\mu_2+\frac{\gamma_2}{\alpha_2}h_2(1+\mu_2)
\end{bmatrix}$$

$$\text{and } \vec{d}_R = \begin{bmatrix} \left[5+\frac{\gamma_1}{\alpha_1}h_1-\left(1+\frac{\gamma_1}{\alpha_1}h_1\right)\mu_1\right]u_0^n+(1+\mu_1)u_1^n+(LF)^{n+\frac{1}{2}}+(L\Phi)^n \\ (1+\mu_1)u_0^n+(10-2\mu_1)u_1^n+(1+\mu_1)u_2^n+(MF_1)_1^{n+\frac{1}{2}} \\ (1+\mu_1)u_1^n+(10-2\mu_1)u_2^n+(1+\mu_1)u_3^n+(MF_1)_2^{n+\frac{1}{2}} \\ \vdots \\ (1+\mu_1)u_{m-2}^n+(10-2\mu_1)u_{m-1}^n+(1+\mu_1)u_m^n+(MF_1)_{m-1}^{n+\frac{1}{2}} \\ c_{5n} \\ c_{6n} \\ (1+\mu_2)u_{m+1}^n+(10-2\mu_2)u_{m+2}^n+(1+\mu_2)u_{m+3}^n+(MF_2)_{m+2}^{n+\frac{1}{2}} \\ (1+\mu_2)u_{m+2}^n+(10-2\mu_2)u_{m+3}^n+(1+\mu_2)u_{m+4}^n+(MF_2)_{m+3}^{n+\frac{1}{2}} \\ \vdots \\ (1+\mu_2)u_{M-3}^n+(10-2\mu_2)u_{M-2}^n+(1+\mu_2)u_{M-1}^n+(MF_2)_{M-2}^{n+\frac{1}{2}} \\ (1+\mu_2)u_{M-2}^n+(10-2\mu_2)u_{M-1}^n+(1+\mu_2)u_M^n+(MF_2)_{M-1}^{n+\frac{1}{2}} \\ (1+\mu_2)u_{M-1}^n+\left[5+\frac{\gamma_2}{\alpha_2}h_2-\left(1-\frac{\gamma_2}{\alpha_2}h_2\right)\mu_2\right]+(RF)^{n+\frac{1}{2}}+(R\Phi)^n \end{bmatrix}.$$

Again, A_R is tridiagonal; one can obtain the solution efficiently by the Thomas algorithm. Once the values of u_{m-1}^{n+1}, u_m^{n+1}, u_{m+1}^{n+1} and u_{m+2}^{n+1} are obtained, the values of $u_{I^-}^{n+1}$, $u_{I^+}^{n+1}$, $(u_x)_{I^-}^{n+1}$ and $(u_x)_{I^+}^{n+1}$ can be obtained easily by using Eqs. (5.52)-(5.57).

In summary, we have developed three higher-order accurate finite difference schemes for the unsteady-state heat conduction model with either the Dirichlet boundary condition, the Neumann boundary condition or the Robin boundary condition. The schemes are third-order for Neumann and Robin boundaries, fourth-order at the interface. Again, it should be pointed out that on the derivations of schemes for the Neumann boundary, the Robin boundary and at the interface, we did not discretize the first-order derivative, u_x, which means the GPM has been used.

5.3 Schemes for Nanoscale Heat Conduction Model

To derive higher-order compact finite difference schemes for solving nanoscale heat conduction model, Eqs. (3.29)-(3.36), we first introduce a new function, $v\left(x,t\right)=u_t\left(x,t\right)$. As such, the nanoscale heat conduction model can be changed to

$$\rho_1 C_1(u_t+\tau_q^{(1)}v_t)=k_1\left(u_{xx}+\tau_T^{(1)}v_{xx}\right)+f_1\left(x,t\right),\ 0<x<l,\ 0\le t\le T, \tag{5.63}$$

$$\rho_2 C_2(u_t+\tau_q^{(2)}v_t)=k_2\left(u_{xx}+\tau_T^{(2)}v_{xx}\right)+f_2\left(x,t\right),\ l<x<L,\ 0\le t\le T, \tag{5.64}$$

subject to the initial and temperature-jump boundary conditions as

$$u\left(x,0\right)=\psi_1\left(x\right),\ v\left(x,0\right)=\varphi_1\left(x\right),\ 0\le x\le l, \tag{5.65}$$

$$u\left(x,0\right)=\psi_2\left(x\right),\ v\left(x,0\right)=\varphi_2\left(x\right),\ l\le x\le L, \tag{5.66}$$

$$-\alpha_1 u_x(0,t)+u(0,t)=\phi_1(t),\quad -\alpha_1 v_x(0,t)+v(0,t)=(\phi_1)_t(t),\quad 0\le t\le T, \tag{5.67}$$

$$\alpha_2 u_x\left(L,t\right)+u\left(L,t\right)=\phi_2\left(t\right),\ \alpha_2 v_x\left(L,t\right)+v\left(L,t\right)=\left(\phi_2\right)_t\left(t\right),\quad 0\le t\le T, \tag{5.68}$$

and the interfacial condition at $x=l$ as

$$u_{I^-}\left(t\right)=u_{I^+}\left(t\right),\quad v_{I^-}\left(t\right)=v_{I^+}\left(t\right),\ 0\le t\le T, \tag{5.69}$$

$$k_1\left[(u_x)_{I^-}(t)+\tau_T^{(1)}(u_{xt})_{I^-}(t)\right]=k_2\left[(u_x)_{I^+}(t)+\tau_T^{(2)}(u_{xt})_{I^+}\left(t\right)\right],\quad 0\le t\le T. \tag{5.70}$$

We first design a mesh, as shown in Figure 5.3, where grid sizes and time step are $h_1=l/m$, $h_2=\left(L-l\right)/(M-m)$, $\Delta t=T/N$, respectively, and m, M $(m<M)$ and N are positive integers. Grid points in the mesh are denoted as $x_j=jh_1$, $0\le j\le m$; $x_j=l+\left(j-m\right)h_2$, $m+1\le j\le M$; $t_n=n\Delta t$, $0\le n\le N$ and $\Omega_h=\left\{x_j|0\le j\le M\right\}$, $\Omega_{\Delta t}=\left\{t_n|0\le n\le N\right\}$, where the interface is located at grid point $x_I=\left(m+1\right)h_1=l$.

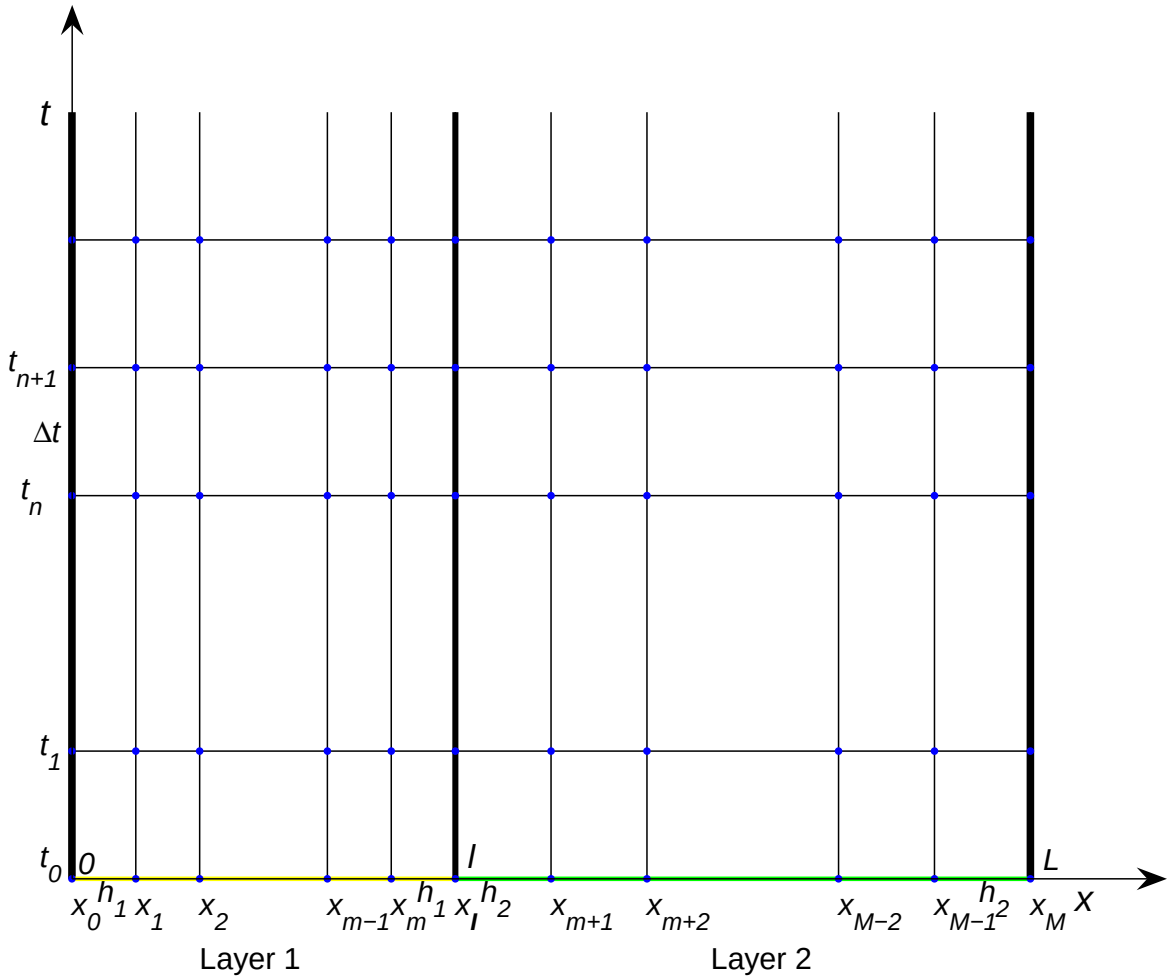

Figure 5.3: Two-dimensional mesh for nanoscale heat conduction model.

Denote u_j^n and v_j^n to be the approximations of $u\left(x_j, t_n\right)$ and $v\left(x_j, t_n\right)$, respectively. For simplicity, we also denote u_j, v_j, $\left(u_t\right)_j$, $\left(v_t\right)_j$, etc. to be the values of $u\left(x_j, t\right)$, $v\left(x_j, t\right)$, $u_t\left(x_j, t\right)$, $v_t\left(x_j, t\right)$, and so on for others.

For the interior points, $x_1 \leq x_j \leq x_{m-1}$, the fourth-order Padé scheme gives

$$\begin{aligned}
&\frac{\rho_1 C_1}{12}\left[\left(\left(u_t\right)_{j-1}+\tau_q^{(1)}\left(v_t\right)_{j-1}\right)+10\left(\left(u_t\right)_j+\tau_q^{(1)}\left(v_t\right)_j\right)+\left(\left(u_t\right)_{j+1}+\tau_q^{(1)}\left(v_t\right)_{j+1}\right)\right] \\
=&\frac{k_1}{h_1^2}\left[\left(u_{j-1}+\tau_T^{(1)} v_{j-1}\right)-2\left(u_j+\tau_T^{(1)} v_j\right)+\left(u_{j+1}+\tau_T^{(1)} v_{j+1}\right)\right] \\
&+\frac{1}{12}\left[\left(f_1\right)_{j-1}+10\left(f_1\right)_j+\left(f_1\right)_{j+1}\right]+O\left(h_1^4\right). \qquad (5.71)
\end{aligned}$$

Using the Crank-Nicolson method gives

$$\begin{aligned}
&\frac{\rho_1 C_1}{12\Delta t}\left(u_{j-1}^{n+1}+\tau_q^{(1)}v_{j-1}^{n+1}\right)-\frac{\rho_1 C_1}{12\Delta t}\left(u_{j-1}^{n}+\tau_q^{(1)}v_{j-1}^{n}\right)+\frac{10\rho_1 C_1}{12\Delta t}\left(u_{j}^{n+1}+\tau_q^{(1)}v_{j}^{n+1}\right)\\
&-\frac{10\rho_1 C_1}{12\Delta t}\left(u_{j}^{n}+\tau_q^{(1)}v_{j}^{n}\right)+\frac{\rho_1 C_1}{12\Delta t}\left(u_{j+1}^{n+1}+\tau_q^{(1)}v_{j+1}^{n+1}\right)-\frac{\rho_1 C_1}{12\Delta t}\left(u_{j+1}^{n}+\tau_q^{(1)}v_{j+1}^{n}\right)\\
=&\frac{k_1}{2h_1^2}\left(u_{j-1}^{n+1}+\tau_T^{(1)}v_{j-1}^{n+1}\right)+\frac{k_1}{2h_1^2}\left(u_{j-1}^{n}+\tau_T^{(1)}v_{j-1}^{n}\right)-\frac{k_1}{h_1^2}\left(u_{j}^{n+1}+\tau_T^{(1)}v_{j}^{n+1}\right)\\
&-\frac{k_1}{h_1^2}\left(u_{j}^{n}+\tau_T^{(1)}v_{j}^{n}\right)+\frac{k_1}{2h_1^2}\left(u_{j+1}^{n+1}+\tau_T^{(1)}v_{j+1}^{n+1}\right)+\frac{k_1}{2h_1^2}\left(u_{j+1}^{n}+\tau_T^{(1)}v_{j+1}^{n}\right)\\
&+\frac{1}{12}\left[f_{j-1}^{n+\frac{1}{2}}+10f_{j}^{n+\frac{1}{2}}+f_{j+1}^{n+\frac{1}{2}}\right]+O\left(h_1^4+\Delta t^2\right). \qquad (5.72)
\end{aligned}$$

Separating the time levels t_{n+1} and t_n yields

$$\begin{aligned}
&\frac{\rho_1 C_1}{12\Delta t}\left(u_{j-1}^{n+1}+\tau_q^{(1)}v_{j-1}^{n+1}\right)-\frac{k_1}{2h_1^2}\left(u_{j-1}^{n+1}+\tau_T^{(1)}v_{j-1}^{n+1}\right)+\frac{10\rho_1 C_1}{12\Delta t}\left(u_{j}^{n+1}+\tau_q^{(1)}v_{j}^{n+1}\right)\\
&+\frac{k_1}{h_1^2}\left(u_{j}^{n+1}+\tau_T^{(1)}v_{j}^{n+1}\right)+\frac{\rho_1 C_1}{12\Delta t}\left(u_{j+1}^{n+1}+\tau_q^{(1)}v_{j+1}^{n+1}\right)-\frac{k_1}{2h_1^2}\left(u_{j+1}^{n+1}+\tau_T^{(1)}v_{j+1}^{n+1}\right)\\
=&\frac{\rho_1 C_1}{12\Delta t}\left(u_{j-1}^{n}+\tau_q^{(1)}v_{j-1}^{n}\right)+\frac{k_1}{2h_1^2}\left(u_{j-1}^{n}+\tau_T^{(1)}v_{j-1}^{n}\right)+\frac{10\rho_1 C_1}{12\Delta t}\left(u_{j}^{n}+\tau_q^{(1)}v_{j}^{n}\right)\\
&-\frac{k_1}{h_1^2}\left(u_{j}^{n}+\tau_T^{(1)}v_{j}^{n}\right)+\frac{\rho_1 C_1}{12\Delta t}\left(u_{j+1}^{n}+\tau_q^{(1)}v_{j+1}^{n}\right)+\frac{k_1}{2h_1^2}\left(u_{j+1}^{n}+\tau_T^{(1)}v_{j+1}^{n}\right)\\
&+\frac{1}{12}\left[\left(f_1\right)_{j-1}^{n+\frac{1}{2}}+10\left(f_1\right)_{j}^{n+\frac{1}{2}}+\left(f_1\right)_{j+1}^{n+\frac{1}{2}}\right]+O\left(h_1^4+\Delta t^2\right). \qquad (5.73)
\end{aligned}$$

By dropping the truncation error, multiplying both sides by $\frac{12\Delta t}{\rho_1 C_1}$, and letting $\mu_1=\frac{6k_1\Delta t}{\rho_1 C_1 h_1^2}$, $\lambda_1=\frac{\Delta t}{\rho_1 C_1}$, then introducing two new function $w_{q_1}(x,t)=u(x,t)+\tau_q^{(1)}v(x,t)$, $w_{T_1}(x,t)=u(x,t)+\tau_T^{(1)}v(x,t)$, where $0<x<l$, $0\le t\le T$, the above equation can be expressed as

$$\begin{aligned}
&\left(w_{q_1}\right)_{j-1}^{n+1}-\mu_1\left(w_{T_1}\right)_{j-1}^{n+1}+10\left(w_{q_1}\right)_{j}^{n+1}+2\mu_1\left(w_{T_1}\right)_{j}^{n+1}+\left(w_{q_1}\right)_{j+1}^{n+1}-\mu_1\left(w_{T_1}\right)_{j+1}^{n+1}\\
=&\left(w_{q_1}\right)_{j-1}^{n}+\mu_1\left(w_{T_1}\right)_{j-1}^{n}+10\left(w_{q_1}\right)_{j}^{n}-2\mu_1\left(w_{T_1}\right)_{j}^{n}+\left(w_{q_1}\right)_{j+1}^{n}+\mu_1\left(w_{T_1}\right)_{j+1}^{n}\\
&+\lambda_1\left[\left(f_1\right)_{j-1}^{n+\frac{1}{2}}+10\left(f_1\right)_{j}^{n+\frac{1}{2}}+\left(f_1\right)_{j+1}^{n+\frac{1}{2}}\right],\ 1\le j\le m-1. \qquad (5.74)
\end{aligned}$$

For $v(x,t) = u_t(x,t)$, a second-order approximation in time gives

$$\frac{v_j^{n+1} + v_j^n}{2} = \frac{u_j^{n+1} - u_j^n}{\Delta t} + O\left(\Delta t^2\right),\ 0 \le j \le M, \tag{5.75}$$

implying that $v_j^{n+1} = \frac{2}{\Delta t}\left(u_j^{n+1} - u_j^n\right) - v_j^n$. Substituting it into Eq. (5.74) gives

$$\begin{aligned}
&\left[\left(1 + \tau_q^{(1)}\frac{2}{\Delta t}\right) - \mu_1\left(1 + \tau_T^{(1)}\frac{2}{\Delta t}\right)\right] u_{j-1}^{n+1} \\
&+ \left[-\tau_q^{(1)}\frac{2}{\Delta t} + \mu_1\tau_T^{(1)}\frac{2}{\Delta t}\right] u_{j-1}^n + \left[-\tau_q^{(1)} + \mu_1\tau_T^{(1)}\right] v_{j-1}^n \\
&+ \left[10\left(1 + \tau_q^{(1)}\frac{2}{\Delta t}\right) + 2\mu_1\left(1 + \tau_T^{(1)}\frac{2}{\Delta t}\right)\right] u_j^{n+1} \\
&+ \left[-10\tau_q^{(1)}\frac{2}{\Delta t} - 2\mu_1\tau_T^{(1)}\frac{2}{\Delta t}\right] u_j^n + \left[-10\tau_q^{(1)} - 2\mu_1\tau_T^{(1)}\right] v_j^n \\
&+ \left[\left(1 + \tau_q^{(1)}\frac{2}{\Delta t}\right) - \mu_1\left(1 + \tau_T^{(1)}\frac{2}{\Delta t}\right)\right] u_{j+1}^{n+1} \\
&+ \left[-\tau_q^{(1)}\frac{2}{\Delta t} + \mu_1\tau_T^{(1)}\frac{2}{\Delta t}\right] u_{j+1}^n + \left[-\tau_q^{(1)} + \mu_1\tau_T^{(1)}\right] v_{j+1}^n \\
=&\left[1 + \mu_1\right] u_{j-1}^n + \left[10 - 2\mu_1\right] u_j^n + \left[1 + \mu_1\right] u_{j+1}^n \\
&+ \left[\tau_q^{(1)} + \mu_1\tau_T^{(1)}\right] v_{j-1}^n + \left[10\tau_q^{(1)} - 2\mu_1\tau_T^{(1)}\right] v_j^n + \left[\tau_q^{(1)} + \mu_1\tau_T^{(1)}\right] v_{j+1}^n \\
&+ \lambda_1\left[\left(f_1\right)_{j-1}^{n+\frac{1}{2}} + 10\left(f_1\right)_j^{n+\frac{1}{2}} + \left(f_1\right)_{j+1}^{n+\frac{1}{2}}\right].
\end{aligned} \tag{5.76}$$

Thus, we obtain a fourth-order compact finite difference scheme as

$$\begin{aligned}
&A_1 \cdot u_{j-1}^{n+1} + B_1 \cdot u_j^{n+1} + A_1 \cdot u_{j+1}^{n+1} \\
=&A_2 \cdot u_{j-1}^n + B_2 \cdot u_j^n + A_2 \cdot u_{j+1}^n \\
&+ A_3 \cdot v_{j-1}^n + B_3 \cdot v_j^n + A_3 \cdot v_{j+1}^n + \left(F_1\right)_j^{n+\frac{1}{2}},\ 1 \le j \le m,
\end{aligned} \tag{5.77}$$

where $A_1 = \left(1 + \tau_q^{(1)}\frac{2}{\Delta t}\right) - \mu_1\left(1 + \tau_T^{(1)}\frac{2}{\Delta t}\right)$, $B_1 = 10\left(1 + \tau_q^{(1)}\frac{2}{\Delta t}\right) + 2\mu_1\left(1 + \tau_T^{(1)}\frac{2}{\Delta t}\right)$,
$A_2 = \left(1 + \tau_q^{(1)}\frac{2}{\Delta t}\right) + \mu_1\left(1 - \tau_T^{(1)}\frac{2}{\Delta t}\right)$, $B_2 = 10\left(1 + \tau_q^{(1)}\frac{2}{\Delta t}\right) - 2\mu_1\left(1 - \tau_T^{(1)}\frac{2}{\Delta t}\right)$,
$A_3 = 2\tau_q^{(1)}$, $B_3 = 20\tau_q^{(1)}$, $\left(F_1\right)_j^{n+\frac{1}{2}} = \lambda_1\left[\left(f_1\right)_{j-1}^{n+\frac{1}{2}} + 10\left(f_1\right)_j^{n+\frac{1}{2}} + \left(f_1\right)_{j+1}^{n+\frac{1}{2}}\right]$.

Similarly, for interior points, $x_{m+2} \le x_j \le x_{M-1}$, a fourth-order compact finite difference scheme can be obtained as

$$\begin{aligned}
&\tilde{A}_1 \cdot u_{j-1}^{n+1} + \tilde{B}_1 \cdot u_j^{n+1} + \tilde{A}_1 \cdot u_{j+1}^{n+1} \\
=&\tilde{A}_2 \cdot u_{j-1}^{n} + \tilde{B}_2 \cdot u_j^{n} + \tilde{A}_2 \cdot u_{j+1}^{n} \\
&+ \tilde{A}_3 \cdot v_{j-1}^{n} + \tilde{B}_3 \cdot v_j^{n} + \tilde{A}_3 \cdot v_{j+1}^{n} + (F_2)_j^{n+\frac{1}{2}}, \ m+1 \le j \le M-1,
\end{aligned} \tag{5.78}$$

where $\tilde{A}_1 = \left(1 + \tau_q^{(2)} \frac{2}{\Delta t}\right) - \mu_2 \left(1 + \tau_T^{(2)} \frac{2}{\Delta t}\right)$, $\tilde{B}_1 = 10 \left(1 + \tau_q^{(2)} \frac{2}{\Delta t}\right) + 2\mu_2 \left(1 + \tau_T^{(2)} \frac{2}{\Delta t}\right)$, $\tilde{A}_2 = \left(1 + \tau_q^{(2)} \frac{2}{\Delta t}\right) + \mu_2 \left(1 - \tau_T^{(2)} \frac{2}{\Delta t}\right)$, $\tilde{B}_2 = 10 \left(1 + \tau_q^{(2)} \frac{2}{\Delta t}\right) - 2\mu_2 \left(1 - \tau_T^{(2)} \frac{2}{\Delta t}\right)$, $\tilde{A}_3 = 2\tau_q^{(2)}$, $\tilde{B}_3 = 20\tau_q^{(2)}$, $(F_2)_j^{n+\frac{1}{2}} = \lambda_2 \left[(f_2)_{j-1}^{n+\frac{1}{2}} + 10\,(f_2)_j^{n+\frac{1}{2}} + (f_2)_{j+1}^{n+\frac{1}{2}}\right]$, $\mu_2 = \frac{6k_2 \Delta t}{\rho_2 C_2 h_2^2}$, $\lambda_2 = \frac{\Delta t}{\rho_2 C_2}$.

For left boundary conditions, which are

$$-\alpha_1 u_x(0,t) + u(0,t) = \phi_1, \tag{5.79}$$

$$-\alpha_1 v_x(0,t) + v(0,t) = (\phi_1)_t, \tag{5.80}$$

by Eq. (4.2a), we have

$$u_1 = u_0 + h_1 (u_x)_0 + \frac{h_1^2}{12}(u_{xx})_1 + \frac{5h_1^2}{12}(u_{xx})_0 + \frac{h_1^3}{12}(u_{x^3})_0, \tag{5.81}$$

$$v_1 = v_0 + h_1 (v_x)_0 + \frac{h_1^2}{12}(v_{xx})_1 + \frac{5h_1^2}{12}(v_{xx})_0 + \frac{h_1^3}{12}(v_{x^3})_0. \tag{5.82}$$

Multiplying Eq. (5.82) by $\tau_T^{(1)}$, then adding it to Eq. (5.81), we obtain

$$\begin{aligned}
u_1 + \tau_T^{(1)} v_1 =& u_0 + \tau_T^{(1)} v_0 + h_1 \left[(u_x)_0 + \tau_T^{(1)} (v_x)_0\right] \\
&+ \frac{h_1^2}{12}\left[(u_{xx})_1 + \tau_T^{(1)} (v_{xx})_1\right] \\
&+ \frac{5h_1^2}{12}\left[(u_{xx})_0 + \tau_T^{(1)} (v_{xx})_0\right] \\
&+ \frac{h_1^3}{12}\left[(u_{x^3})_0 + \tau_T^{(1)} (v_{x^3})_0\right].
\end{aligned} \tag{5.83}$$

Eq. (5.63) gives

$$\rho_1 C_1 \left((u_t)_1 + \tau_q^{(1)} (v_t)_1\right) = k_1 \left[(u_{xx})_1 + \tau_T^{(1)} (v_{xx})_1\right] + (f_1)_1 \,, \tag{5.84a}$$

$$\rho_1 C_1 \left((u_t)_0 + \tau_q^{(1)} (v_t)_0\right) = k_1 \left[(u_{xx})_0 + \tau_T^{(1)} (v_{xx})_0\right] + (f_1)_0 \,, \tag{5.84b}$$

$$\rho_1 C_1 \left((u_{xt})_0 + \tau_q^{(1)} (v_{xt})_0\right) = k_1 \left[(u_{x^3})_0 + \tau_T^{(1)} (v_{x^3})_0\right] + ((f_1)_x)_0 \,. \tag{5.84c}$$

Solving $(u_{xx})_1 + \tau_T^{(1)}(v_{xx})_1$, $(u_{xx})_0 + \tau_T^{(1)}(v_{xx})_0$ and $(u_{x^3})_0 + \tau_T^{(1)}(v_{x^3})_0$, then substituting them into Eq. (5.83), we obtain

$$\begin{aligned} u_1 + \tau_T^{(1)} v_1 =& u_0 + \tau_T^{(1)} v_0 + h_1 \left[(u_x)_0 + \tau_T^{(1)} (v_x)_0\right] \\ &+ \frac{h_1^2}{12k_1} \left[\rho_1 C_1 \left((u_t)_1 + \tau_q^{(1)} (v_t)_1\right) - (f_1)_1\right] \\ &+ \frac{5h_1^2}{12k_1} \left[\rho_1 C_1 \left((u_t)_0 + \tau_q^{(1)} (v_t)_0\right) - (f_1)_0\right] \\ &+ \frac{h_1^3}{12k_1} \left[\rho_1 C_1 \left((u_{xt})_0 + \tau_q^{(1)} (v_{xt})_0\right) - ((f_1)_x)_0\right] . \end{aligned} \tag{5.85}$$

Applying the Crank-Nicolson method to Eq. (5.85) gives

$$\begin{aligned} &\frac{\rho_1 C_1 h_1^2}{12k_1} \left[\frac{\left(u_1^{n+1} + \tau_q^{(1)} v_1^{n+1}\right) - \left(u_1^n + \tau_q^{(1)} v_1^n\right)}{\Delta t}\right] \\ &+ \frac{5\rho_1 C_1 h_1^2}{12k_1} \left[\frac{\left(u_0^{n+1} + \tau_q^{(1)} v_0^{n+1}\right) - \left(u_0^n + \tau_q^{(1)} v_0^n\right)}{\Delta t}\right] \\ &+ \frac{\rho_1 C_1 h_1^3}{12k_1} \left[\frac{\left((u_x)_0^{n+1} + \tau_q^{(1)} (v_x)_0^{n+1}\right) - \left((u_x)_0^n + \tau_q^{(1)} (v_x)_0^n\right)}{\Delta t}\right] \\ =& \frac{1}{2}\left[u_1^{n+1} + \tau_T^{(1)} v_1^{n+1}\right] + \frac{1}{2}\left[u_1^n + \tau_T^{(1)} v_1^n\right] \\ &- \frac{1}{2}\left[u_0^{n+1} + \tau_T^{(1)} v_0^{n+1}\right] - \frac{1}{2}\left[u_0^n + \tau_T^{(1)} v_0^n\right] \\ &- \frac{h_1}{2}\left[(u_x)_0^{n+1} + \tau_T^{(1)} (v_x)_0^{n+1}\right] - \frac{h_1}{2}\left[(u_x)_0^n + \tau_T^{(1)} (v_x)_0^n\right] \\ &+ \frac{h_1^2}{12k_1} (f_1)_1^{n+\frac{1}{2}} + \frac{5h_1^2}{12k_1} (f_1)_0^{n+\frac{1}{2}} + \frac{h_1^3}{12k_1} ((f_1)_x)_0^{n+\frac{1}{2}} \,. \end{aligned} \tag{5.86}$$

Multiplying both sides by $\frac{12k_1\Delta t}{\rho_1 C_1 h_1^2}$, letting $\lambda_1 = \frac{\Delta t}{\rho_1 C_1}$, $\mu_1 = \frac{6k_1\Delta t}{\rho_1 C_1 h_1^2}$, $w_{q_1}(x,t) = u(x,t)$ $+ \tau_q^{(1)} v(x,t)$, and $w_{T_1}(x,t) = u(x,t) + \tau_T^{(1)} v(x,t)$, where $0 < x < l$, $0 \le t \le T$, rearranging the terms, we rewrite the above equation in a simple way as

$$\begin{aligned}
&(w_{q_1})_1^{n+1} - \mu_1 (w_{T_1})_1^{n+1} + 5(w_{q_1})_0^{n+1} + \mu_1 (w_{T_1})_0^{n+1} \\
&+ h_1 \left[\left((w_{q_1})_x\right)_0^{n+1} + \mu_1 \left((w_{T_1})_x\right)_0^{n+1} \right] \\
=& (w_{q_1})_1^{n} + \mu_1 (w_{T_1})_1^{n} + 5(w_{q_1})_0^{n} - \mu_1 (w_{T_1})_0^{n} \\
&+ h_1 \left[\left((w_{q_1})_x\right)_0^{n} - \mu_1 \left((w_{T_1})_x\right)_0^{n} \right] \\
&+ \lambda_1 \left[(f_1)_1^{n+\frac{1}{2}} + 5(f_1)_0^{n+\frac{1}{2}} + h_1 \left((f_1)_x\right)_0^{n+\frac{1}{2}} \right]. \qquad (5.87)
\end{aligned}$$

Eqs. (5.79)-(5.80) give

$$(u_x)_0^{n+1} = \frac{1}{\alpha_1}\left(u_0^{n+1} - (\phi_1)^{n+1}\right), \qquad (5.88a)$$

$$(v_x)_0^{n+1} = \frac{1}{\alpha_1}\left[v_0^{n+1} - ((\phi_1)_t)^{n+1}\right], \qquad (5.88b)$$

$$(u_x)_0^{n} = \frac{1}{\alpha_1}\left(u_0^{n} - (\phi_1)^{n}\right), \qquad (5.88c)$$

$$(v_x)_0^{n} = \frac{1}{\alpha_1}\left[v_0^{n} - ((\phi_1)_t)^{n}\right]. \qquad (5.88d)$$

Substituting them into Eq. (5.87) yields

$$\begin{aligned}
&(w_{q_1})_1^{n+1} - \mu_1 (w_{T_1})_1^{n+1} + 5(w_{q_1})_0^{n+1} + \mu_1 (w_{T_1})_0^{n+1} \\
&+ \frac{1}{\alpha_1} h_1 (1+\mu_1)\left(u_0^{n+1} - (\phi_1)^{n+1}\right) + \frac{1}{\alpha_1} h_1 \left(\tau_q^{(1)} + \mu_1 \tau_T^{(1)}\right)\left[v_0^{n+1} - ((\phi_1)_t)^{n+1}\right] \\
=& (w_{q_1})_1^{n} + \mu_1 (w_{T_1})_1^{n+1} + 5(w_{q_1})_0^{n} - \mu_1 (w_{T_1})_0^{n} \\
&+ \frac{1}{\alpha_1} h_1 (1-\mu_1)\left(u_0^{n} - (\phi_1)^{n}\right) + \frac{1}{\alpha_1} h_1 \left(\tau_q^{(1)} - \mu_1 \tau_T^{(1)}\right)\left[v_0^{n} - ((\phi_1)_t)^{n}\right] \\
&+ \lambda_1 \left[(f_1)_1^{n+\frac{1}{2}} + 5(f_1)_0^{n+\frac{1}{2}} + h_1 \left((f_1)_x\right)_0^{n+\frac{1}{2}} \right]. \qquad (5.89)
\end{aligned}$$

Substituting $v_j^{n+1}=\frac{2}{\Delta t}\left(u_j^{n+1}-u_j^n\right)-v_j^n$, $j=0,1$, into the above equation, we obtain

$$\begin{aligned}
&\left(1-\mu_1\right)u_1^{n+1}+\left(\tau_q^{(1)}-\mu_1\tau_T^{(1)}\right)\left[\frac{2}{\Delta t}\left(u_1^{n+1}-u_1^n\right)-v_1^n\right]\\
&+\left(5+\mu_1\right)u_0^{n+1}+\left(5\tau_q^{(1)}+\mu_1\tau_T^{(1)}\right)\left[\frac{2}{\Delta t}\left(u_0^{n+1}-u_0^n\right)-v_0^n\right]\\
&+\frac{1}{\alpha_1}h_1\left(1+\mu_1\right)\left(u_0^{n+1}-\left(\phi_1\right)^{n+1}\right)\\
&+\frac{1}{\alpha_1}h_1\left(\tau_q^{(1)}+\mu_1\tau_T^{(1)}\right)\left[\frac{2}{\Delta t}\left(u_0^{n+1}-u_0^n\right)-v_0^n-\left(\left(\phi_1\right)_t\right)^{n+1}\right]\\
=&\left(1+\mu_1\right)u_1^n+\left(\tau_q^{(1)}+\mu_1\tau_T^{(1)}\right)v_1^n+\left(5-\mu_1\right)u_0^n+\left(5\tau_q^{(1)}-\mu_1\tau_T^{(1)}\right)v_0^n\\
&+\frac{1}{\alpha_1}h_1\left(1-\mu_1\right)\left(u_0^n-\left(\phi_1\right)^n\right)+\frac{1}{\alpha_1}h_1\left(\tau_q^{(1)}-\mu_1\tau_T^{(1)}\right)\left[v_0^n-\left(\left(\phi_1\right)_t\right)^n\right]\\
&+\lambda_1\left[\left(f_1\right)_1^{n+\frac{1}{2}}+5\left(f_1\right)_0^{n+\frac{1}{2}}+h_1\left(\left(f_1\right)_x\right)_0^{n+\frac{1}{2}}\right].
\end{aligned}\tag{5.90}$$

After some algebraic simplifications, a third-order scheme can be obtained as

$$\begin{aligned}
&LB_1\cdot u_0^{n+1}+LC_1\cdot u_1^{n+1}\\
=&LB_2\cdot u_0^n+LC_2\cdot u_1^n\\
&+LB_3\cdot v_0^n+LC_3\cdot v_1^n+\left(LF\right)^{n+\frac{1}{2}}+\left(L\Phi\right)^n,
\end{aligned}\tag{5.91}$$

where $LB_1=5+\mu_1+\left(5\tau_q^{(1)}+\mu_1\tau_T^{(1)}\right)\frac{2}{\Delta t}+\frac{h_1}{\alpha_1}\left(1+\mu_1\right)+\frac{h_1}{\alpha_1}\left(\tau_q^{(1)}+\mu_1\tau_T^{(1)}\right)\frac{2}{\Delta t}$,
$LC_1=1-\mu_1+\left(\tau_q^{(1)}-\mu_1\tau_T^{(1)}\right)\frac{2}{\Delta t}$, $LB_2=5-\mu_1+\left(5\tau_q^{(1)}+\mu_1\tau_T^{(1)}\right)\frac{2}{\Delta t}+\frac{h_1}{\alpha_1}\left(1-\mu_1\right)$
$+\frac{h_1}{\alpha_1}\left(\tau_q^{(1)}+\mu_1\tau_T^{(1)}\right)\frac{2}{\Delta t}$, $LC_2=1+\mu_1+\left(\tau_q^{(1)}-\mu_1\tau_T^{(1)}\right)\frac{2}{\Delta t}$, $LB_3=\left(10+\frac{2}{\alpha_1}h_1\right)\tau_q^{(1)}$,
$LC_3=2\tau_q^{(1)}$, $\left(LF\right)^{n+\frac{1}{2}}=\lambda_1\left[\left(f_1\right)_1^{n+\frac{1}{2}}+5\left(f_1\right)_0^{n+\frac{1}{2}}+h_1\left(\left(f_1\right)_x\right)_0^{n+\frac{1}{2}}\right]$, $\left(L\Phi\right)^n=\frac{h_1}{\alpha_1}\left(1+\mu_1\right)$
$\left(\left(\phi_1\right)^{n+1}\right)-\frac{h_1}{\alpha_1}\left(1-\mu_1\right)\left(\left(\phi_1\right)^n\right)+\frac{h_1}{\alpha_1}\left(\tau_q^{(1)}+\mu_1\tau_T^{(1)}\right)\left(\left(\phi_1\right)_t\right)^{n+1}-\frac{h_1}{\alpha_1}\left(\tau_q^{(1)}-\mu_1\tau_T^{(1)}\right)\left(\left(\phi_1\right)_t\right)^n$.

For right boundary conditions, which are

$$\alpha_2 u_x\left(L,t\right)+u\left(L,t\right)=\phi_2\left(t\right),\tag{5.92}$$

$$\alpha_2 v_x\left(L,t\right)+v\left(L,t\right)=\left(\phi_2\right)_t\left(t\right),\tag{5.93}$$

by Eq. (4.2b), we have

$$u_{M-1} = u_M - h_2(u_x)_M + \frac{h_2^2}{12}(u_{xx})_{M-1} + \frac{5h_2^2}{12}(u_{xx})_M - \frac{h_2^3}{12}(u_{x^3})_M, \tag{5.94}$$

$$v_{M-1} = v_M - h_2(v_x)_M + \frac{h_2^2}{12}(v_{xx})_{M-1} + \frac{5h_2^2}{12}(v_{xx})_M - \frac{h_2^3}{12}(v_{x^3})_M. \tag{5.95}$$

Multiplying Eq. (5.95) by $\tau_T^{(2)}$, then adding it to Eq. (5.94), we obtain

$$\begin{aligned}
&u_{M-1} + \tau_T^{(2)} v_{M-1} \\
=&u_M + \tau_T^{(2)} v_M - h_2 \left[(u_x)_M + \tau_T^{(2)}(v_x)_M\right] \\
&+ \frac{h_2^2}{12}\left[(u_{xx})_1 + \tau_T^{(2)}(v_{xx})_{M-1}\right] \\
&+ \frac{5h_2^2}{12}\left[(u_{xx})_M + \tau_T^{(2)}(v_{xx})_M\right] \\
&- \frac{h_2^3}{12}\left[(u_{x^3})_M + \tau_T^{(2)}(v_{x^3})_M\right],
\end{aligned} \tag{5.96}$$

Eq. (5.64) gives

$$(u_{xx})_{M-1} + \tau_T^{(2)}(v_{xx})_{M-1} = \frac{1}{k_2}\left[\rho_2 C_2\left((u_t)_{M-1} + \tau_q^{(2)}(v_t)_{M-1}\right) - (f_2)_{M-1}\right], \tag{5.97a}$$

$$(u_{xx})_M + \tau_T^{(2)}(v_{xx})_M = \frac{1}{k_2}\left[\rho_2 C_2\left((u_t)_M + \tau_q^{(2)}(v_t)_M\right) - (f_2)_M\right], \tag{5.97b}$$

$$(u_{x^3})_M + \tau_T^{(2)}(v_{x^3})_M = \frac{1}{k_2}\left[\rho_2 C_2\left((u_{xt})_M + \tau_q^{(2)}(v_{xt})_M\right) - ((f_2)_x)_M\right]. \tag{5.97c}$$

Substituting them into Eq. (5.96) yields

$$\begin{aligned}
&u_{M-1} + \tau_T^{(2)} v_{M-1} \\
=&u_M + \tau_T^{(2)} v_M - h_2 \left[(u_x)_M + \tau_T^{(2)}(v_x)_M\right] \\
&+ \frac{h_2^2}{12k_2}\left[\rho_2 C_2\left((u_t)_{M-1} + \tau_q^{(2)}(v_t)_{M-1}\right) - (f_2)_{M-1}\right] \\
&+ \frac{5h_2^2}{12k_2}\left[\rho_2 C_2\left((u_t)_M + \tau_q^{(2)}(v_t)_M\right) - (f_2)_M\right] \\
&- \frac{h_2^3}{12k_2}\left[\rho_2 C_2\left((u_{xt})_M + \tau_q^{(2)}(v_{xt})_M\right) - ((f_2)_x)_M\right].
\end{aligned} \tag{5.98}$$

Applying the Crank-Nicolson method to Eq. (5.98) gives

$$\begin{aligned}
&\frac{\rho_2 C_2 h_2^2}{12k_2}\left[\frac{\left(u_{M-1}^{n+1}+\tau_q^{(2)}v_{M-1}^{n+1}\right)-\left(u_{M-1}^{n}+\tau_q^{(2)}v_{M-1}^{n}\right)}{\Delta t}\right]\\
&+\frac{5\rho_2 C_2 h_2^2}{12k_2}\left[\frac{\left(u_{M}^{n+1}+\tau_q^{(2)}v_{M}^{n+1}\right)-\left(u_{M}^{n}+\tau_q^{(2)}v_{M}^{n}\right)}{\Delta t}\right]\\
&-\frac{\rho_2 C_2 h_2^3}{12k_2}\left[\frac{\left((u_x)_M^{n+1}+\tau_q^{(2)}(v_x)_M^{n+1}\right)-\left((u_x)_M^{n}+\tau_q^{(2)}(v_x)_M^{n}\right)}{\Delta t}\right]\\
=&\frac{1}{2}\left[u_{M-1}^{n+1}+\tau_T^{(2)}v_{M-1}^{n+1}\right]+\frac{1}{2}\left[u_{M-1}^{n}+\tau_T^{(2)}v_{M-1}^{n}\right]-\frac{1}{2}\left[u_{M}^{n+1}+\tau_T^{(2)}v_{M}^{n+1}\right]\\
&-\frac{1}{2}\left[u_{M}^{n}+\tau_T^{(2)}v_{M}^{n}\right]+\frac{h_2}{2}\left[(u_x)_M^{n+1}+\tau_T^{(2)}(v_x)_M^{n+1}\right]+\frac{h_2}{2}\left[(u_x)_M^{n}+\tau_T^{(2)}(v_x)_M^{n}\right]\\
&+\frac{h_2^2}{12k_2}(f_2)_{M-1}^{n+\frac{1}{2}}+\frac{5h_2^2}{12k_2}(f_2)_{M}^{n+\frac{1}{2}}-\frac{h_2^3}{12k_2}((f_2)_x)_{M}^{n+\frac{1}{2}}. \qquad (5.99)
\end{aligned}$$

Multiplying both sides by $\frac{12k_2\Delta t}{\rho_2 C_2 h_2^2}$, letting $\lambda_2=\frac{\Delta t}{\rho_2 C_2}$, $\mu_2=\frac{6k_2\Delta t}{\rho_2 C_2 h_2^2}$, $w_{q_2}(x,t)=u(x,t)+\tau_q^{(2)}v(x,t)$, and $w_{T_2}(x,t)=u(x,t)+\tau_T^{(2)}v(x,t)$, where $0<x<l$, $0\le t\le T$, rearranging the terms, we rewrite the above equation as

$$\begin{aligned}
&(w_{q_2})_{M-1}^{n+1}-\mu_2(w_{T_2})_{M-1}^{n+1}+5(w_{q_2})_{M}^{n+1}+\mu_2(w_{T_2})_{M}^{n+1}-h_2\left[\left((w_{q_2})_x\right)_0^{n+1}-\mu_2((w_{T_2})_x)_0^{n+1}\right]\\
=&(w_{q_2})_{M-1}^{n}+\mu_2(w_{T_2})_{M-1}^{n}+5(w_{q_2})_{M}^{n}-\mu_2(w_{T_2})_{M}^{n}-h_2\left[\left((w_{q_2})_x\right)_0^{n}+\mu_2((w_{T_2})_x)_0^{n}\right]\\
&+\lambda_2\left[(f_2)_{M-1}^{n+\frac{1}{2}}+5(f_2)_{M}^{n+\frac{1}{2}}-h_2((f_2)_x)_{M}^{n+\frac{1}{2}}\right]. \qquad (5.100)
\end{aligned}$$

Eqs. (5.92)-(5.93) give

$$(u_x)_M^{n+1}=-\frac{1}{\alpha_2}\left(u_M^{n+1}-(\phi_2)^{n+1}\right), \qquad (5.101a)$$

$$(v_x)_M^{n+1}=-\frac{1}{\alpha_2}\left[v_M^{n+1}-((\phi_2)_t)^{n+1}\right], \qquad (5.101b)$$

$$(u_x)_M^{n}=-\frac{1}{\alpha_2}\left(u_M^{n}-(\phi_2)^{n}\right), \qquad (5.101c)$$

$$(v_x)_M^{n}=-\frac{1}{\alpha_2}\left[v_M^{n}-((\phi_2)_t)^{n}\right]. \qquad (5.101d)$$

Substituting them into Eq. (5.100) yields

$$
\begin{aligned}
&\left(w_{q_2}\right)_{M-1}^{n+1}-\mu_2\left(w_{T_2}\right)_{M-1}^{n+1}+5\left(w_{q_2}\right)_M^{n+1}+\mu_2\left(w_{T_2}\right)_M^{n+1}\\
&+\frac{h_2}{\alpha_2}\left(1+\mu_2\right)\left(u_M^{n+1}-\left(\phi_2\right)^{n+1}\right)+\frac{h_2}{\alpha_2}\left(\tau_q^{(2)}+\mu_2\tau_T^{(2)}\right)\left[v_M^{n+1}-\left(\left(\phi_2\right)_t\right)^{n+1}\right]\\
=&\left(w_{q_2}\right)_{M-1}^{n}+\mu_2\left(w_{T_2}\right)_{M-1}^{n}+5\left(w_{q_2}\right)_M^{n}-\mu_2\left(w_{T_2}\right)_M^{n}\\
&+\frac{h_2}{\alpha_2}\left(1-\mu_2\right)\left(u_M^{n}-\left(\phi_2\right)^{n}\right)+\frac{h_2}{\alpha_2}\left(\tau_q^{(2)}-\mu_2\tau_T^{(2)}\right)\left[v_M^{n}-\left(\left(\phi_2\right)_t\right)^{n}\right]\\
&+\lambda_2\left[\left(f_2\right)_{M-1}^{n+\frac{1}{2}}+5\left(f_2\right)_M^{n+\frac{1}{2}}-h_2\left(\left(f_2\right)_x\right)_M^{n+\frac{1}{2}}\right].
\end{aligned}
\tag{5.102}
$$

Substituting $v_j^{n+1}=\frac{2}{\Delta t}\left(u_j^{n+1}-u_j^n\right)-v_j^n$, $j=M-1$, M, into Eq. (5.102) gives

$$
\begin{aligned}
&\left(1-\mu_2\right)u_{M-1}^{n+1}+\left(\tau_q^{(2)}-\mu_2\tau_T^{(2)}\right)\left[\frac{2}{\Delta t}\left(u_{M-1}^{n+1}-u_{M-1}^{n}\right)-v_{M-1}^{n}\right]\\
&+\left(5+\mu_2\right)u_M^{n+1}+\left(5\tau_q^{(2)}+\mu_2\tau_T^{(2)}\right)\left[\frac{2}{\Delta t}\left(u_M^{n+1}-u_M^{n}\right)-v_M^{n}\right]\\
&+\frac{h_2}{\alpha_2}\left(1+\mu_2\right)\left(u_M^{n+1}-\left(\phi_2\right)^{n+1}\right)\\
&+\frac{h_2}{\alpha_2}\left(\tau_q^{(2)}+\mu_2\tau_T^{(2)}\right)\left[\frac{2}{\Delta t}\left(u_M^{n+1}-u_M^{n}\right)-v_M^{n}-\left(\left(\phi_2\right)_t\right)^{n+1}\right]\\
=&\left(1+\mu_2\right)u_{M-1}^{n}+\left(\tau_q^{(2)}+\mu_2\tau_T^{(2)}\right)v_{M-1}^{n}+\left(5-\mu_2\right)u_M^{n}+\left(5\tau_q^{(2)}-\mu_2\tau_T^{(2)}\right)v_M^{n}\\
&+\frac{h_2}{\alpha_2}\left(1-\mu_2\right)\left(u_M^{n}-\left(\phi_2\right)^{n}\right)+\frac{h_2}{\alpha_2}\left(\tau_q^{(2)}-\mu_2\tau_T^{(2)}\right)\left[v_M^{n}-\left(\left(\phi_2\right)_t\right)^{n}\right]\\
&+\lambda_2\left[\left(f_2\right)_{M-1}^{n+\frac{1}{2}}+5\left(f_2\right)_M^{n+\frac{1}{2}}-h_2\left(\left(f_2\right)_x\right)_M^{n+\frac{1}{2}}\right].
\end{aligned}
\tag{5.103}
$$

After some algebraic simplifications, we obtain a third-order scheme as

$$
\begin{aligned}
&RA_1\cdot u_{M-1}^{n+1}+RB_1\cdot u_M^{n+1}\\
=&RA_2\cdot u_{M-1}^{n}+RB_2\cdot u_M^{n}\\
&+RA_3\cdot v_{M-1}^{n}+RB_3\cdot v_M^{n}+\left(RF\right)^{n+\frac{1}{2}}+\left(R\Phi\right)^{n},
\end{aligned}
\tag{5.104}
$$

where $RA_1 = 1-\mu_2+\left(\tau_q^{(2)}-\mu_2\tau_T^{(2)}\right)\frac{2}{\Delta t}$, $RB_1 = 5+\mu_2+\left(5\tau_q^{(2)}+\mu_2\tau_T^{(2)}\right)\frac{2}{\Delta t}+\frac{h_2}{\alpha_2}(1+\mu_2)$
$+\frac{h_2}{\alpha_2}\left(\tau_q^{(2)}+\mu_2\tau_T^{(2)}\right)\frac{2}{\Delta t}$, $RA_2 = 1+\mu_2+\left(\tau_q^{(2)}-\mu_2\tau_T^{(2)}\right)\frac{2}{\Delta t}$, $RB_2 = 5-\mu_2+\left(5\tau_q^{(2)}+\mu_2\tau_T^{(2)}\right)\frac{2}{\Delta t}$
$+\frac{h_2}{\alpha_2}\left[(1-\mu_2)+\left(\tau_q^{(2)}+\mu_2\tau_T^{(2)}\right)\frac{2}{\Delta t}\right]$, $RA_3 = 2\tau_q^{(2)}$, $RB_3 = \left(10+\frac{2h_2}{\alpha_2}\right)\tau_q^{(2)}$,
$(R\Phi)^n = \frac{h_2}{\alpha_2}\left[(1+\mu_2)\,(\phi_2)^{n+1}+\left(\tau_q^{(2)}+\mu_2\tau_T^{(2)}\right)((\phi_2)_t)^{n+1}-(1-\mu_2)(\phi_2)^n-\left(\tau_q^{(2)}-\mu_2\tau_T^{(2)}\right)((\phi_2)_t)^n\right]$,
$(RF)^{n+\frac{1}{2}} = \lambda_2\left[(f_2)_{M-1}^{n+\frac{1}{2}}+5\,(f_2)_M^{n+\frac{1}{2}}-h_2((f_2)_x)_M^{n+\frac{1}{2}}\right]$.

At the interface, by using Eqs. (4.21a)-(4.21b), we have

$$\begin{aligned}
&u_{m-1}-32u_m+31u_{I^-}-30h_1\,(u_x)_{I^-}\\
=&-\frac{h_1^2}{3}\left[35\,(u_{xx})_{I^-}+8\,(u_{xx})_m-(u_{xx})_{m-1}\right]+2h_1^3\,(u_{x^3})_{I^-}\,, \qquad (5.105)\\
&v_{m-1}-32v_m+31v_{I^-}-30h_1\,(v_x)_{I^-}\\
=&-\frac{h_1^2}{3}\left[35\,(v_{xx})_{I^-}+8\,(v_{xx})_m-(v_{xx})_{m-1}\right]+2h_1^3\,(v_{x^3})_{I^-}\,, \qquad (5.106)\\
&u_{m+2}-32u_{m+1}+31u_{I^+}+30h_2\,(u_x)_{I^+}\\
=&-\frac{h_2^2}{3}\left[35\,(u_{xx})_{I^+}+8\,(u_{xx})_{m+1}-(u_{xx})_{m+2}\right]-2h_2^3\,(u_{x^3})_{I^+}\,, \qquad (5.107)\\
&v_{m+2}-32v_{m+1}+31v_{I^+}+30h_2\,(v_x)_{I^+}\\
=&-\frac{h_2^2}{3}\left[35\,(v_{xx})_{I^+}+8\,(v_{xx})_{m+1}-(v_{xx})_{m+2}\right]-2h_2^3\,(v_{x^3})_{I^+}\,. \qquad (5.108)
\end{aligned}$$

Multiplying Eq. (5.106) and Eq. (5.108) by $\tau_T^{(1)}$, $\tau_T^{(2)}$, respectively, then adding them to Eq. (5.105) and Eq. (5.107), respectively, we obtain

$$\begin{aligned}
&\left(u_{m-1}+\tau_T^{(1)}v_{m-1}\right)-32\left(u_m+\tau_T^{(1)}v_m\right)\\
&+31\left(u_{I^-}+\tau_T^{(1)}v_{I^-}\right)-30h_1\left((u_x)_{I^-}+\tau_T^{(1)}(v_x)_{I^-}\right)\\
=&-\frac{h_1^2}{3}\left[35\left((u_{xx})_{I^-}+\tau_T^{(1)}(v_{xx})_{I^-}\right)+8\left((u_{xx})_m+\tau_T^{(1)}(v_{xx})_m\right)\right.\\
&\left.-\left((u_{xx})_{m-1}+\tau_T^{(1)}(v_{xx})_{m-1}\right)\right]+2h_1^3\left((u_{x^3})_{I^-}+\tau_T^{(1)}(v_{x^3})_{I^-}\right), \qquad (5.109)
\end{aligned}$$

and

$$\begin{aligned}
&\left(u_{m+2}+\tau_T^{(2)}v_{m+2}\right)-32\left(u_{m+1}+\tau_T^{(2)}v_{m+1}\right)\\
&+31\left(u_{I^+}+\tau_T^{(2)}v_{I^+}\right)+30h_2\left((u_x)_{I^+}+\tau_T^{(2)}(v_x)_{I^+}\right)\\
=&-\frac{h_2^2}{3}\left[35\left((u_{xx})_{I^+}+\tau_T^{(2)}(v_{xx})_{I^+}\right)+8\left((u_{xx})_{m+1}+\tau_T^{(2)}(v_{xx})_{m+1}\right)\right.\\
&\left.-\left((u_{xx})_{m+2}+\tau_T^{(2)}(v_{xx})_{m+2}\right)\right]-2h_2^3\left(\left(u_{x^3}\right)_{I^+}+\tau_T^{(2)}\left(v_{x^3}\right)_{I^+}\right). \qquad (5.110)
\end{aligned}$$

Eqs. (5.63)-(5.64) give

$$\rho_1C_1\left((u_t)_i+\tau_q^{(1)}(v_t)_i\right)=k_1\left((u_{xx})_i+\tau_T^{(1)}(v_{xx})_i\right)+(f_1)_i\,,\ i=m-1,m,I^-, \qquad (5.111a)$$

$$\rho_2C_2\left((u_t)_i+\tau_q^{(2)}(v_t)_i\right)=k_2\left((u_{xx})_i+\tau_T^{(2)}(v_{xx})_i\right)+(f_2)_i\,,\ i=m+2,m+1,I^+, \qquad (5.111b)$$

$$\rho_1C_1\left((u_{xt})_{I^-}+\tau_q^{(1)}\left(v_{xt}\right)_{I^-}\right)=k_1\left(\left(u_{x^3}\right)_{I^-}+\tau_T^{(1)}\left(v_{x^3}\right)_{I^-}\right)+\left((f_1)_x\right)_{I^-}, \qquad (5.111c)$$

$$\rho_2C_2\left((u_{xt})_{I^+}+\tau_q^{(2)}\left(v_{xt}\right)_{I^+}\right)=k_2\left(\left(u_{x^3}\right)_{I^+}+\tau_T^{(2)}\left(v_{x^3}\right)_{I^+}\right)+\left((f_2)_x\right)_{I^+}. \qquad (5.111d)$$

Solving $(u_{xx})_i+\tau_T^{(1)}(v_{xx})_i$, $(u_{xx})_i+\tau_T^{(2)}(v_{xx})_i$, $(u_{x^3})_{I^-}+\tau_T^{(1)}(v_{x^3})_{I^-}$ and $(u_{x^3})_{I^+}+\tau_T^{(2)}(v_{x^3})_{I^+}$, then substituting them into Eq. (5.109) and Eq. (5.110), respectively, we obtain

$$\begin{aligned}
&\left(u_{m-1}+\tau_T^{(1)}v_{m-1}\right)-32\left(u_m+\tau_T^{(1)}v_m\right)\\
&+31\left(u_{I^-}+\tau_T^{(1)}v_{I^-}\right)-30h_1\left((u_x)_{I^-}+\tau_T^{(1)}(v_x)_{I^-}\right)\\
=&-\frac{35h_1^2}{3}\left[\frac{\rho_1C_1}{k_1}\left((u_t)_{I^-}+\tau_q^{(1)}\left(v_t\right)_{I^-}\right)-\frac{1}{k_1}\left(f_1\right)_{I^-}\right]\\
&-\frac{8h_1^2}{3}\left[\frac{\rho_1C_1}{k_1}\left((u_t)_m+\tau_q^{(1)}\left(v_t\right)_m\right)-\frac{1}{k_1}\left(f_1\right)_m\right]\\
&+\frac{h_1^2}{3}\left[\frac{\rho_1C_1}{k_1}\left((u_t)_{m-1}+\tau_q^{(1)}\left(v_t\right)_{m-1}\right)-\frac{1}{k_1}\left(f_1\right)_{m-1}\right],\\
&+2h_1^3\left[\frac{\rho_1C_1}{k_1}\left((u_{xt})_{I^-}+\tau_q^{(1)}\left(v_{xt}\right)_{I^-}\right)-\frac{1}{k_1}\left(\left(f_1\right)_x\right)_{I^-}\right], \qquad (5.112)
\end{aligned}$$

and

$$\begin{aligned}
&\left(u_{m+2}+\tau_T^{(2)}v_{m+2}\right)-32\left(u_{m+1}+\tau_T^{(2)}v_{m+1}\right)\\
&+31\left(u_{I^+}+\tau_T^{(2)}v_{I^+}\right)+30h_2\left(\left(u_x\right)_{I^+}+\tau_T^{(2)}\left(v_x\right)_{I^+}\right)\\
=&-\frac{35h_2^2}{3}\left[\frac{\rho_2C_2}{k_2}\left(u_t\right)_{I^+}+\tau_q^{(2)}\left(v_t\right)_{I^+}-\frac{1}{k_2}\left(f_2\right)_{I^+}\right]\\
&-\frac{8h_2^2}{3}\left[\frac{\rho_2C_2}{k_2}\left(u_t\right)_{m+1}+\tau_q^{(2)}\left(v_t\right)_{m+1}-\frac{1}{k_2}\left(f_2\right)_{m+1}\right]\\
&+\frac{h_2^2}{3}\left[\frac{\rho_2C_2}{k_2}\left(u_t\right)_{m+2}+\tau_q^{(2)}\left(v_t\right)_{m+2}-\frac{1}{k_2}\left(f_2\right)_{m+2}\right]\\
&-2h_2^3\left[\frac{\rho_2C_2}{k_2}\left(u_{xt}\right)_{I^+}+\tau_q^{(2)}\left(v_{xt}\right)_{I^+}-\frac{1}{k_2}\left(\left(f_2\right)_x\right)_{I^+}\right].
\end{aligned}\tag{5.113}$$

Then, the Crank-Nicolson method gives

$$\begin{aligned}
&\frac{1}{2}\left[\left(u_{m-1}^{n+1}+\tau_T^{(1)}v_{m-1}^{n+1}\right)+\left(u_{m-1}^{n}+\tau_T^{(1)}v_{m-1}^{n}\right)\right]\\
&-16\left[\left(u_{m}^{n+1}+\tau_T^{(1)}v_{m}^{n+1}\right)+\left(u_{m}^{n}+\tau_T^{(1)}v_{m}^{n}\right)\right]\\
&+\frac{31}{2}\left[\left(u_{I^-}^{n+1}+\tau_T^{(1)}v_{I^-}^{n+1}\right)+\left(u_{I^-}^{n}+\tau_T^{(1)}v_{I^-}^{n}\right)\right]\\
&-15h_1\left[\left(\left(u_x\right)_{I^-}^{n+1}+\tau_T^{(1)}\left(v_x\right)_{I^-}^{n+1}\right)+\left(\left(u_x\right)_{I^-}^{n}+\tau_T^{(1)}\left(v_x\right)_{I^-}^{n}\right)\right]\\
=&-\frac{35\rho_1C_1h_1^2}{3k_1\Delta t}\left[\left(u_{I^-}^{n+1}+\tau_q^{(1)}v_{I^-}^{n+1}\right)-\left(u_{I^-}^{n}+\tau_q^{(1)}v_{I^-}^{n}\right)\right]\\
&-\frac{8\rho_1C_1h_1^2}{3k_1\Delta t}\left[\left(u_{m}^{n+1}+\tau_q^{(1)}v_{m}^{n+1}\right)-\left(u_{m}^{n}+\tau_q^{(1)}v_{m}^{n}\right)\right]\\
&+\frac{\rho_1C_1h_1^2}{3k_1\Delta t}\left[\left(u_{m-1}^{n+1}+\tau_q^{(1)}v_{m-1}^{n+1}\right)-\left(u_{m-1}^{n}+\tau_q^{(1)}v_{m-1}^{n}\right)\right]\\
&+\frac{2\rho_1C_1h_1^3}{k_1\Delta t}\left[\left(\left(u_x\right)_{I^-}^{n+1}+\tau_q^{(1)}\left(v_x\right)_{I^-}^{n+1}\right)-\left(\left(u_x\right)_{I^-}^{n}+\tau_q^{(1)}\left(v_x\right)_{I^-}^{n}\right)\right]\\
&+\frac{h_1^2}{3k_1}\left[35\left(f_1\right)_{I^-}^{n+\frac{1}{2}}+8\left(f_1\right)_{m}^{n+\frac{1}{2}}-\left(f_1\right)_{m-1}^{n+\frac{1}{2}}-6h_1\left(\left(f_1\right)_x\right)_{I^-}^{n+\frac{1}{2}}\right],
\end{aligned}\tag{5.114}$$

and

$$
\begin{aligned}
&\frac{1}{2}\left[\left(u_{m+2}^{n+1}+\tau_T^{(2)}v_{m+2}^{n+1}\right)+\left(u_{m+2}^{n}+\tau_T^{(2)}v_{m+2}^{n}\right)\right]\\
&-16\left[\left(u_{m+1}^{n+1}+\tau_T^{(2)}v_{m+1}^{n+1}\right)+\left(u_{m+1}^{n}+\tau_T^{(2)}v_{m+1}^{n}\right)\right]\\
&+\frac{31}{2}\left[\left(u_{I^+}^{n+1}+\tau_T^{(2)}v_{I^+}^{n+1}\right)+\left(u_{I^+}^{n}+\tau_T^{(2)}v_{I^+}^{n}\right)\right]\\
&+15h_2\left[\left((u_x)_{I^+}^{n+1}+\tau_T^{(2)}\left(v_x\right)_{I^+}^{n+1}\right)+\left((u_x)_{I^+}^{n}+\tau_T^{(2)}\left(v_x\right)_{I^+}^{n}\right)\right]\\
=&-\frac{35\rho_2C_2h_2^2}{3k_2\Delta t}\left[\left(u_{I^+}^{n+1}+\tau_q^{(2)}v_{I^+}^{n+1}\right)-\left(u_{I^+}^{n}+\tau_q^{(2)}v_{I^+}^{n}\right)\right]\\
&-\frac{8\rho_2C_2h_2^2}{3k_2\Delta t}\left[\left(u_{m+1}^{n+1}+\tau_q^{(2)}v_{m+1}^{n+1}\right)-\left(u_{m+1}^{n}+\tau_q^{(2)}v_{m+1}^{n}\right)\right]\\
&+\frac{\rho_2C_2h_2^2}{3k_2\Delta t}\left[\left(u_{m+2}^{n+1}+\tau_q^{(2)}v_{m+2}^{n+1}\right)-\left(u_{m+2}^{n}+\tau_q^{(2)}v_{m+2}^{n}\right)\right]\\
&-\frac{2\rho_2C_2h_2^3}{k_2\Delta t}\left[\left((u_x)_{I^+}^{n+1}+\tau_q^{(2)}\left(v_x\right)_{I^+}^{n+1}\right)-\left((u_x)_{I^+}^{n}+\tau_q^{(2)}\left(v_x\right)_{I^+}^{n}\right)\right]\\
&+\frac{h_2^2}{3k_2}\left[35\left(f_2\right)_{I^+}^{n+\frac{1}{2}}+8\left(f_2\right)_{m+1}^{n+\frac{1}{2}}-\left(f_2\right)_{m+2}^{n+\frac{1}{2}}+6h_2\left(\left(f_2\right)_x\right)_{I^+}^{n+\frac{1}{2}}\right].
\end{aligned}
\tag{5.115}
$$

It should be pointed out that we only discretized u_{xt} at time direction without discretization on spatial direction, which means the GPM has been used here.

Multiplying Eq. (5.114) and Eq. (5.115) by $\frac{12k_1\Delta t}{\rho_1C_1h_1^2}$ and $\frac{12k_2\Delta t}{\rho_2C_2h_2^2}$, respectively, we obtain a simple form of the above two equations as

$$
\begin{aligned}
&\left[4\left(w_{q_1}\right)_{m-1}^{n+1}-\mu_1\left(w_{T_1}\right)_{m-1}^{n+1}\right]-\left[32\left(w_{q_1}\right)_{m}^{n+1}-32\mu_1\left(w_{T_1}\right)_{m}^{n+1}\right]\\
&-\left[140\left(w_{q_1}\right)_{I^-}^{n+1}+31\mu_1\left(w_{T_1}\right)_{I^-}^{n+1}\right]\\
&+h_1\left[24\left(\left(w_{q_1}\right)_x\right)_{I^-}^{n+1}+30\mu_1\left(\left(w_{T_1}\right)_x\right)_{I^-}^{n+1}\right]\\
=&\left[4\left(w_{q_1}\right)_{m-1}^{n}+\mu_1\left(w_{T_1}\right)_{m-1}^{n}\right]-\left[32\left(w_{q_1}\right)_{m}^{n}+32\mu_1\left(w_{T_1}\right)_{m}^{n}\right]\\
&-\left[140\left(w_{q_1}\right)_{I^-}^{n+1}-31\mu_1\left(w_{T_1}\right)_{I^-}^{n+1}\right]\\
&+h_1\left[24\left(\left(w_{q_1}\right)_x\right)_{I^-}^{n+1}-30\mu_1\left(\left(w_{T_1}\right)_x\right)_{I^-}^{n+1}\right]\\
&-4\lambda_1\left(35\left(f_1\right)_{I^-}^{n+\frac{1}{2}}+8\left(f_1\right)_{m}^{n+\frac{1}{2}}-\left(f_1\right)_{m}^{n+\frac{1}{2}}-6h_1\left(\left(f_1\right)_x\right)_{I^-}^{n+\frac{1}{2}}\right),
\end{aligned}
\tag{5.116}
$$

and

$$
\begin{aligned}
&\left[4\left(w_{q_2}\right)_{m+2}^{n+1}-\mu_2\left(w_{T_2}\right)_{m+2}^{n+1}\right]-\left[32\left(w_{q_2}\right)_{m+1}^{n+1}-32\mu_2\left(w_{T_2}\right)_{m+1}^{n+1}\right]\\
&-\left[140\left(w_{q_2}\right)_{I^+}^{n+1}+31\mu_2\left(w_{T_2}\right)_{I^+}^{n+1}\right]\\
&-h_2\left[24\left(\left(w_{q_2}\right)_x\right)_{I^+}^{n+1}+30\mu_2\left(\left(w_{T_2}\right)_x\right)_{I^+}^{n+1}\right]\\
=&\left[4\left(w_{q_2}\right)_{m+2}^{n}+\mu_2\left(w_{T_2}\right)_{m+2}^{n}\right]-\left[32\left(w_{q_2}\right)_{m+1}^{n}+32\mu_2\left(w_{T_2}\right)_{m+1}^{n}\right]\\
&-\left[140\left(w_{q_2}\right)_{I^+}^{n}-31\mu_2\left(w_{T_2}\right)_{I^+}^{n}\right]\\
&-h_2\left[24\left(\left(w_{q_2}\right)_x\right)_{I^+}^{n}-30\mu_2\left(\left(w_{T_2}\right)_x\right)_{I^+}^{n}\right]\\
&-4\lambda_2\left(35\left(f_2\right)_{I^+}^{n+\frac{1}{2}}+8\left(f_2\right)_{m+1}^{n+\frac{1}{2}}-\left(f_2\right)_{m+2}^{n+\frac{1}{2}}+6h_2\left(\left(f_2\right)_x\right)_{I^+}^{n+\frac{1}{2}}\right). \qquad (5.117)
\end{aligned}
$$

Substituting $v_j^{n+1}=\frac{2}{\Delta t}\left(u_j^{n+1}-u_j^n\right)-v_j^n$, where $j=m-1,\, m,\, I^-,\, I^+,\, m+1,\, m+2$, and $\left(v_x\right)_j^{n+1}=\frac{2}{\Delta t}\left(\left(u_x\right)_j^{n+1}-\left(u_x\right)_j^n\right)-\left(v_x\right)_j^n$, where $j=I^-,\, I^+$, into the above equations, we obtain

$$
\begin{aligned}
&\left(4-\mu_1\right)u_{m-1}^{n+1}+\left(4\tau_q^{(1)}-\mu_1\tau_T^{(1)}\right)\left[\frac{2}{\Delta t}\left(u_{m-1}^{n+1}-u_{m-1}^n\right)-v_{m-1}^n\right]\\
&-\left(32-32\mu_1\right)u_m^{n+1}-\left(32\tau_q^{(1)}-32\mu_1\tau_T^{(1)}\right)\left[\frac{2}{\Delta t}\left(u_m^{n+1}-u_m^n\right)-v_m^n\right]\\
&-\left(140+31\mu_1\right)u_{I^-}^{n+1}-\left(140\tau_q^{(1)}+31\mu_1\tau_T^{(1)}\right)\left[\frac{2}{\Delta t}\left(u_{I^-}^{n+1}-u_{I^-}^n\right)-v_{I^-}^n\right]\\
&+\left(24+30\mu_1\right)h_1\left(u_x\right)_{I^-}^{n+1}\\
&+24\left(\tau_q^{(1)}+30\mu_1\tau_T^{(1)}\right)h_1\left[\frac{2}{\Delta t}\left(\left(u_x\right)_{I^-}^{n+1}-\left(u_x\right)_{I^-}^n\right)-\left(v_x\right)_{I^-}^n\right]\\
=&\left[4\left(w_{q_1}\right)_{m-1}^{n}+\mu_1\left(w_{T_1}\right)_{m-1}^{n}\right]-\left[32\left(w_{q_1}\right)_{m}^{n}+32\mu_1\left(w_{T_1}\right)_{m}^{n}\right]\\
&-\left[140\left(w_{q_1}\right)_{I^-}^{n}-31\mu_1\left(w_{T_1}\right)_{I^-}^{n}\right]+h_1\left[24\left(\left(w_{q_1}\right)_x\right)_{I^-}^{n}-30\mu_1\left(\left(w_{T_1}\right)_x\right)_{I^-}^{n}\right]\\
&-4\lambda_1\left(35\left(f_1\right)_{I^-}^{n+\frac{1}{2}}+8\left(f_1\right)_{m}^{n+\frac{1}{2}}-\left(f_1\right)_{m-1}^{n+\frac{1}{2}}-6h_1\left(\left(f_1\right)_x\right)_{I^-}^{n+\frac{1}{2}}\right), \qquad (5.118)
\end{aligned}
$$

and

$$
\begin{aligned}
&(4-\mu_2)\,u_{m+2}^{n+1}+\left(4\tau_q^{(2)}-\mu_2\tau_T^{(2)}\right)\left[\frac{2}{\Delta t}\left(u_{m+2}^{n+1}-u_{m+2}^{n}\right)-v_{m+2}^{n}\right]\\
&-(32-32\mu_2)\,u_{m+1}^{n+1}-\left(32\tau_q^{(2)}-32\mu_2\tau_T^{(2)}\right)\left[\frac{2}{\Delta t}\left(u_{m+1}^{n+1}-u_{m+1}^{n}\right)-v_{m+1}^{n}\right]\\
&-(140+31\mu_2)\,u_{I^+}^{n+1}-\left(140\tau_q^{(2)}+31\mu_2\tau_T^{(2)}\right)\left[\frac{2}{\Delta t}\left(u_{I^+}^{n+1}-u_{I^+}^{n}\right)-v_{I^+}^{n}\right]\\
&-(24+30\mu_2)\,h_2\,(u_x)_{I^-}^{n+1}\\
&-\left(24\tau_q^{(2)}+30\mu_2\tau_T^{(2)}\right)h_2\left[\frac{2}{\Delta t}\left((u_x)_{I^+}^{n+1}-(u_x)_{I^+}^{n}\right)-(v_x)_{I^+}^{n}\right]\\
=&\left[4\,(w_{q_2})_{m+2}^{n}+\mu_2\,(w_{T_2})_{m+2}^{n}\right]-\left[32\,(w_{q_2})_{m+1}^{n}+32\mu_2\,(w_{T_2})_{m+1}^{n}\right]\\
&-\left[140\,(w_{q_2})_{I^+}^{n}-31\mu_2\,(w_{T_2})_{I^+}^{n}\right]-h_2\left[24\left((w_{q_2})_x\right)_{I^+}^{n}-30\mu_2\left((w_{T_2})_x\right)_{I^+}^{n}\right]\\
&-4\lambda_2\left(35\,(f_2)_{I^+}^{n+\frac{1}{2}}+8\,(f_2)_{m+1}^{n+\frac{1}{2}}-(f_2)_{m+2}^{n+\frac{1}{2}}+6h_2\left((f_2)_x\right)_{I^+}^{n+\frac{1}{2}}\right),
\end{aligned}
\tag{5.119}
$$

After simplification, we obtain

$$
\begin{aligned}
&M_1A_1\cdot u_{m-1}^{n+1}+M_1B_1\cdot u_m^{n+1}+M_1C_1\cdot u_{I^-}^{n+1}+M_1D_1\cdot(u_x)_{I^-}^{n+1}\\
=&M_1A_2\cdot u_{m-1}^{n}+M_1B_2\cdot u_m^{n}+M_1C_2\cdot u_{I^-}^{n}+M_1D_2\cdot(u_x)_{I^-}^{n}\\
&M_1A_3\cdot v_{m-1}^{n}+M_1B_3\cdot v_m^{n}+M_1C_3\cdot v_{I^-}^{n}+M_1D_3\cdot(v_x)_{I^-}^{n}\\
&-4\lambda_1\left(35\,(f_1)_{I^-}^{n+\frac{1}{2}}+8\,(f_1)_{m}^{n+\frac{1}{2}}-(f_1)_{m-1}^{n+\frac{1}{2}}-6h_1\left((f_1)_x\right)_{I^-}^{n+\frac{1}{2}}\right),
\end{aligned}
\tag{5.120}
$$

and

$$
\begin{aligned}
&M_2A_1\cdot u_{m+2}^{n+1}+M_2B_1\cdot u_{m+1}^{n+1}+M_2C_1\cdot u_{I^+}^{n+1}+M_2D_1\cdot(u_x)_{I^+}^{n+1}\\
=&M_2A_2\cdot u_{m+2}^{n}+M_2B_2\cdot u_{m+1}^{n}+M_2C_2\cdot u_{I^+}^{n}+M_2D_2\cdot(u_x)_{I^+}^{n}\\
&M_2A_3\cdot v_{m+2}^{n}+M_2B_3\cdot v_{m+1}^{n}+M_2C_3\cdot v_{I^+}^{n}+M_2D_3\cdot(v_x)_{I^+}^{n}\\
&-4\lambda_2\left(35\,(f_2)_{I^+}^{n+\frac{1}{2}}+8\,(f_2)_{m+1}^{n+\frac{1}{2}}-(f_2)_{m+2}^{n+\frac{1}{2}}+6h_2\left((f_2)_x\right)_{I^+}^{n+\frac{1}{2}}\right),
\end{aligned}
\tag{5.121}
$$

where $M_1A_1 = 4(1+\tau_q^{(1)}\frac{2}{\Delta t})-\mu_1(1+\tau_T^{(1)}\frac{2}{\Delta t})$, $M_1B_1 = -32(1+\tau_q^{(1)}\frac{2}{\Delta t})+32\mu_1(1+\tau_T^{(1)}\frac{2}{\Delta t})$,

$M_1C_1 = -140\left(1+\tau_q^{(1)}\right)\frac{2}{\Delta t}-31\mu_1(1+\tau_T^{(1)}\frac{2}{\Delta t})$, $M_1D_1 = 24h_1(1+\tau_q^{(1)}\frac{2}{\Delta t})+30\mu_1h_1(1+\tau_T^{(1)}\frac{2}{\Delta t})$,

$M_1A_2 = 4(1+\tau_q^{(1)}\frac{2}{\Delta t})+\mu_1(1-\tau_T^{(1)}\frac{2}{\Delta t})$, $M_1B_2 = -32(1+\tau_q^{(1)}\frac{2}{\Delta t})-32\mu_1(1-\tau_T^{(1)}\frac{2}{\Delta t})$,

$M_1C_2 = -140\left(1+\tau_q^{(1)}\frac{2}{\Delta t}\right)+31\mu_1(1-\tau_T^{(1)}\frac{2}{\Delta t})$, $M_1D_2 = 24h_1(1+\tau_q^{(1)}\frac{2}{\Delta t})-30\mu_1h_1(1-\tau_T^{(1)}\frac{2}{\Delta t})$,

$M_1A_3 = 8\tau_q^{(1)}$, $M_1B_3 = -64\tau_q^{(1)}$, $M_1C_3 = -280\tau_q^{(1)}$, $M_1D_3 = 48h_1\tau_q^{(1)}$;

$M_2A_1 = 4(1+\tau_q^{(2)}\frac{2}{\Delta t})-\mu_2(1+\tau_T^{(2)}\frac{2}{\Delta t})$, $M_2B_1 = -32(1+\tau_q^{(2)}\frac{2}{\Delta t})+32\mu_2(1+\tau_T^{(2)}\frac{2}{\Delta t})$,

$M_2C_1 = -140\left(1+\tau_q^{(2)}\frac{2}{\Delta t}\right)-31\mu_2(1+\tau_T^{(2)}\frac{2}{\Delta t})$, $M_2D_1 = -24h_2(1+\tau_q^{(2)}\frac{2}{\Delta t})-30\mu_2h_2(1+\tau_T^{(2)}\frac{2}{\Delta t})$,

$M_2A_2 = 4(1+\tau_q^{(2)}\frac{2}{\Delta t})+\mu_2(1-\tau_T^{(2)}\frac{2}{\Delta t})$, $M_2B_2 = -32(1+\tau_q^{(2)}\frac{2}{\Delta t})-32\mu_2(1-\tau_T^{(2)}\frac{2}{\Delta t})$,

$M_2C_2 = -140\left(1+\tau_q^{(2)}\frac{2}{\Delta t}\right)+31\mu_2(1-\tau_T^{(2)}\frac{2}{\Delta t})$, $M_2D_2 = -24h_2(1+\tau_q^{(2)}\frac{2}{\Delta t})+30\mu_2h_2(1-\tau_T^{(2)}\frac{2}{\Delta t})$,

$M_2A_3 = 8\tau_q^{(2)}$, $M_2B_3 = -64\tau_q^{(2)}$, $M_2C_3 = -280\tau_q^{(2)}$, $M_2D_3 = -48h_2\tau_q^{(2)}$.

Applying the Crank-Nicolson method to interfacial conditions Eqs. (5.69)-(5.70) yields

$$u_{I^+}^{n+1} - u_{I^-}^{n+1} = u_{I^-}^{n} - u_{I^+}^{n}, \tag{5.122}$$

$$\begin{aligned} &k_2\left(1+\tau_T^{(2)}\frac{2}{\Delta t}\right)(u_x)_{I^+}^{n+1} - k_1\left(1+\tau_T^{(1)}\frac{2}{\Delta t}\right)(u_x)_{I^-}^{n+1} \\ =&k_1\left(1-\tau_T^{(1)}\frac{2}{\Delta t}\right)(u_x)_{I^-}^{n} - k_2\left(1-\tau_T^{(2)}\frac{2}{\Delta t}\right)(u_x)_{I^+}^{n}. \end{aligned} \tag{5.123}$$

From Eqs. (5.77)-(5.78), when $j = m$, $m+1$, we have

$$\begin{aligned} &A_1u_{m-1}^{n+1} + B_1u_m^{n+1} + A_1u_{I^-}^{n+1} \\ =&A_2u_{m-1}^{n} + B_2u_m^{n} + A_2u_{j+1}^{n} + D_1v_{m-1}^{n} + D_2v_m^{n} + D_1v_{I^-}^{n} + + (F_1)_m^{n+\frac{1}{2}}, \end{aligned} \tag{5.124}$$

and

$$\begin{aligned} &\tilde{A}_1u_{I^+}^{n+1} + \tilde{B}_1u_{m+1}^{n+1} + \tilde{A}_1u_{m+2}^{n+1} \\ =&\tilde{A}_2u_{I^+}^{n} + \tilde{B}_2u_{m+1}^{n} + \tilde{A}_2u_{m+2}^{n} + \tilde{D}_1v_{I^+}^{n} + \tilde{D}_2v_{m+1}^{n} + \tilde{D}_1v_{m+2}^{n} + (F_2)_{m+1}^{n+\frac{1}{2}}, \end{aligned} \tag{5.125}$$

respectively. Combining Eqs. (5.120)-(5.125) together, we obtain a similar system to Eqs. (5.52)-(5.57) as follows:

$$u_{I^+}^{n+1} - u_{I^-}^{n+1} = a_n, \tag{5.126}$$

$$K_2 \left(u_x\right)_{I^+}^{n+1} - K_1 \left(u_x\right)_{I^-}^{n+1} = b_n, \tag{5.127}$$

$$c_{11} \cdot u_{m-1}^{n+1} + c_{12} \cdot u_m^{n+1} + c_{13} \cdot u_{I^-}^{n+1} + c_{14} \cdot \left(u_x\right)_{I^-}^{n+1} = c_{1n}, \tag{5.128}$$

$$c_{21} \cdot u_{m+2}^{n+1} + c_{22} \cdot u_{m+1}^{n+1} + c_{23} \cdot u_{I^+}^{n+1} + c_{24} \cdot \left(u_x\right)_{I^+}^{n+1} = c_{2n}, \tag{5.129}$$

$$c_{31} \cdot u_{m-1}^{n+1} + c_{32} \cdot u_m^{n+1} + c_{33} \cdot u_{I^-}^{n+1} = c_{3n}, \tag{5.130}$$

$$c_{41} \cdot u_{m+2}^{n+1} + c_{42} \cdot u_{m+1}^{n+1} + c_{43} \cdot u_{I^+}^{n+1} = c_{4n}, \tag{5.131}$$

where $a_n = u_{I^-}^n - u_{I^+}^n$, $K_1 = k_1 \left(1 + \tau_T^{(1)} \frac{2}{\Delta t}\right)$, $K_2 = k_2 \left(1 + \tau_T^{(2)} \frac{2}{\Delta t}\right)$,

$b_n = k_1 \left(1 - \tau_T^{(1)} \frac{2}{\Delta t}\right) \left(u_x\right)_{I^-}^n - k_2 \left(1 - \tau_T^{(2)} \frac{2}{\Delta t}\right) \left(u_x\right)_{I^+}^n$,

$c_{11} = M_1 A_1$, $c_{12} = M_1 B_1$, $c_{13} = M_1 C_1$, $c_{14} = M_1 D_1$,

$$c_{1n} = M_1 A_2 \cdot u_{m-1}^n + M_1 B_2 \cdot u_m + M_1 C_2 \cdot u_{I^-}^n + M_1 D_2 \cdot \left(u_x\right)_{I^-}^n + M_1 A_3 \cdot v_{m-1}^n + M_1 B_3 \cdot v_m$$
$$+ M_1 C_3 \cdot v_{I^-}^n + M_1 D_3 \cdot \left(v_x\right)_{I^-}^n - 4\lambda_1 \left[\left(f_1\right)_m^{n+\frac{1}{2}} + 5 \left(f_1\right)_{I^-}^{n+\frac{1}{2}} + h_1 \left(\left(f_1\right)_x\right)_{I^-}^{n+\frac{1}{2}}\right];$$

$c_{21} = M_2 A_1$, $c_{22} = M_2 B_1$, $c_{23} = M_2 C_1$, $c_{24} = M_2 D_1$,

$$c_{2n} = M_2 A_2 \cdot u_{m+2}^n + M_2 B_2 \cdot u_{m+1} + M_2 C_2 \cdot u_{I^+}^n + M_2 D_2 \cdot \left(u_x\right)_{I^+}^n + M_2 A_3 \cdot v_{m+2}^n + M_2 B_3 \cdot v_{m+1}$$
$$+ M_2 C_3 \cdot v_{I^+}^n + M_2 D_3 \cdot \left(v_x\right)_{I^+}^n - 4\lambda_2 \left[\left(f_2\right)_{m+1}^{n+\frac{1}{2}} + 5 \left(f_2\right)_{I^+}^{n+\frac{1}{2}} + h_2 \left(\left(f_2\right)_x\right)_{I^+}^{n+\frac{1}{2}}\right];$$

$c_{31} = A_1$, $c_{32} = B_1$, $c_{33} = c_{31} = A_1$,

$$c_{3n} = A_2 u_{m-1}^n + B_2 u_m^n + A_2 u_{j+1}^n + D_1 v_{m-1}^n + D_2 v_m^n + D_1 v_{I^-}^n + + \left(F_1\right)_m^{n+\frac{1}{2}};$$

$c_{41} = \tilde{A}_1$, $c_{42} = \tilde{A}_2$, $c_{43} = c_{41} = \tilde{A}_1$,

$$c_{4n} = \tilde{A}_2 u_{I^+}^n + \tilde{B}_2 u_{m+1}^n + \tilde{A}_2 u_{m+2}^n + \tilde{D}_1 v_{I^+}^n + \tilde{D}_2 v_{m+1}^n + \tilde{D}_1 v_{m+2}^n + \left(F_2\right)_{m+1}^{n+\frac{1}{2}}.$$

Using a similar argument as in the steady-state case, we can delete $u_{I^-}^{n+1}$, $u_{I^+}^{n+1}$, $(u_x)_{I^-}^{n+1}$, $(u_x)_{I^+}^{n+1}$ in the above equations and obtain two equations as follows:

$$c_{51} \cdot u_{m-1}^{n+1} + c_{52} \cdot u_m^{n+1} + c_{53} \cdot u_{m+1}^{n+1} = c_{5n}, \tag{5.132}$$

$$c_{61} \cdot u_m^{n+1} + c_{62} \cdot u_{m+1}^{n+1} + c_{63} \cdot u_{m+2}^{n+1} = c_{6n}, \tag{5.133}$$

where $c_{51} = K_1 c_{24} c_{41} \left(c_{13} c_{31} - c_{11} c_{33}\right) - K_2 c_{14} c_{31} \left(c_{23} c_{41} - c_{21} c_{43}\right)$,

$c_{52} = K_1 c_{24} c_{41} \left(c_{13} c_{32} - c_{12} c_{33}\right) - K_2 c_{14} c_{32} \left(c_{23} c_{41} - c_{21} c_{43}\right)$,

$c_{53} = K_2 c_{14} c_{33} \left(c_{22} c_{41} - c_{21} c_{42}\right)$,

$c_{5n} = -K_1 c_{24} c_{33} c_{41} c_{1n} + K_2 c_{14} c_{33} c_{41} c_{2n} + [K_1 c_{24} c_{13} c_{41} - K_2 c_{14} \left(c_{23} c_{41} - c_{21} c_{43}\right)] c_{3n}$

$\quad -K_2 c_{14} c_{21} c_{33} c_{4n} + K_2 c_{14} c_{33} (c_{21} c_{43} - c_{23} c_{41}) a_n - c_{14} c_{24} c_{33} c_{41} b_n;$

$c_{61} = K_1 c_{24} c_{43} \left(c_{12} c_{31} - c_{11} c_{32}\right)$,

$c_{62} = K_2 c_{14} c_{31} \left(c_{23} c_{42} - c_{22} c_{43}\right) - K_1 c_{24} c_{42} \left(c_{13} c_{31} - c_{11} c_{33}\right)$,

$c_{63} = K_2 c_{14} c_{31} \left(c_{23} c_{41} - c_{21} c_{43}\right) - K_1 c_{24} c_{41} \left(c_{13} c_{31} - c_{11} c_{33}\right)$,

$c_{6n} = K_1 c_{24} c_{31} c_{43} c_{1n} - K_2 c_{14} c_{31} c_{43} c_{2n} + \left[\frac{K_1 c_{24} c_{13} c_{31} c_{43}}{-c_{33}} - K_1 c_{24} c_{43} \left(c_{11} + \frac{c_{13} c_{31}}{-c_{33}}\right)\right] c_{3n}$

$\quad + \left[K_2 c_{14} c_{23} c_{31} + K_1 c_{24} c_{33} \left(c_{11} + \frac{c_{13} c_{31}}{-c_{33}}\right)\right] c_{4n} - K_1 c_{24} c_{33} c_{43} \left(c_{11} + \frac{c_{13} c_{31}}{-c_{33}}\right) a_n$

$\quad + c_{14} c_{24} c_{31} c_{43} b_n.$

As the same as before, the GPM was used again here.

Thus, Eqs. (5.77)-(5.78), Eqs. (5.91) and (5.104), and Eqs. (5.132)-(5.133) together form a higher-order accurate finite difference scheme for the heat conduction model in nanoscale. We can rewrite the scheme in matrix form as

$$A\vec{u}^{n+1} = \vec{d}, \tag{5.134}$$

where $\vec{u}^{n+1} = \left[u_0^{n+1}, u_1^{n+1}, u_2^{n+1}, ..., u_{m-1}^{n+1}, u_m^{n+1}, u_{m+1}^{n+1}, u_{m+2}^{n+1}, ..., u_{M-2}^{n+1}, u_{M-1}^{n+1}, u_M^{n+1}\right]^T$,

$$A=\begin{bmatrix}
LB_1 & LC_1 & & & & & & & & & \\
A_1 & B_1 & A_1 & & & & & & & & \\
 & \ddots & \ddots & \ddots & & & & & & & \\
 & & A_1 & B_1 & A_1 & & & & & & \\
 & & & c_{51} & c_{52} & c_{53} & & & & & \\
 & & & & c_{61} & c_{62} & c_{63} & & & & \\
 & & & & & \tilde{A}_1 & \tilde{B}_1 & \tilde{A}_1 & & & \\
 & & & & & & \ddots & \ddots & \ddots & & \\
 & & & & & & & & \tilde{A}_1 & \tilde{B}_1 & \tilde{A}_1 \\
 & & & & & & & & & RA_1 & RB_1
\end{bmatrix}$$

and $\vec{d}=$

$$\begin{bmatrix}
LB_2u_0^n+LC_2u_1^n+LB_3v_0^n+LC_3v_1^n+(LF)^{n+\frac{1}{2}}+(L\Phi)^n \\
A_2u_0^n+B_2u_1^n+A_2u_2^n+A_3v_0^n+B_3v_1^n+A_3v_2^n+(F_1)_1^{n+\frac{1}{2}} \\
A_2u_1^n+B_2u_2^n+A_2u_3^n+A_3v_1^n+B_3v_2^n+A_3v_3^n+(F_1)_2^{n+\frac{1}{2}} \\
\vdots \\
A_2u_{m-2}^n+B_2u_{m-1}^n+A_2u_m^n+A_3v_{m-2}^n+B_3v_{m-1}^n+A_3v_m^n+(F_1)_{m-1}^{n+\frac{1}{2}} \\
c_{5n} \\
c_{6n} \\
\tilde{A}_2u_{m+1}^n+\tilde{B}_2u_{m+2}^n+\tilde{A}_2u_{m+3}^n+\tilde{A}_3v_{m+1}^n+\tilde{B}_3v_{m+2}^n+\tilde{A}_3v_{m+3}^n+(F_2)_{m+2}^{n+\frac{1}{2}} \\
\tilde{A}_2u_{m+2}^n+\tilde{B}_2u_{m+3}^n+\tilde{A}_2u_{m+4}^n+\tilde{A}_3v_{m+2}^n+\tilde{B}_3v_{m+3}^n+\tilde{A}_3v_{m+4}^n+(F_2)_{m+3}^{n+\frac{1}{2}} \\
\vdots \\
\tilde{A}_2u_{M-3}^n+\tilde{B}_2u_{M-2}^n+\tilde{A}_2u_{M-1}^n+\tilde{A}_3v_{M-3}^n+\tilde{B}_3v_{M-2}^n+\tilde{A}_3v_{M-1}^n+(F_2)_{M-2}^{n+\frac{1}{2}} \\
\tilde{A}_2u_{M-2}^n+\tilde{B}_2u_{M-1}^n+\tilde{A}_2u_M^n+\tilde{A}_3v_{M-2}^n+\tilde{B}_3v_{M-1}^n+\tilde{A}_3v_M^n+(F_2)_{M-1}^{n+\frac{1}{2}} \\
RA_2u_{M-1}^n+RB_2u_M^n+RA_3v_{M-1}^n+RB_3v_M^n+(RF)^{n+\frac{1}{2}}+(R\Phi)^n
\end{bmatrix}.$$

Note that A is a tridiagonal matrix, one can use the Thomas algorithm to obtain the solution efficiently. Once the values of u_{m-1}^{n+1}, u_m^{n+1}, u_{m+1}^{n+1} and u_{m+2}^{n+1} are obtained, the values of $u_{I^-}^{n+1}$, $u_{I^+}^{n+1}$, $(u_x)_{I^-}^{n+1}$ and $(u_x)_{I^+}^{n+1}$ can be easily obtained by using Eqs. (5.126)-(5.131). After all the values of u^{n+1} (including $u_{I^-}^{n+1}$, $u_{I^+}^{n+1}$, $(u_x)_{I^-}^{n+1}$ and $(u_x)_{I^+}^{n+1}$) are obtained, we can use Eq. (5.75) to obtain the corresponding values of v^{n+1} for preparing the next time iteration.

In summary, we have developed a higher-order finite difference scheme for the nanoscale heat conduction model, which is the dual-phase-lagging equation. The scheme is third-order at boundary, fourth-order at the interface. Hence, the overall schemes are at least third-order. Again, it should be pointed out that the GPM has been used in the derivations of the scheme.

CHAPTER 6

NUMERICAL EXAMPLES

In this chapter, we will test the accuracy and applicability of those compact finite difference schemes obtained in Chapters 4 and 5 by four examples. In particular, the first three examples are to verify the accuracy of the numerical solutions obtained based on our present schemes for solving the steady-state heat conduction model, unsteady-state heat conduction model, and nanoscale heat conduction model, respectively. Numerical results will be compared with the exact solutions and numerical solutions based on the existing methods. The fourth example is to demonstrate the applicability of the scheme for the nanoscale heat conduction case by obtaining the temperature rise in a double-layered nanoscale thin film, where a gold layer is on a chromium padding layer and is irradiated by an ultrashort-pulsed laser.

Example 1. Consider a steady-state heat conduction problem in [65] as

$$u_{xx} = 2, \quad 0 < x < \frac{1}{3}, \tag{6.1}$$

$$10u_{xx} = 10e^x, \quad \frac{1}{3} < x < 1, \tag{6.2}$$

with interfacial condition:

$$u_{I^+} - u_{I^-} = e^{\frac{1}{3}} - \frac{1}{9}, \quad 10\left(u_x\right)_{I^+} - \left(u_x\right)_{I^-} = 10e^{\frac{1}{3}} - \frac{2}{3}, \tag{6.3}$$

and boundary condition either of Dirichlet boundary:

$$u(0) = 0,\ u(1) = e, \tag{6.4a}$$

Neumann boundary:

$$u_x(0) = 0,\quad u_x(1) = e, \tag{6.4b}$$

Robin boundary:

$$-u_x(0) + u(0) = 0,\ u_x(1) + u(1) = 2e. \tag{6.4b}$$

It can be seen that the exact solution is $u(x) = x^2$, if $0 \le x \le \frac{1}{3}$; $u(x) = e^x$, if $\frac{1}{3} \le x \le 1$. We use the three schemes Eq. (4.55), Eq. (5.14) (combining with Eq. (5.15)), and Eq. (5.16), to solve the above problem corresponding to the three types of boundaries, respectively.

Table 6.1: Numerical errors and convergence order for Example 1.

Present schemes						
	Eq. (4.55) (Dirichlet)		Eq. (5.14) (Neumann)		Eq. (5.16) (Robin)	
M	$\|E_M\|_\infty$	Order	$\|E_M\|_\infty$	Order	$\|E_M\|_\infty$	Order
9	1.6044×10^{-7}	–	2.0465×10^{-6}	–	6.6332×10^{-7}	–
18	1.1584×10^{-8}	3.79	1.6070×10^{-7}	3.67	5.1046×10^{-8}	3.70
36	7.7137×10^{-10}	3.91	1.1090×10^{-8}	3.86	3.4904×10^{-9}	3.87
72	4.9705×10^{-11}	3.96	7.2617×10^{-10}	3.93	2.2759×10^{-10}	3.94
144	3.1535×10^{-12}	3.98	4.6425×10^{-11}	3.97	1.4520×10^{-11}	3.97
Methods for Dirichlet boundary in [65]						
	GFM (1st-order)		IIM (2nd-order)		IMIB (2nd-order)	
M	$\|E_M\|_\infty$	Order	$\|E_M\|_\infty$	Order	$\|E_M\|_\infty$	Order
10	1.07×10^{-2}	–	5.71×10^{-4}	–	2.42×10^{-4}	–
40	2.70×10^{-3}	0.99	3.66×10^{-5}	1.98	1.13×10^{-5}	2.21
160	6.91×10^{-4}	0.98	2.30×10^{-6}	2.00	6.40×10^{-7}	2.07
640	1.73×10^{-4}	1.00	1.44×10^{-7}	2.00	3.90×10^{-8}	2.02
2560	4.32×10^{-5}	1.00	8.99×10^{-9}	2.00	2.42×10^{-9}	2.01

In our computation, we choose $h_1 = h_2 = h = \frac{1}{M}$. We calculate the error $u_j - u(x_j)$ and obtain the maximum error $\|E_M\|_\infty = \max_{0\le j\le M} |u_j - u(x_j)|$. If $\|E_{M_1}\|_\infty = O(h^q)$, then $\|E_{M_2}\|_\infty = O((M_2/M_1)^q h^q)$. It can be seen that $q = \frac{\log(\|E_{M_2}\|_\infty / \|E_{M_1}\|_\infty)}{\log(M_1/M_2)}$, which gives the convergence order. We choose M to 9, 18, 36, 72, 144, respectively. The maximum error and convergence order are obtained, which are listed in Table 6.1. It can be seen from Table 6.1, the convergence order is around 4.0, which coincides with the theoretical analysis in Chapters 4 and 5. This example (with Dirichlet boundary) was also calculated by three other methods in [65]. The numerical results of these methods are also listed in Table 6.1. It can be seen that the present schemes are much more accurate than the existing three methods, the ghost fluid method (GFM), the immersed interface method (IIM) and the interpolation matched interface and boundary method (IMIB) in [65].

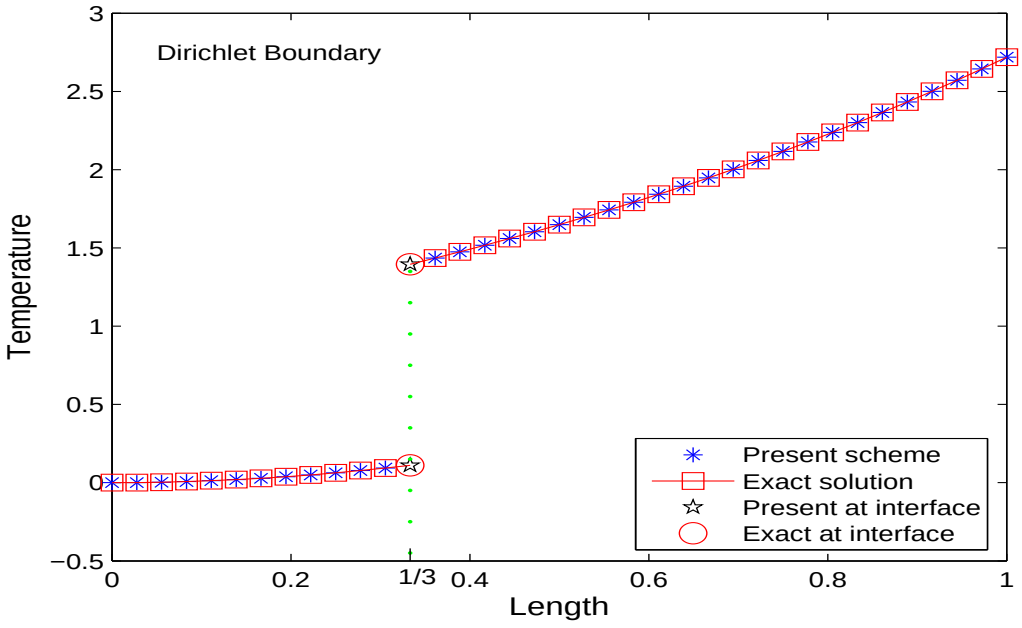

Figure 6.1: Temperature profiles along the spatial direction when $M = 36$ using the present scheme for Dirichlet boundary in Example 1.

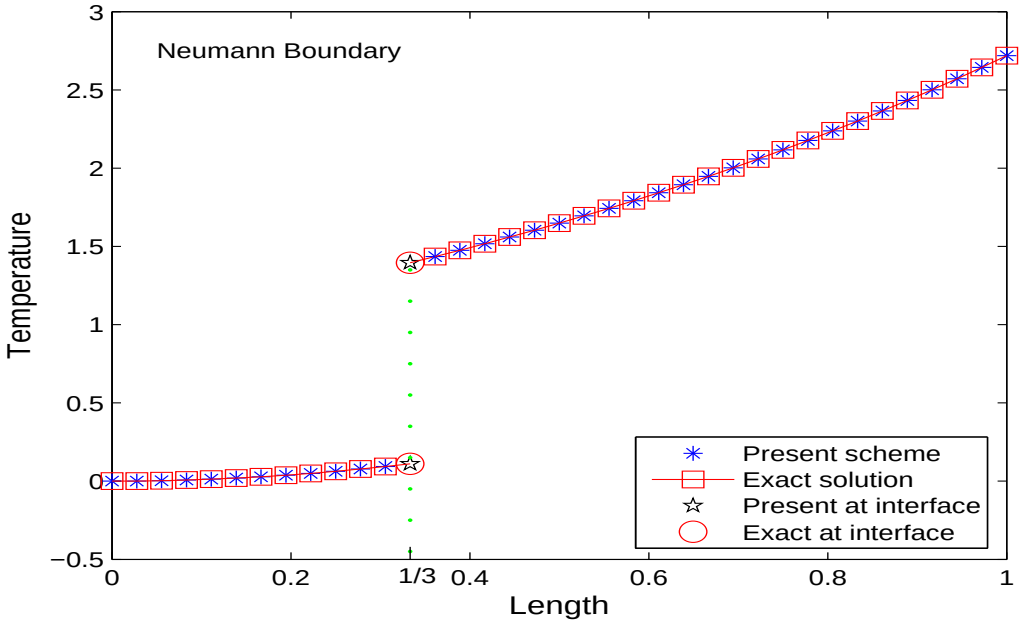

Figure 6.2: Temperature profiles along the spatial direction when $M = 36$ using the present scheme for Neumann boundary in Example 1.

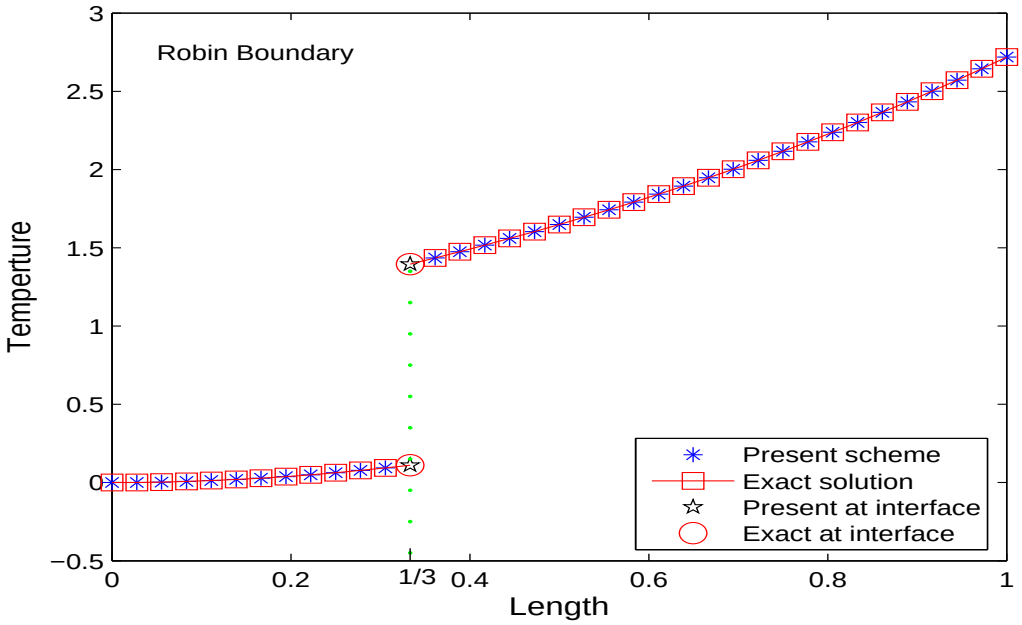

Figure 6.3: Temperature profiles along the spatial direction when $M = 36$ using the present scheme for Robin boundary in Example 1.

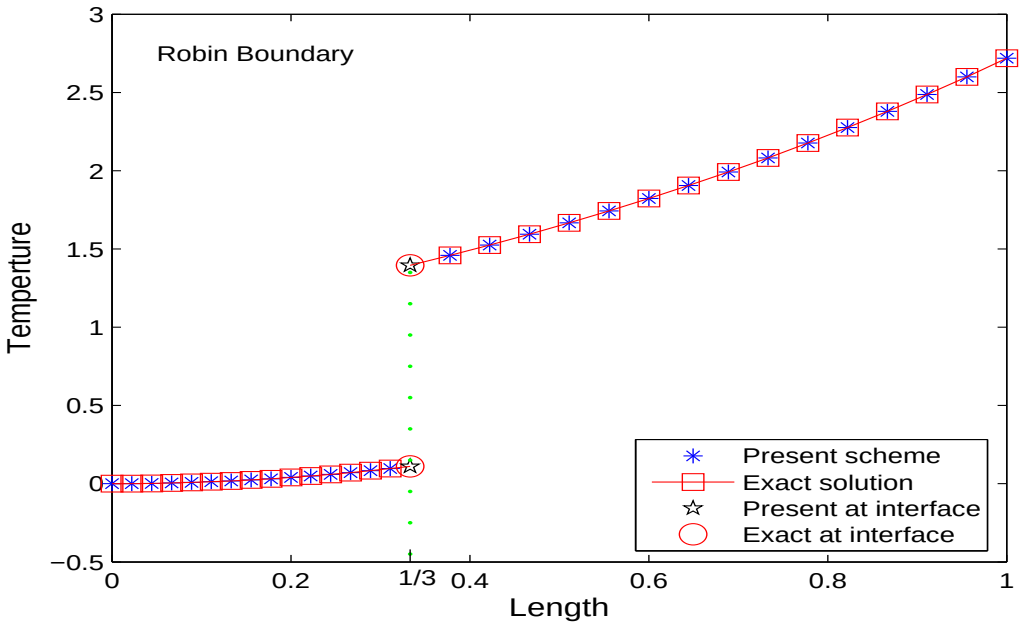

Figure 6.4: Temperature profiles along the spatial direction when $m = 15, M = 30$ using the present scheme for Robin boundary in Example 1.

Figures 6.1-6.3 show the temperature profiles along the spatial direction when $M = 36$ using the present schemes for different types of boundaries, respectively. From these figures, one may see a clear discontinuity at the interface and that there is not significantly different between the exact solutions and numerical solutions.

Our schemes can be also used for $h_1 \neq h_2$, where $h_1 = \frac{1/3}{m}$, $h_2 = \frac{2/3}{M-m}$. Figure 6.4 shows the temperature profiles along the spatial direction when $m = 15, M = 30$ using the present scheme for Robin boundary. It can be observed from this figure that there is no significant difference between the exact solution and numerical solution.

Example 2. Consider a heat conduction problem as [70]:

$$u_t(x,t) = u_{xx}(x,t), \ 0 \leq x \leq \frac{1}{2}, \ 0 \leq t \leq T, \tag{6.5}$$

$$5u_t(x,t) = \frac{1}{5}u_{xx}(x,t), \ \frac{1}{2} \leq x \leq 1, \ 0 \leq t \leq T, \tag{6.6}$$

with initial conditions:

$$u(x,0) = \cos(\pi x),\ 0 \le x \le \frac{1}{2}, \tag{6.7}$$

$$u(x,0) = \frac{1}{5}\cos(5\pi x),\ \frac{1}{2} \le x \le 1, \tag{6.8}$$

boundary conditions either of Dirichlet boundary:

$$u(0,t) = e^{-\pi^2 t},\ u(1,t) = -e^{-\pi^2 t},\ 0 \le t \le T, \tag{6.9a}$$

Neumann boundary:

$$u_x(0,t) = u_x(1,t) = 0,\ 0 \le t \le T, \tag{6.9b}$$

Robin boundary:

$$-u_x(0,t) + u(0,t) = e^{-\pi^2 t},\ u_x(1,t) + u(1,t) = -e^{-\pi^2 t},\ 0 \le t \le T, \tag{6.9c}$$

and the interfacial condition at $x = \frac{1}{2}$ as

$$u_{I^+}(t) - u_{I^-}(t) = 0,\ \ (u_x)_{I^+}(t) - \frac{1}{5}(u_x)_{I^-}(t) = 0,\ 0 \le t \le T. \tag{6.10}$$

It can be seen that the exact solution is $u(x,t) = e^{-\pi^2 t}\cos(\pi x)$, if $0 \le x \le \frac{1}{2}$; $u(x,t) = e^{-\pi^2 t}\cos(5\pi x)$, if $\frac{1}{2} \le x \le 1$. We use the three schemes Eq. (5.60), Eq. (5.61) and Eq. (5.62) to solve the above example corresponding to three different boundary conditions, respectively. In our computation, we choose $h_1 = h_2 = h = \frac{1}{M}$, $\Delta t = \frac{1}{N}$. We calculate the error $u_j^n - u(x_j, t_n)$ and obtain the maximum error $\|E_{M,N}\|_\infty = \max\limits_{0\le j\le M,\ 0\le n\le N,} \left|u_j^n - u(x_j,t_n)\right|$. If $\|E_{M_1,N}\|_\infty = O\left(h^q + (\Delta t)^p\right)$, then $\|E_{M_2,N}\|_\infty = O\left((M_2/M_1)^q h^q + (\Delta t)^p\right)$. It can be seen that $q \simeq \frac{\log\left(\|E_{M_2,N}\|_\infty / \|E_{M_1,N}\|_\infty\right)}{\log(M_1/M_2)}$ if Δt is very small, which gives the convergence order in space. In our computation, we choose $N = 10^5$ and M to be 10, 20, 40, 80, 160, respectively. The maximum

Table 6.2: Numerical errors and convergence order for Example 2.

Present scheme ($N = \frac{1}{\Delta t} = 10^5$)						
	Eq. (5.60) (Dirichlet)		Eq. (5.61) (Neumann)		Eq. (5.62) (Robin)	
M	$\|E_{M,N}\|_\infty$	Order	$\|E_{M,N}\|_\infty$	Order	$\|E_{M,N}\|_\infty$	Order
20	6.0497×10^{-4}	–	6.0101×10^{-4}	–	6.0102×10^{-4}	–
40	3.8483×10^{-5}	3.9746	3.8486×10^{-5}	3.9650	3.8486×10^{-5}	3.9650
80	2.4370×10^{-6}	3.9810	2.4381×10^{-6}	3.9805	2.4380×10^{-6}	3.9806
120	4.8285×10^{-7}	3.9925	4.8303×10^{-7}	3.9927	4.8301×10^{-7}	3.9927
160	1.5277×10^{-7}	4.0002	1.5282×10^{-7}	4.0003	1.5281×10^{-7}	4.0004
Methods for Neumann boundary in [70] ($N = \frac{1}{\Delta t} = 10^6$)						
	4th order scheme		1st-order scheme		2nd-order scheme	
M	$\|E_{M,N}\|_\infty$	Order	$\|E_{M,N}\|_\infty$	Order	$\|E_{M,N}\|_\infty$	Order
20	4.6704×10^{-4}	–	7.6308×10^{-2}	–	1.4597×10^{-2}	–
40	2.8689×10^{-5}	4.0250	3.1961×10^{-2}	1.2555	3.6516×10^{-3}	1.9990
80	1.7764×10^{-6}	4.0135	1.4944×10^{-2}	1.0969	9.1471×10^{-4}	1.9971
120	3.5195×10^{-7}	3.9926	9.7533×10^{-3}	1.0552	4.0684×10^{-4}	1.9982
160	1.2332×10^{-7}	3.6454	7.2389×10^{-3}	1.0363	2.2893×10^{-4}	1.9988

error and convergence order are obtained, which are listed in Table 6.2. It can be seen from Table 6.2 that the convergence order in space is around 4.0, which coincides with the theoretical analysis in Chapter 5. This example (with Neumann boundary) was also calculated by three other methods in [70]. The numerical results of these methods are also listed in Table 6.2. It can be observed that the present scheme is much more accurate than the first-order and second-order schemes, and has the same order accuracy as the 4th-order scheme in [70].

Figures 6.5, 6.6, and 6.7 show the temperature profiles along the spatial direction when $M = 40$, $N = 10^5$ at $t = 0.5$, using the present schemes for different types of boundaries, respectively. From these figures, one may see that there is no significant difference between the exact solutions and numerical solutions.

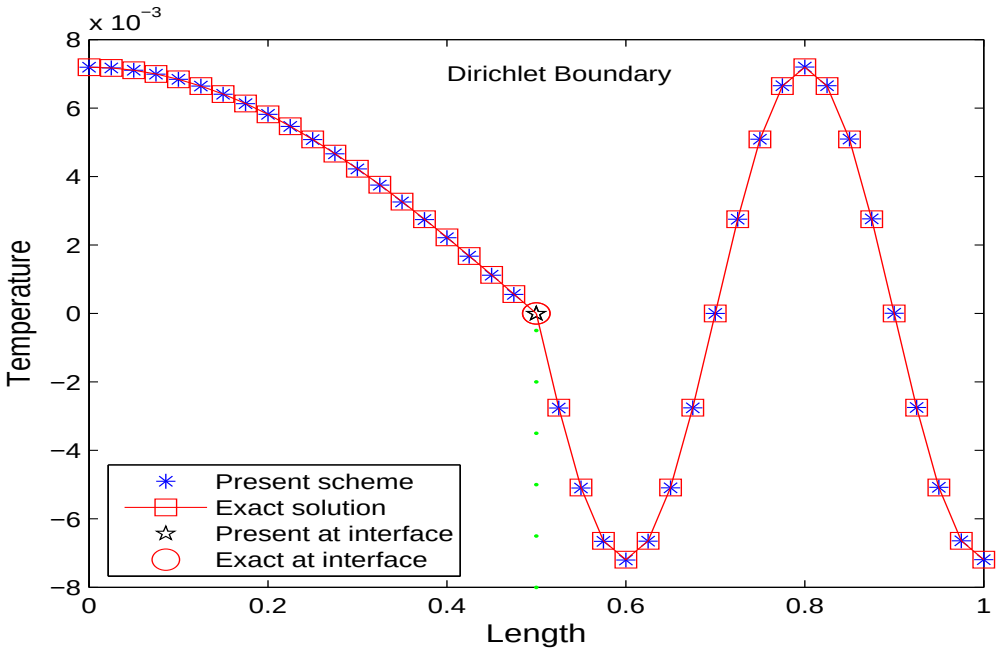

Figure 6.5: Temperature profiles along the spatial direction when $M = 40$, $N = 10^5$ at $t = 0.5$, using the present scheme for Dirichlet boundary in Example 2.

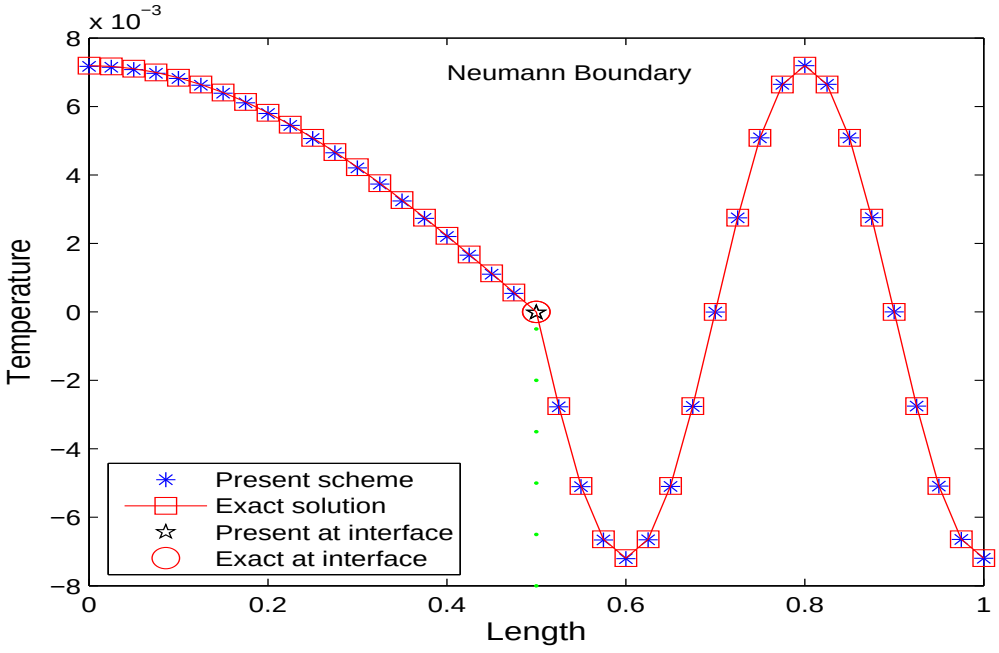

Figure 6.6: Temperature profiles along the spatial direction when $M = 40$, $N = 10^5$ at $t = 0.5$, using the present scheme for Neumann boundary in Example 2.

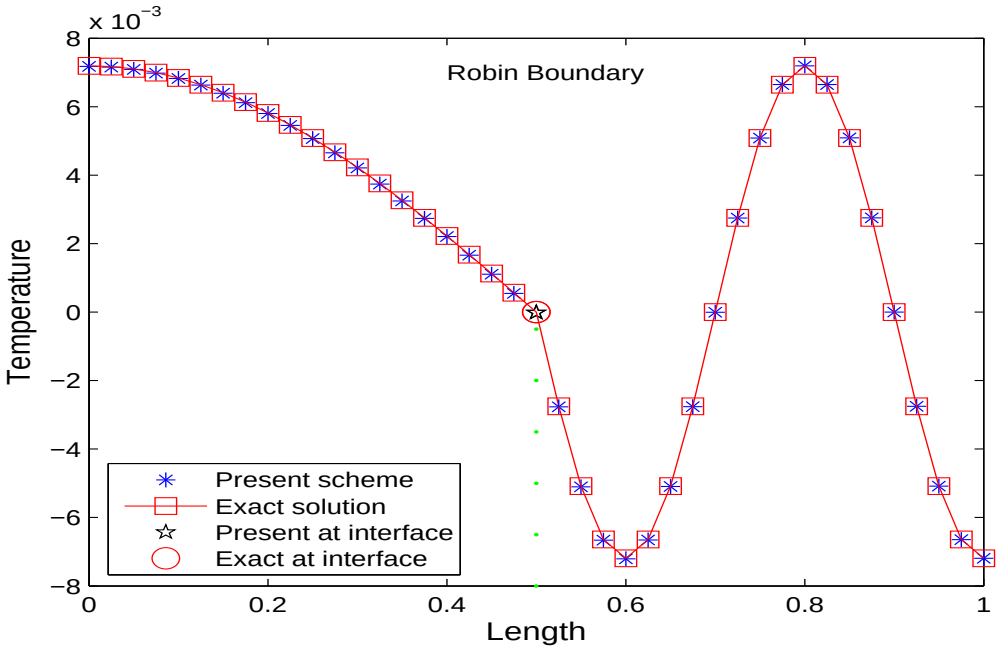

Figure 6.7: Temperature profiles along the spatial direction when $M = 40$, $N = 10^5$ at $t = 0.5$, using the present scheme for Robin boundary in Example 2.

Example 3. Consider a dual-phase-lagging heat conduction problem as [76]:

$$\begin{aligned}&\left(u_t\left(x,t\right)+u_{tt}\left(x,t\right)\right)\\ =&\frac{2}{3\pi^2}\left(u_{xx}\left(x,t\right)+u_{xxt}\left(x,t\right)\right)-\frac{1}{6}e^{-\frac{t}{2}}\sin\left(\frac{\pi}{2}x\right),\quad 0<x<\frac{1}{2},\ 0<t\leq 1,\end{aligned}\tag{6.11}$$

$$\begin{aligned}&\left(u_t\left(x,t\right)+u_{tt}\left(x,t\right)\right)\\ =&\frac{1}{3\pi^2}\left(u_{xx}\left(x,t\right)+4u_{xxt}\left(x,t\right)\right)-\frac{1}{3}e^{-\frac{t}{2}}\cos\left(\frac{\pi}{2}x\right),\quad \frac{1}{2}<x<1,\ 0<t\leq 1,\end{aligned}\tag{6.12}$$

subject to the initial and temperature-jump boundary conditions as

$$u\left(x,0\right)=\sin\left(\frac{\pi}{2}x\right),\ u_t\left(x,0\right)=-\frac{1}{2}\sin\left(\frac{\pi}{2}x\right),\ 0\leq x\leq\frac{1}{2},\tag{6.13}$$

$$u\left(x,0\right)=\cos\left(\frac{\pi}{2}x\right),\quad u_t\left(x,0\right)=-\frac{1}{2}\cos\left(\frac{\pi}{2}x\right),\quad \frac{1}{2}\leq x\leq 1,\tag{6.14}$$

$$-\frac{1}{2}u_x\left(0,t\right)+u\left(0,t\right)=-\frac{\pi}{4}e^{-\frac{t}{2}},\quad 0\leq t\leq 1,\tag{6.15}$$

$$\frac{1}{2}u_x\left(L,t\right)+u\left(L,t\right)=-\frac{\pi}{4}e^{-\frac{t}{2}},\quad 0\leq t\leq 1,\tag{6.16}$$

and the interfacial conditions at $x = l$ as

$$u_{I^+}(t) - u_{I^+}(t) = 0, \quad 0 \le t \le 1, \tag{6.17}$$

$$\frac{1}{3\pi^2}\left((u_x)_{I^+}(t) + 4\,(u_{xt})_{I^+}(t)\right) - \frac{2}{3\pi^2}\left((u_x)_{I^-}(t) + (u_{xt})_{I^-}(t)\right)$$

$$=0, \quad 0 \le t \le 1. \tag{6.18}$$

It can be seen that the exact solution is $u(x,t) = e^{-\frac{1}{2}}\sin(\frac{\pi}{2}x)$, if $0 \le x \le \frac{1}{2}$; $u(x,t) = e^{-\frac{1}{2}}\cos(\frac{\pi}{2}x)$, if $\frac{1}{2} \le x \le 1$. We use the scheme Eq. (5.134) to solve the above example.

Table 6.3: Numerical errors and convergence order in space for Example 3.

	Present scheme $\left(N = \frac{1}{\Delta t} = 10^5\right)$		2nd-order scheme in [76] $\left(N = \frac{1}{\Delta t} = 10^3\right)$	
M	$\|E_{M,N}\|_\infty$	Order	$\|E_{M,N}\|_\infty$	Order
10	1.9612×10^{-7}	–	$2.4247e-4$	–
20	1.2327×10^{-8}	3.9918	$6.0984e-5$	1.9913
40	7.4945×10^{-10}	4.0398	$1.5268e-5$	1.9979
80	4.6033×10^{-11}	4.0251	$3.8187e-6$	1.9997

In our computation, we choose $h_1 = h_2 = h = \frac{1}{M}$, $\Delta t = \frac{1}{N}$. We calculate the error $u_j^n - u(x_j, t_n)$ and obtain the maximum error $\|E_{M,N}\|_\infty = \max\limits_{0\le j\le M,\ 0\le n\le N,} \left|u_j^n - u(x_j,t_n)\right|$. If $\|E_{M_1,N}\|_\infty = O\left(h^q + (\Delta t)^p\right)$, then $\|E_{M_2,N}\|_\infty = O\left((M_2/M_1)^q h^q + (\Delta t)^p\right)$. It can be seen that $q \simeq \frac{\log\left(\|E_{M_2,N}\|_\infty / \|E_{M_1,N}\|_\infty\right)}{\log(M_1/M_2)}$ if Δt is very small, which gives the convergence order in space. We choose $N = 10^5$ and M to be 10, 20, 40, 80, respectively. The maximum error and convergence order are obtained, which are listed in Table 6.3. It is noted from Table 6.3 that the spatial convergence order of the present scheme is approximately 4.0. The result coincides with the theoretical analysis in Chapter 5. It can be seen that the present scheme is much more accurate than the second-order scheme in [76].

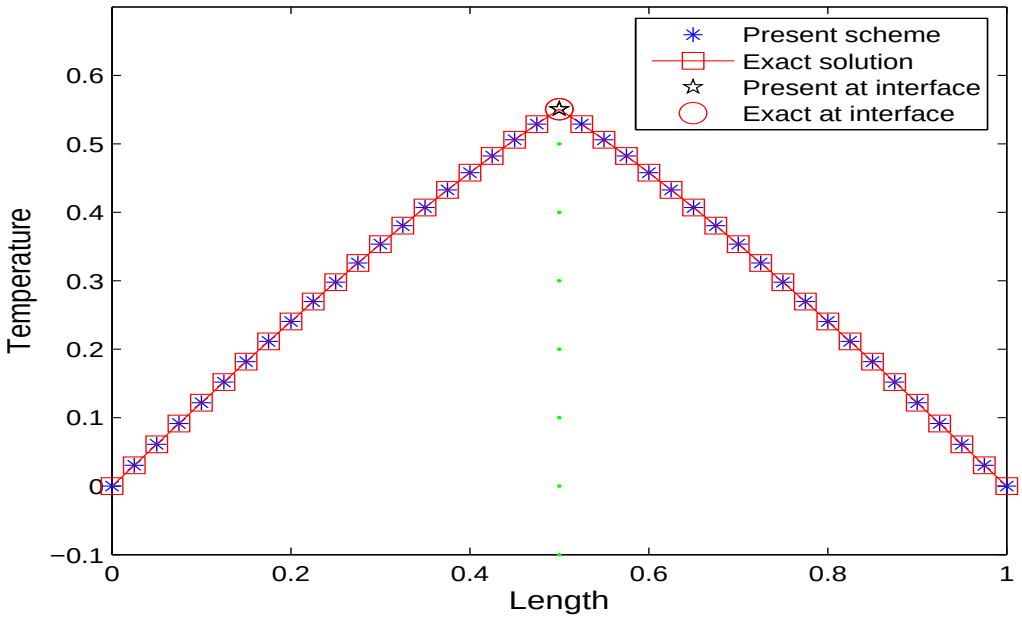

Figure 6.8: Temperature profiles along the spatial direction when $M = 40$, $N = 10^5$ at $t = 0.5$ using the present scheme in Example 3.

Figure 6.8 shows the temperature profiles along the spatial direction when $M = 40$, $N = 10^5$ at $t = 0.5$ using the present scheme. It can be observed from this figure that there is not significantly different between the exact solution and numerical solution.

Example 4. Consider a double-layered nanoscale thin film, where a gold layer is on a chromium padding layer and is irradiated by an ultrashort-pulsed laser, as shown in Figure 6.9. Each thickness of the gold layer and the chromium layer is 1 (nm), implying that $l = 1$ (nm), $L = 2$ (nm).

The thermal properties of gold and chromium used in the analysis are listed in Table 6.4 [53, 72, 98]. The heat source for both layers is given as [53]:

$$Q(x,t) = 0.94J\frac{1-R}{t_p\delta}\exp\left[-\frac{x}{\delta} - 2.77(\frac{t-2t_\rho}{t_\rho^2})^2\right],$$

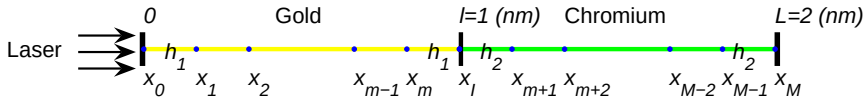

Figure 6.9: A double-layered nanoscale thin film in Example 4.

where $J = 13.7$ (J/m^2), $\delta = 15.3$ (nm), $t_p = 100$ (fs) and $R = 0.93$. Here, 1 (ps)= 10^{-12}(s), 1 (fs) =10^{-15} (s), and 1 (nm) = 10^{-9} (m). The initial temperature is chosen to be 300 (K).

Table 6.4: Properties of gold and chromium for Example 4 [53, 72, 98].

Property	c_p (J/kg/K)	K (ω/m/K)	ρ (kg/m^3)	τ_q (ps)	τ_T (ps)
Gold	129	317	193000	8.5	90
Chromium	449	94	7160	0.136	7.86

In our model, we choose $f_1(x,t) = Q + \tau_q^{(1)} \frac{\partial Q}{\partial t}$, $f_2(x,t) = Q + \tau_q^{(2)} \frac{\partial Q}{\partial t}$. For the parameters in the boundary condition, we choose $\alpha_1 = \alpha_2 = \alpha = 0.05$, 0.5, 5.0, respectively, to indicate that how fast the heat exchanges with the surroundings. A large α means that the heat transfer is close to the insulated situation. The solutions are obtained using scheme Eq. (5.134). Again, we take $h_1 = h_2 = h$ for simplicity.

Figures 6.10-6.12 show the temperature profiles along the spatial direction for three different values, $\alpha_1 = \alpha_2 = \alpha = 0.05$, 0.5, 5, at $t = 0.2$ (ps), 0.32 (ps), 0.5 (ps), based on a mesh of 40 grid points with a time increment of 0.0001 (ps). At $t = 0.2$ (ps), the temperature rises to about 311 (K); at $t = 0.32$ (ps), the temperature at the gold layer is almost uniform due to the very thin layer. It can be seen that the larger the α is, the higher the temperature level is.

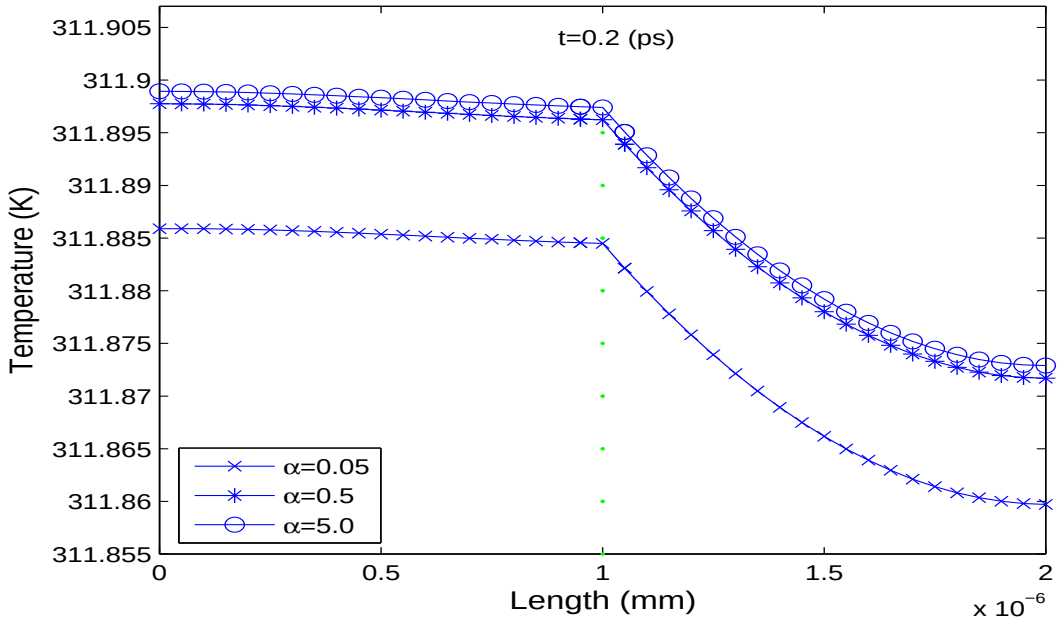

Figure 6.10: Temperature profiles along the spatial direction for three different values, $\alpha_1 = \alpha_2 = \alpha = 0.05, 0.5, 5$, at $t = 0.2$ (ps), based on a mesh of 40 grid points with a time increment of 0.0001 (ps) in Example 4.

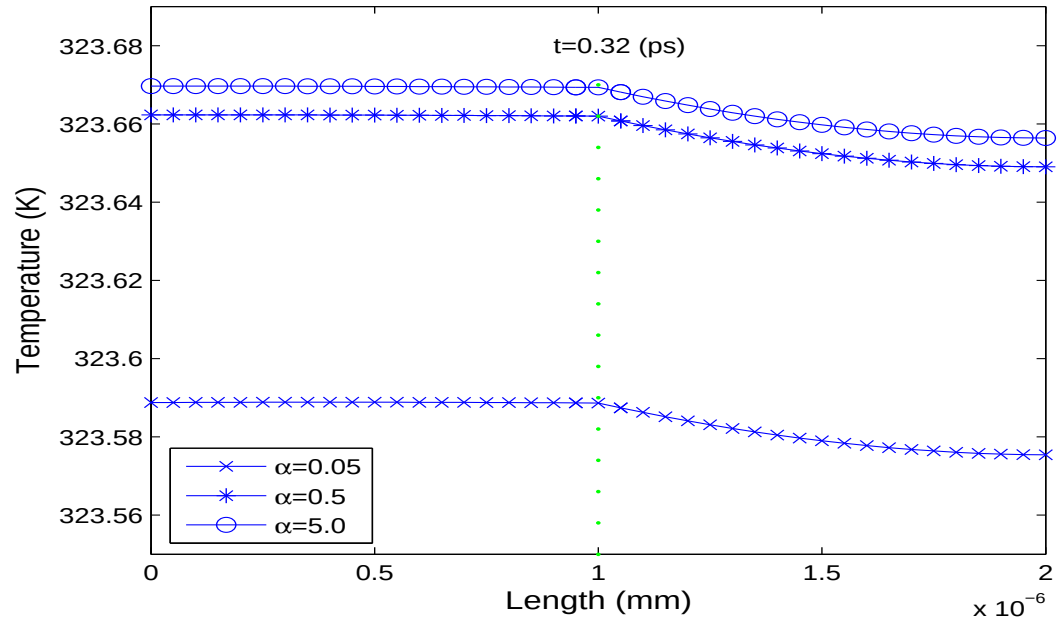

Figure 6.11: Temperature profiles along the spatial direction for three different values, $\alpha_1 = \alpha_2 = \alpha = 0.05, 0.5, 5$, at 0.32 (ps), based on a mesh of 40 grid points with a time increment of 0.0001 (ps) in Example 4.

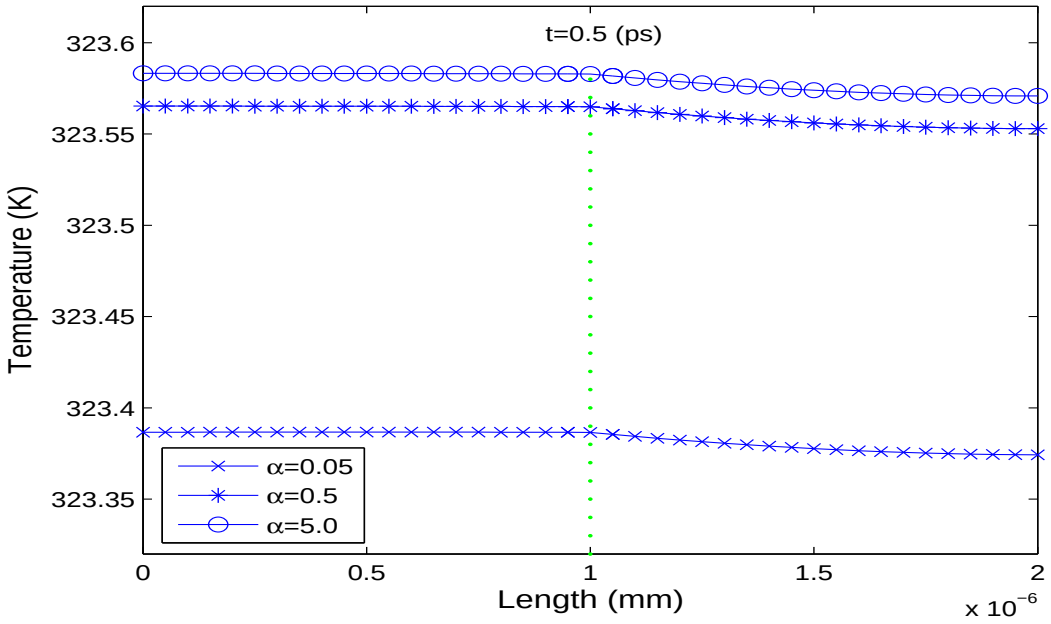

Figure 6.12: Temperature profiles along the spatial direction for three different values, $\alpha_1 = \alpha_2 = \alpha = 0.05, 0.5, 5$, at 0.5 (ps), based on a mesh of 40 grid points with a time increment of 0.0001 (ps) in Example 4.

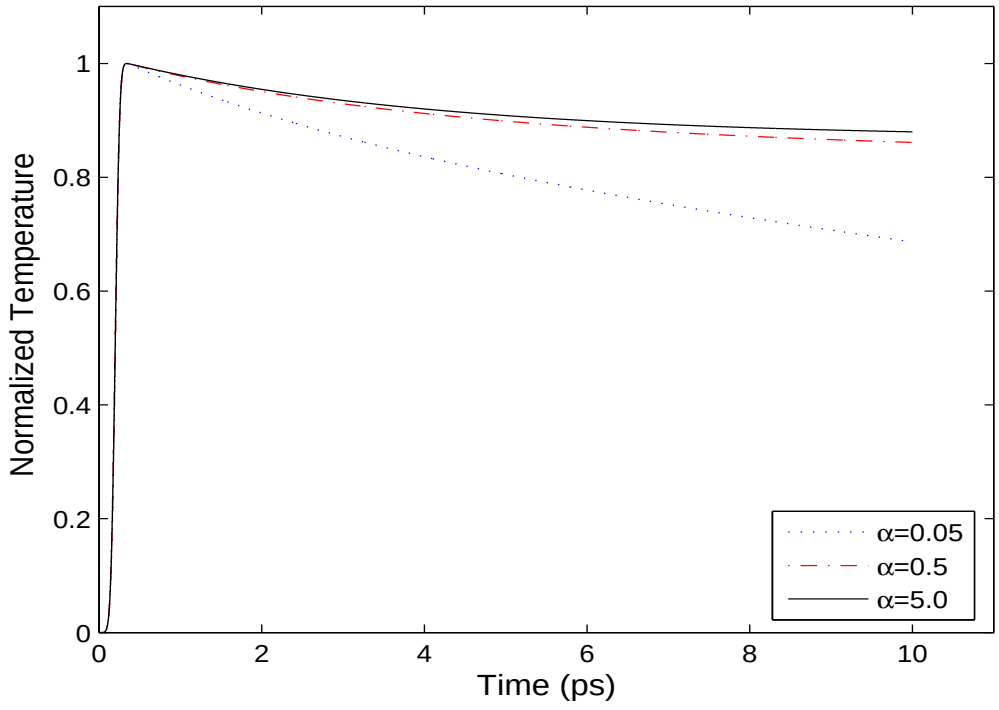

Figure 6.13: Normalized temperature ($\frac{u-u^0}{u_{\max}-u^0}$) profiles along the time direction at location x_0 for three different values, $\alpha_1 = \alpha_2 = \alpha = 0.05, 0.5, 5$, based on a mesh of 40 grid points with a time increment of 0.0001 (ps) in Example 4.

Figure 6.13 shows the normalized temperature ($\frac{u-u^0}{u_{\max}-u^0}$) profiles along the time direction at location x_0, i.e. the gold layer surface. This figure shows that the temperature rises quickly to the maximum around $t = 0.32$ (ps). After that, due to laser heating decreases, the heat transfers through the gold layer to chromium layer. Thus, the temperature at the gold surface is gradually falling with time increase.

In summary, numerical results have verified the accuracy and efficiency of the present finite difference schemes with the convergence order of four in space in L_∞ -norm. Moreover, the scheme for nanoscale heat conduction model is applied to the thermal analysis for a double-layered nanoscale thin film where a gold layer is on a chromium padding layer and is irradiated by an ultrashort-pulsed laser.

CHAPTER 7

CONCLUSIONS AND FUTURE WORK

In this dissertation research, we have developed several higher-order compact finite difference schemes that can accurately determine the temperature distribution in double-layered solid structures. Three mathematical models, the steady-state heat conduction model, the unsteady-state heat conduction model and the nanoscale heat conduction model, have been considered. We have proved the well-posedness of these three models. In our derivations of the compact finite difference schemes, we employ a well-known Padé fourth-order compact finite difference scheme for the interior points, while on the boundary and interface, the derivative u_x is kept without discretization, which we call the gradient preserved method (GPM). As a result, we obtain several fourth-order accurate three-points in space finite difference scheme for the interface. At the same time, we obtain third-order or fourth-order schemes for the Neumann boundary condition or the Robin boundary condition. We have analyzed the solvability, stability and convergence order of the numerical scheme for the steady-state heat conduction model with the Dirichlet boundary, which is proved to be solvable, unconditionally stable and fourth-order. Four numerical examples have been used to test the present schemes. Numerical results show that the present schemes are applicable and provide a higher-order accurate solution. The convergence

order based on the numerical examples is round about 4.0, which coincides with the theoretical analysis.

Future study will focus on the analysis of the stability and convergence order of the present schemes for the unsteady-state heat conduction model and the nanoscale heat conduction model as well as the extension of our schemes to multidimensional cases, and the application to multi-layer structures.

BIBLIOGRAPHY

[1] J. Ghazanfarian, Z. Shomali, A. Abbassi, Macro to nanoscale heat transfer: the lagging behaviour, *International Journal of Thermophysics*, 36: 1416-1467, 2015.

[2] J. Ho, C. Kuo, W. Jiaung, Study of heat transfer in multilayered structure within the framework of dual-phase-lag heat conduction model using lattice Boltzmann method, *International Journal of Heat and Mass Transfer*, 43: 55-69, 2003.

[3] K. Liu, Analysis of dual-phase-lag thermal behavior in layered films with temperature-dependent interface thermal resistance, *Journal of Physics D: Applied Physics*, 38: 3722-3732, 2005.

[4] M. Shen, P. Keblinski, Ballistic vs. diffusive heat transfer across nanoscopic films of layered crystals, *Journal of Applied Physics*, 115: 144310, 2014.

[5] M. Pillers, M. Lieberman, Rapid thermal processing of DNA origami on silicon creates embedded silicon carbide replicas, *13th Annual Conference on Foundations of Nanoscience*, Snowbird, Utah, April 11-16, 2016.

[6] F. Shah, K. Kim, M. Lieberman, G. Bernstein, Roughness optimization of electron-beam exposed hydrogen silsesquioxane for immobilization of DNA origami, *Journal of Vacuum Science and Technology Volume B*, 30: 011806, 2014.

[7] T. Tsai, Y. Lee, Analysis of microscale heat transfer and ultrafast thermoelasticity in a multi-layered metal film with nonlinear thermal boundary resistance, *International Journal of Heat and Mass Transfer*, 62: 87-98, 2013.

[8] S. Sadasivam, U. Waghmare, T. Fisher, Electron-phonon coupling and thermal conductance at metal-semiconductor interface: first-principles analysis, *Journal of Applied Physics*, 117: 134502, 2015.

[9] B. Griffith, C. Peskin, On the order of accuracy of the immersed boundary method: Higher order convergence rates for sufficiently smooth problems, *Journal of Computational Physics*, 208: 75-105, 2005.

[10] M. Lai, C. Peskin, An immersed boundary method with formal second-order accuracy and reduced numerical viscosity, *Journal of Computational Physics*, 160: 705-719, 2000.

[11] C. Peskin, Numerical analysis of blood flow in heart, *Journal of Computational Physics*, 25: 220-252, 1977.

[12] C. Peskin, Lectures on mathematical aspects of physiology, *Lectures in Applied Mathematics*, 19: 69-109, 1981.

[13] C. Peskin, D. McQueen, A 3-dimensional computational method for blood-flow in the heart. 1. immersed elastic fibers in a viscous incompressible fluid, *Journal Computational Physics*, 81: 372-405, 1989.

[14] C. Peskin, B. Printz, Improved volume conservation in the computation of flows with immersed elastic boundaries, *Journal of Computational Physics*, 105: 33-46, 1993.

[15] L. Adams, Z. Li, The immersed interface/multigrid methods for interface problems, *SIAM Journal on Scientific Computing*, 24: 463-479, 2002.

[16] S. Deng, K. Ito, Z. Li, Three-dimensional elliptic solvers for interface problems and applications, *Journal of Computational Physics*, 184: 215-243, 2003.

[17] J. Sethian, A. Wiegmann, Structural boundary design via level set and immersed interface methods, *Journal of Computational Physics*, 163: 489-528, 2000.

[18] R. Leveque, Z. Li, The immersed interface method for elliptic equations with discontinuous coefficients and singular sources, *SIAM Journal on Numerical Analysis*, 31: 1019-1044, 1994.

[19] Z. Li, K. Ito, Maximum principle preserving schemes for interface problems with discontinuous coefficients, *SIAM Journal on Scientific Computing*, 23: 339-361, 2001.

[20] Z. Li, An overview of the immersed interface method and its application, *Taiwanese Journal of Mathematics*, 7: 1-49, 2003.

[21] Z. Li, A fast iterative algorithm for elliptic interface problems, *SIAM Journal on*

Numerical Analysis, 35: 230-254, 1998.

[22] A. Wiegmann, K. Bube, The explicit-jump immersed interface method: Finite difference methods for pdes with piecewise smooth solutions, *SIAM Journal on Numerical Analysis*, 37, 827-862, 2000.

[23] Z. Li, The immersed interface method using a finite element formulation, *Applied Numerical Mathematics*, 27: 253-267, 1998.

[24] S. Hou, X. Liu, A numerical method for solving variable cofficient elliptic equation with interfaces, *Journal of Computational Physics*, 202: 411-445, 2005.

[25] H. Huang, Z. Li, Convergence analysis of the immersed interface method, *IMA Journal on Numerical Analysis*, 19: 583-608, 1999.

[26] R. Fedkiw, T. Aslam, B. Merriman, S. Osher, A non-oscillatory eulerian approach to interfaces in multimaterial flows (the ghost fluid method), *Journal of Computational Physics*, 152: 457-492,1999.

[27] X. Liu, R. Fedkiw, M. Kang, A boundary condition capturing method for poissons equation on irregular domains, *Journal of Computational Physics*, 160: 151-178, 2000.

[28] M. Kang, R. Fedkiw, X. Liu, A boundary condition capuring method for multiphase incompressible flow, *Journal of Scientific Computing*, 15: 323-360, 2000.

[29] S. Yu, Y. Zhou, G. Wei, Matched interface and boundary (MIB) method for elliptic problems with sharp-edged interfaces, *Journal of Computational Physics*, 224: 729-756, 2007.

[30] S. Yu, G. Wei, Three-dimensional mathed interface and boundary (MIB) method for treating geometric singularities, *Journal of Computational Physics*, 227: 602-623, 2007.

[31] S. Zhao, G. Wei, High order FDTD methods via derivative matching for maxwell equations with material interfaces, J*ournal of Computational Physics*, 200: 60-103, 2004.

[32] Y. Zhou, S. Zhao, M. Feig, G. Wei, High order matched interface and boundary method for elliptic equations with discontinuous coefficients and singular sources, *Journal of Computational Physics*, 213: 1-30, 2006.

[33] Y. Zhou, G. Wei, On the fictious-domain and interpolation formulations of the matched interface and boundary method, *Journal of Computational Physics*, 219: 228-246, 2006.

[34] S. Zhao, G. Wei, Matched interface and boundary (MIB) for the implementation of boundary conditions in high-order central finite differences, *International Journal for Numerical Methods in Engineering*, 77: 1690-1730, 2009.

[35] I. Babuska, The finite element method for elliptic equations with discontinuous coeffcients, *Computing*, 5: 207-213, 1970.

[36] Z. Chen, J. Zou, Finite element methods and their convergence for elliptic and parabolic interface problems, *Numerische Mathematik*, 79: 175-202, 1998.

[37] J. Bramble, J. King, A finite element method for interface problems in domains with smooth boundaries and interfaces, *Advances in Computational Mathematics*, 6: 109-138, 1996.

[38] Z. Li, T. Lin, X. Wu, New cartesian grid methods for interface problems using the finite element formulation, *Numerische Mathematik*, 96: 61-98, 2003.

[39] W. Liu, Y. Liu, D. Farrell, L. Zhang, X. Wang, Y. Fukui, N. Patankar, Y. Zhang, C. Bajaj, J. Lee, J. Hong, X. Chen, H. Hsua, Immersed finite element method and its applications to biological systems, *Computer Methods in Applied Mechanics and Engineering*, 195: 1722-1749, 2006.

[40] R. Sinha, B. Deka, On the convergence of finite element method for second order elliptic interface problems, *Numerical Functional Analysis and Optimization*, 27: 99-115, 2006.

[41] J. Huang, J. Zou, A mortar element method for elliptic problems with discontinuous coefficients, *IMA Journal on Numerical Analysis*, 22: 549-576, 2002.

[42] S. Hou, P. Song, L. Wang and H. Zhao, A weak formulation for solving elliptic interface problems without body fitted grid, *Journal of Computational Physics*,

249: 80-95, 2013.

[43] L. Wang, S. Hou and L. Shi, An improved non-traditional finite element formulation for solving the elliptic interface problems, *Journal of Computational Mathematics*, 32: 39-57, 2014.

[44] L. Wang, S. Hou and L. Shi, A weak formulation for solving elliptic interface problems with imperfect contact, *Applied Mathematics and Mechanics*, 9: 1189-1205, 2017.

[45] W. Wang, A jump condition capturing finite difference scheme for elliptic interface problems, *SIAM Journal on Scientific Computing*, 25: 1479-1496, 2004.

[46] Z. Li, W. Wang, I. Chern, M. Lai, New formulations for interface problems in polar coordinates, *SIAM Journal on Scientific Computing*, 25: 224-245, 2003.

[47] B. Strand, Summation by parts for finite difference approximations for d/dx, *Journal of Computational Physics*, 110: 47-67, 1994.

[48] K. Mattsson, J. Nordstrom, Summation by parts operators for finite difference approximations of second derivatives, *Journal of Computational Physics*, 199: 503-540, 2004.

[49] B. Gustafsson, High Order Difference Methods for Time Dependent PDE, Springer: Berlin, 2008.

[50] C. David, D. Fernández, J. Hicken, D. Zingg, Review of summation-by-parts operators with simultaneous approximation terms for the numerical solution of partial differential equations, *Computers & Fluids Elsevier*, 95: 171-196, 2014.

[51] S. Lele, Compact finite difference schemes with spectral-like resolution, *Journal of Computational Physics*, 103: 16-42, 1992.

[52] Y. Zhou, G. Wei, On the fictitious-domain and interpolation formulations of the matched interface and boundary (MIB) method, *Journal of Computational Physics*, 219: 228-246, 2016.

[53] D. Tzou, Macro to Microscale Heat Transfer: the Lagging Behaviour, Taylor and Francis, Washinton, 1997.

[54] C. Cattaneo, A form of heat conduction equation which eliminates the paradox of instantaneous propagation, *Comptes Rendus*, 247: 431-433, 1958.

[55] P. Vernotte, Some possible complications in the phenomena of thermal conduction, *Comptes Rendus*, 252: 2190-2191, 1961.

[56] E. Fadlun, R. Verzicco, P. Orlandi, J. Mohd-Yusof, Combined immersed-boundary finite-difference methods for three-dimensional complex flow simulations, *Journal of Computational Physics*, 161: 30-60, 2000.

[57] M. Francois, W. Shyy, Computations of drop dynamics with the immersed boundary method, part 2: drop impact and heat transfer, *Numerical Heat Transfer*, 44: 119-143, 2003.

[58] G. Iaccarino, R. Verzicco, Immersed boundary technique for turbulent flow simulations, *Applied Mechanics Reviews*, 56: 331-347, 2003.

[59] A. Tornberg, B. Engquist, Numerical approximations of singular source terms in differential equations, *Journal of Computational Physics*, 200: 462-488, 2004.

[60] T. Hou, Z. Li, S. Osher, H. Zhao, A hybrid method for moving interface problems with application to the Hele–Shaw flow, *Journal of Computational Physics*, 134: 236-252, 1997.

[61] J. Jin, X. Wang, Robust numerical simulation of porosity evolution in chemical vapor infiltration II. Two-dimensional anisotropic fronts, *Journal of Computational Physics*, 179: 557-577, 2002.

[62] J. Kandilarov, Immersed interface method for a reaction-diffusion equation with a moving own concentrated source, *Lecture Notes in Computer Science*, 2542: 506-513, 2003.

[63] Z. Li, K. Ito, The Immeresed Interface Method, SIAM Frontiers in Applied Mathematics, Philadelphia, 2006.

[64] S. Zhao, G. Wei, Tensor product derivative matching for wave propagation in inhomogeneous media, *Microwave and Optical Technology Letters*, 43: 69-77, 2004.

[65] K. Pan, Y. Tan, H. Hu, An interpolation matched interface and boundary method for elliptic interface problems, *Journal of Computational and Applied Mathematics*, 234: 73-94, 2010.

[66] M. Svärd, J. Nordström, Review of summation-by-parts schemes for initial–boundary-value problems, *Journal of Computational Physics*, 268: 17-38, 2014.

[67] M. Giles, Stability analysis of numerical interface conditions in fluid-structure thermal analysis, *International Journal for Numerical Methods in Fluids*, 25: 421-436, 1997.

[68] B. Roe, R. Jaiman, A. Haselbacher, P.H. Geubelle, Combined interface boundary condition method for coupled thermal simulations, *International Journal for Numerical Methods in Fluids*, 57: 329-354, 2008.

[69] W. Henshaw, K. Chand, A composite grid solver for conjugate heat transfer in fluid-structure systems, *Journal of Computational Physics*, 228: 3708-3741, 2009.

[70] Z. Sun, W. Dai, A new higher-order accurate numerical method for solving heat conduction in a double-layered film with the Neumann boundary condition, *Numerical Methods for Partial Differential Equations*, 30: 1291-1314, 2014.

[71] W. Dai, H. Yu, R. Nassar, A fourth-order compact finite difference scheme for solving a 1-D Pennes' bioheat transfer equation in a triple-layered skin structure, *Numerical Heat Transfer, Part B*, 46: 447-461, 2004.

[72] W. Dai, R. Nassar, A hybrid finite element-finite difference method for solving three-dimensional heat transport equations in a double-layered thin film with microscale thickness, *Numerical Heat Transfer, Part A*, 38: 573-588, 2000.

[73] W. Dai, T. Niu, A finite difference method for solving nonlinear hyperbolic two-step model in a double-layered thin film exposed to ultrashort pulsed lasers with nonlinear interfacial conditions, *Nonlinear Analysis: Hybrid Systems*, 2: 121-143, 2008.

[74] T. Niu, W. Dai, A hyperbolic two-step model based finite difference scheme for studying thermal deformation in a double-layered thin film exposed to ultrashort pulsed lasers, *International Journal of Thermal Sciences*, 48: 34-49, 2009.

[75] H. Wang, W. Dai, L. Hewavitharana, A finite difference method for studying thermal deformation in a double-layered thin film with imperfect interfacial contact exposed to ultrashort pulsed lasers, *International Journal of Thermal Sciences*, 47: 7-24, 2008.

[76] H. Sun, Z. Sun, W. Dai, A second-order finite difference dcheme for dolving the dual-phase-lagging equation in a double-layered nanoscale thin film, *Numerical Methods for Partial Differential Equations*, 33: 142-173, 2017.

[77] G. Guyomarc'h, C. Lee, K. Jeon , A discontinuous Galerkin method for elliptic interface problems with application to electroporation, *International Journal for Numerical Methods in Biomedical Engineering*, 25: 991-1008, 2009.

[78] A. Mayo, A. Greengard, Fast parallel solution of Poisson's and the biharmonic equations on irregular regions, *SIAM Journal on Scientific and Statistical Computing*, 13: 101-118, 1992.

[79] W. Liao, J. Zhu, A. Khaliq, A fourth-order compact algorithm for nonlinear reactiondiffusion equations with Neumann boundary conditions, *Numerical Methods for Partial Differential Equations*, 22: 600-616, 2006.

[80] W. Dai, A new accurate finite difference scheme for Neumann (insulated) boundary condition of heat conduction, *International Journal of Thermal Sciences*, 49: 571-579, 2010.

[81] Z. Sun, Compact difference schemes for heat equation with Neumann boundary conditions, *Numer Methods Partial Differential Equations*, 25: 1320-1341, 2009.

[82] G. Gao, Z. Sun, Compact difference schemes for heat equation with Neumann boundary conditions (II), *Numerical Methods for Partial Differential Equations*, 29: 1459–1486, 2013.

[83] A. Mohebbi, M. Dehghan, High-order compact solution of the one-dimensional heat and advection-diffusion equations, *Applied Mathematical Modelling*, 34: 3071-3084, 2010.

[84] H. Cao, L. Liu, Y. Zhang, S. Fu, fourth-order method of the convection-diffusion equations with Neumann boundary conditions, *Applied Mathematics and Computation*, 217: 9133-9141, 2011.

[85] D. You, A high-order Padé ADI method for unsteady convection-diffusion equations, *Journal of Computational Physics*, 214: 1-11, 2006.

[86] W. Liao, A compact high-order finite difference method for unsteady convection-fiffusion equation, *International Journal for Computational Methods in Engineering Science and Mechanics*, 13: 135-145, 2012.

[87] R. Mohanty, W. Dai, F. Han, Compact operator method of accuracy two in time and four in space for the numerical solution of coupled viscous Burgers' equations, *Applied Mathematics and Computation*, 256: 381-393, 2015.

[88] F. Han, W. Dai, New higher-order compact finite difference schemes for 1D heat conduction equations, *Applied Mathematical Modelling*, 37: 7940-7953, 2013.

[89] D. Liu, W. Kuang, A. Tangborn, High-order compact implicit difference methods for parabolic equations in geodynamo simulation, *Advances in Mathematical Physics*, ID: 568296, 2009.

[90] F. Gelu, G. Duressa, T.Bullo, Sixth-order compact finite difference method for singularly perturbed 1D reaction diffusion problems, *Journal of Taibah University for Science*, 11: 302-308, 2017.

[91] X. Hu, S. Chen, Q. Chang, Fourth-order compact difference schemes for 1D nonlinear Kuramoto-Tsuzuki equation, *Numerical Methods for Partial Differential Equations*, 31: 2080-2109, 2015.

[92] Y. Yan, F. Moxley III, W. Dai, A new compact finite difference scheme for solving the complex Ginzburg-Landau equation, *Applied Mathematics and Computation*, 260: 269-287, 2015.

[93] W. Dai, R. Nassar, A compact finite difference scheme for solving a one-dimensional heat transport equation at the micro-scale, *Journal of Computational and Applied Mathematics*, 132: 431-441, 2001.

[94] W. Dai, F. Han, Z. Sun, Accurate numerical method for solving dual-phase-lagging equation with temperature jump boundary condition in nano heat conduction, *International Journal of Heat and Mass Transfer*, 64: 966-975, 2013.

[95] W. Lor, H. Chu, Hyperbolic heat conduction in thin-film high Tc superconductors with interface thermal resistance, *Cryogenics*, 39: 739-750,1999.

[96] W. Lor, H. Chu, Effect of interface thermal resistance on heat transfer in a composite medium using the thermal wave model, *International Journal of Heat and Mass Transfer*, 43: 653-663, 2000.

[97] K. Atkinson, An Introduction to Numerical Analysis, Wiley, New York, 1989.

[98] E. Incropera, D. Dewitt, Fundamentals of Heat Mass Transfer, Wiley, New York, 1990.

[99] W. Dai, G. Li, R. Nassar, L. Shen, An unconditionally stable three level finite difference scheme for solving parabolic two-step micro heat transport equations in a three-dimensional double-layered thin film, *International Journal for Numerical Methods in Engineering*, 59: 493–509, 2004.